Mechanisms of Immunodeficiency Due To NFkappaB Signaling Defects

Mechanisms of immunodeficiency due to NFκB signaling defects

ABSTRACT

Ectodermal dysplasia with immunodeficiency (ED-ID) is a rare primary immunodeficiency syndrome characterized by defects in ectodermal tissues (skin, hair and sweat glands), recurrent infections, impaired response to Toll-like receptor ligands, hypogammaglobulinemia and deficient antibody production. It is caused by defective NFκB signaling.

The most common form of ED-ID is X-linked. It is caused by hypomorphic mutations in the NFκB essential modifier gene *NEMO*, which is an important regulatory component in the NFκB signaling pathway. We report the first case of ED-ID caused by insufficient expression of a NEMO protein of normal sequence, due to a mutation in the 5' untranslated region of the *NEMO* gene.

Autosomal dominant ED-ID, a rare form of ED-ID, has been reported to be caused by a heterozygous S32I mutation in the IκBα. This mutation prevents IκBα phosphorylation and inhibits its degradation. The mutant sequesters NFκB in the cytoplasm and acts as a dominant negative. We report the first ED-ID patient with a heterozygous mutation (W11X) that causes N-terminal truncation of IκBα and results in functional haploinsufficiency.

We have constructed a knock-in mouse model of ED-ID caused by a heterozygous S32I mutation in IκBα. The mutant mice had ED, increased mortality, complete lack of lymph nodes and Peyer's patches, and disorganized spleens that

lacked follicles, marginal zone B cells and follicular dendritic cells. T cell proliferation and cytokine production was normal *in vitro*, but *in vivo* contact hypersensitivity was severely impaired, B cell function *in vitro* and specific antibody response to antigens were severely reduced. All immune defects, except those that affected B cell function, were absent in IκBα S32I mutant $Rag2^{-/-}$ bone marrow chimeras, indicating that defects in non-lymphiod cells play a major role in the immunodeficiency of patients with ED-ID due to mutations in IκBα. This has important clinical implications, as bone marrow transplant may not be able to correct immune function in such patients.

The lessons learned in these chapters may be applicable to other mutations that impair NFκB signaling and have important implications for the treatment of patients who carry these mutations.

Mechanisms of immunodeficiency due to NFκB signaling defects

Introduction: An Overview of Relevant Immune System Functions

Introduction: An Overview of Relevant Immune System Functions

Innate and adaptive immunity

The immune system uses two layers of defense to protect the body from attack by pathogens. The innate immune system launches an immediate, non-specific response, then activates the adaptive immune system, which allows the body to recognize and remember specific pathogens[1]. The innate immune system includes the barrier functions of the skin and the mucosa, as well as the complement system and pro-inflammatory cytokine production[2]. Many types of cells in the body, from fibroblasts to macrophages, use pathogen-associated molecular pattern (PAMP) receptors such as the Toll-like receptors to detect pathogenic antigens, and send out cytokine danger signals to alert and recruit members of the immune system[1, 2].

The adaptive immune system

The adaptive immune system recognizes antigens when they bind to T and B lymphocyte receptors (T cell receptor, TCR, and B cell receptor, BCR). Antigens are phagocytosed, processed and presented to lymphocytes by antigen presenting cells, such as dendritic cells. Each naïve lymphocyte bears antigen receptors of a single specificity. When activated, lymphocytes proliferate and differentiate to form a clone of effector cells[3].

T cells

T cells recognize antigen-derived peptide that is bound to a major histocompatibility complex (MHC) molecule and presented on the surface of cells that display T cell co-stimulatory receptors. There are two major classes of T cells that have different functions. $CD4^+$ T cells recognize antigen in the context of MHC class II molecules, and activated $CD4^+$ T cells proliferate and produce cytokines that attract the appropriate immune cells to the site of infection, or help B cells produce specific antibodies. $CD8^+$ T cells recognize antigen in the context of MHC class I molecules which generally present peptides derived from intracellular antigens, and mature into cytotoxic "killer" T cells upon activation[3].

Immunoglobulins and B cell development

The BCR is a cell surface bound antibody molecule, or immunoglobulin (Ig). B cells are an essential part of the adaptive immune system; they produce immunoglobulin against antigens, act as antigen presenting cells and preserve immunological memory by developing into memory B cells[4]. It is estimated that the human body can make up to 10^{11} different antibodies and B cells can make antibodies even to new antigens never before seen in evolution. This variability and adaptability is due to antigen receptor gene rearrangement, also known as VDJ recombination, and somatic hypermutation[3].

Immunoglobulins are made up of two protein chains, heavy and light, each with a variable and a constant region. The variable regions are encoded by several pieces, known as variable (V), diversity (D), and joining (J) segments.

There are multiple copies of the V, D and J gene segments, and in the bone marrow, each developing B cell will

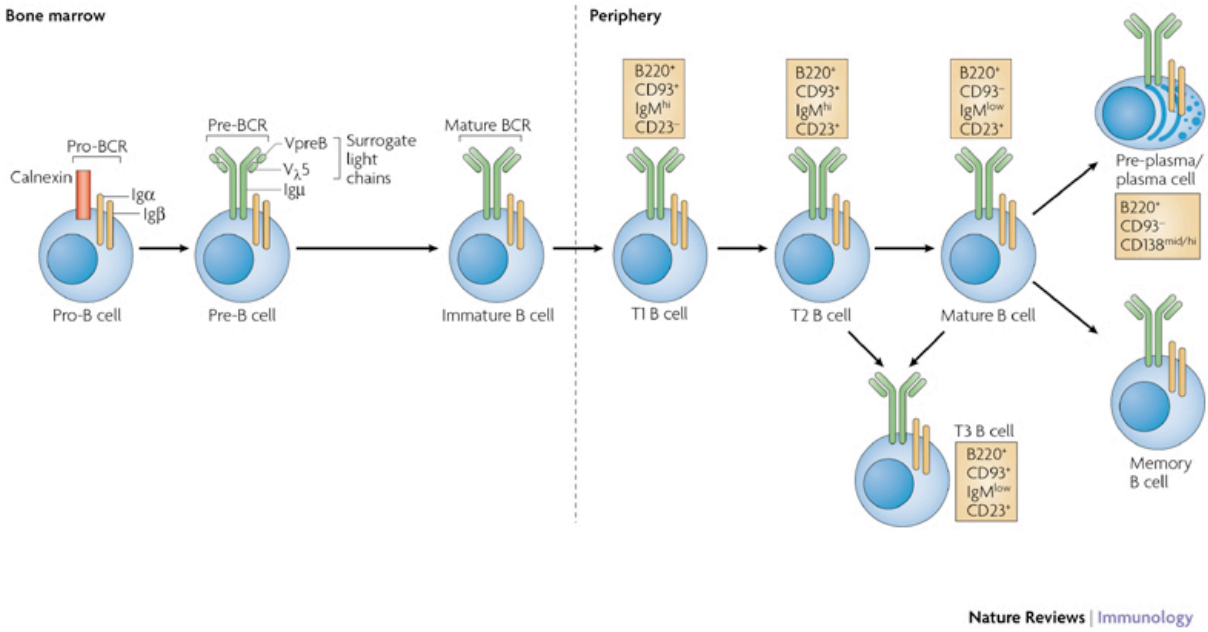

Figure I.1. B-cell development occurs in both the bone marrow and peripheral lymphoid tissues such as the spleen. In the bone marrow, development progresses through the pro-B-cell, pre-B-cell and immature-B-cell stages. During this differentiation, rearrangements at the immunoglobulin locus result in the generation and surface expression of the pre-B-cell receptor (pre-BCR, which is comprised of an Ig heavy chain and surrogate light chains (VpreB or V5)) and finally a mature BCR (comprised of rearranged heavy- and light-chain genes) that is capable of binding antigen. At this immature stage of development, B cells undergo a selection process to prevent any further development of self-reactive cells. Both receptor editing and clonal deletion have a role at this stage. Cells successfully completing this checkpoint leave the bone marrow as transitional B cells, eventually maturing into mature follicular B cells (or marginal-zone B cells). Following an immune response, antigen-specific B cells develop into either plasma (antibody-secreting) cells or memory B cells. From Cambier, et al[7].

assemble its immunoglobulin variable region by randomly selecting and combining one V, one D and one J gene segment (or one V and one J segment in the light chain)[5, 6]. The heavy chain undergoes VDJ recombination first, and it is expressed on the cell surface. If the heavy chain is functional, the receptor signals through several pathways, including the nuclear factor κB (NFκB) signaling pathway, inhibiting apoptosis and giving positive feedback that allows

the B cell to initiate light chain rearrangement. A similar checkpoint occurs after light chain rearrangement[5] (see Figure I.1 for a depiction of B cell development and differentiation). T cell receptor gene rearrangement of α and β chains also undergoes V-J recombination to produce diverse TCRs[3].

B cells with functional surface immunoglobulin (BCR) exit the bone marrow and migrate to the spleen where they may encounter their antigen. Following activation by antigen, the B cells proliferate rapidly and the variable regions undergo a high rate of point mutation called somatic hypermutation. The daughter cells then have acquired specific amino acid differences in their BCR that change the affinity of the receptor. B cells that express high affinity immunoglobulins on their surface will receive a strong survival signal through the NFκB pathway, whereas those with low affinity immunoglobulins will not, and therefore die by apoptosis. This process is also called affinity maturation, and depends in part on helper T cells[5]. Another process that takes place after B cell activation is class switch recombination (CSR). The effector function of an antibody depends on its isotype class. Naïve B cells express only IgM and IgD, but in order to eliminate an antigen, IgG, IgA or IgE are necessary. Since only the constant region is affected, CSR allows daughter cells with the same variable region to produce antibodies with the same specificity but different effector functions[6]. The isotypes produced during CSR depend on the kind of cytokines and other signals present[4, 5, 8].

NFκB and the immune system

NFκB is a key transcription factor required for the expression of many important genes in immune and non-immune cells[9]. Receptors that result in NFκB activation include the BCR and TCR, PAMP receptors like the TLRs, and the tumor necrosis factor receptor (TNFR) and other TNFR family members including CD40. NFκB activation results in the synthesis of inflammatory cytokines and chemokines, anti-bacterial peptides, and anti-apoptotic molecules[10]. Two distinct NFκB signaling pathways have been described. The canonical pathway depends on the IκB kinase (IKK) complex, which contains the kinases IKKα and IKKβ, and the scaffolding protein IKKγ, also known as NFκB essential modulator (NEMO), which links receptor signaling to the IKK complex. The non-canonical NFκB signaling pathway is independent of NEMO and IKKβ, and uses the NFκB activating kinase (NIK) to link signals from surface receptors to IKKα. In immune cells, the canonical NFκB pathway mediates relatively rapid inflammatory responses to antigens and injury, whereas the non-canonical NFκB pathway, results in slower and more sustained NFκB signaling and is used by receptors that are important for the development of lymphoid organs, such as lymphotoxin β receptor (LTβR) which is expressed on stromal cells (see Figure I.2)[10].

In the canonical pathway, homodimers or heterodimers of the three Rel homology domain (RHD)-containing NFκB polypeptides RelA (p65), p50 and cRel are held in the cytoplasm at the basal state by the inhibitor of NFκB (IκB) proteins. These include IκBα, and IκBβ, and IκBε, with IκBα being the most abundant in immune cells bound predominantly to the RelA:p50 dimer. Upon

receptor activation, the IKK complex phosphorylates the IκB proteins at two conserved serine residues, S32 and S36 on IκBα, targeting it for ubiquitination, which is followed by its degradation in the proteasome. This releases the NFκB dimers and allowing them to translocate into the nucleus[11]. Except for dimers of p50, which have no transcriptional activity, all other dimers generated bind to specific promoters and activate transcription of genes involved in inflammation, cell survival, proliferation and differentiation. As a negative feedback loop for NFκB signaling, IκBα expression itself is also regulated by NFκB activation[12, 13].

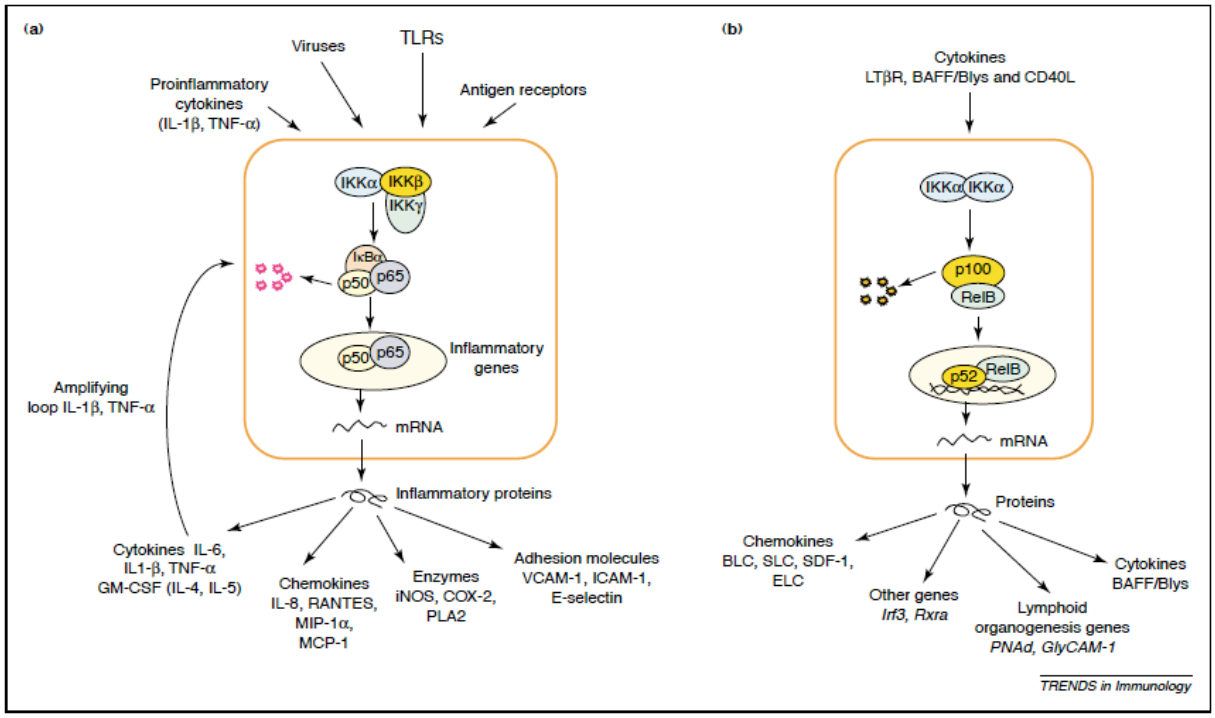

Figure I.2. The canonical and non-canonical NFκB pathways. **a**. The canonical NFκB pathway is activated by a variety of inflammatory signals, resulting in coordinate expression of multiple inflammatory and innate immune genes. The proinflammatory cytokines IL-1 and TNFα activate NFκB, and their expression is induced in response to NFκB activation, thus forming an amplifying feed forward loop. **b**. The non-canonical pathway for NFκB, which is activated by LTβR, BAFF and CD40L by NIK, results in nuclear translocation of p52:RelB dimers and is strictly dependent on IKKα homodimers. From Bonizzi and Karin, Trends in Immunology, 2004[10].

In the non-canonical NFκB signaling pathway, the activation of the NIK-IKKα kinase complex results in the processing of NFκB p100, which under basal conditions forms an inactive dimer with the NFκB protein RelB. Processing of p100 generates p52 and liberates the dimer. The RelB:p52 heterodimer, which slowly accumulates, translocates to the nucleus to activate transcription of chemokines, cytokines, developmental genes and other genes. There is additional cross-talk between the canonical and non-canonical pathways. For example, RelA:p50 is inhibited not only by IκB proteins, but also by a multimeric form of p100 called IκBδ. Furthermore, transcription of p100 and RelB, like that of IκBα, depend on RelA:p50 activation[14].

Ectodermal dysplasia with immune deficiency

Ectodermal dysplasia (ED) with immune deficiency (ED-ID) is a rare primary immunodeficiency syndrome characterized by abnormal development of the ectoderm and severe immunologic dysfunction. Clinical features include those typical of ED (sparse hair, conical teeth, and reduced number of sweat glands) and susceptibility to severe pyogenic infections and to opportunistic infections with mycobacterial, fungal, and viral pathogens. Immunologic features include decreased cytokine production in response to Toll-like receptor (TLR) ligands, impaired T cell proliferation to specific antigen, variably reduced T cell proliferation to mitogens, and deficient specific antibody production, but normal numbers of T and B cells[15]. Normal ectodermal development requires activation of the canonical NFκB pathway downstream of the ectodysplasin A (EDA)

receptor[15, 16]. Similarly, effective innate and adaptive immune responses depend on the activation of the canonical NFκB pathway downstream of several receptors. These include TLRs, IL-1 receptor, TNF receptor, BCR, TCR, and CD40[9]. Two forms of ED-ID have been described: an X-linked form caused by hypomorphic mutations in NEMO, and an autosomal dominant form caused by mutations in IκBα.

Amorphic mutations in NEMO are lethal *in utero*. Several hypomorphic mutations in NEMO have been described in patients with X-linked ED-ID. There is some variability between patients, depending on the location of the mutation, but generally X-linked ED-ID patients have recurrent pyogenic infections; hypogammaglobulinemia with low IgG and variable IgM and IgA; specific antibody deficiency, particularly to polysaccharide antigens; decreased cytokine and type I interferon production; and a decreased response to CD40[17, 18]. Some X-linked ED-ID patients do not have ED, including one patient we followed, the first to be documented with decreased normal NEMO protein instead of a hypomorphic mutation[19]. This is the topic of Chapter 1.

A handful of patients with mutations in IκBα have also been reported[20-24]. Two of these patients carry the serine 32 to isoleucine (S32I) mutation, which abolishes the IKK phosphorylation site. Three other patients carry mutations that result in premature stop codons, resulting in alternatively translated N-terminally truncated IκBα that is missing the S32 and S36, the sites of IKK phosphorylation. All of these mutations affect only one of the two IκBα alleles and impair IκBα degradation. This results in sequestration of NFκB, attenuating but not abolishing

the NFκB signal. We reported the first patient with ED-ID and a truncating mutation of IκBα. The patient had a W11X mutation, that resulted in the degradation of only of 50% of IκBα and in the activation of only 50% of NFκB after stimulation with IL-1 compared to normal controls[22]. This is the topic of chapter 2.

The two patients with the S32I mutation had severe recurrent pyogenic infections, high IgM but low IgG and IgA levels in the serum, made no specific antibodies following immunization, and had an impaired T cell response to anti-CD3. They also had a profound deficiency in memory T cells[20, 21]. Both patients received bone marrow transplantation[25, 26]. Only one survived, but continues to have impaired immune function and requires intravenous gammaglobulin replacement and trimethoprim/ sulfamethoxazole prophylaxis against opportunistic infections[26]. The variable presentation of ED-ID patients is likely due to the heterogeneity of modifier genes within the NFκB pathway as well as the specific mutation within the pathway.

Phenotypes of NFkB knock-out mice

Mouse models have been created where various components of the NFκB signaling pathway have been deleted. NFκB p50 deficient mice have impaired innate and adaptive immune function including increased susceptibility to some pathogens and selective deficiencies in class switch recombination[27]. RelA/p65, IKKβ, and NEMO knock-outs are all embryonically lethal. IKKβ and RelA/p65 knock-out mice die from TNF-induced hepatocyte apoptosis that can be blocked

by crossing these mice to TNFR1 deficient mice[28]. However, these double knock-out mice have increased mortality due to increased susceptibility to microbial infections. IκBα knock-out mice die within 7 to 10 days of birth and have severe inflammatory dermatitis and granulocytosis[29].

A mouse model of ED-ID

The rarity of patients with ED-ID as well as logistical considerations make it difficult to investigate their immune function in detail. It is difficult to obtain samples from young children, and the therapy for treating immunodeficiency - intravenous immunoglobulin and bone marrow transplant - confound the baseline function of the patients' immune systems. While mice do differ from humans in some aspects of the immune system, they are useful models for human immune diseases. We have created an IκBα S32I knock-in mouse model of ED-ID in order to gain insights into the disease.

The IκBα S32I knock-in mutant mouse recapitulates many of the ectodermal and immune abnormalities found in patients with ED-ID caused by IκBα mutations, including poor responses to TLR stimulation and poor antibody responses due to an intrinsic defect in B cell function. In contrast to the ED-ID patients, these mice had no inherent T cell defect. However, they completely lacked lymph nodes (LN) and Peyer's patches (PP), follicular dendritic cells (FDCs) and germinal centers (GCs). Studies of bone marrow chimeras generated by reconstituting $Rag2^{-/-}$ mice with BM from the IκBα mutant strongly

suggest many of these abnormalities resulted from defective NFκB signaling in stromal cells. The IκBα S32I knock-in mouse is the topic of Chapter 3.

NFκB and lymphoid organ development

Both canonical and non-canonical NFκB signaling plays an important role in the development of secondary lymphoid tissues such as LN and PP[28, 30-32]. Interaction between $CD3^{-}CD4^{+}$IL-7Rα^{+} lymphoid-tissue inducer (LTi) cells and stromal organizer cells is crucial for the development of LN and PP. LTi cells express $LT\alpha_1\beta_2$, which engages LTβR on the stromal organizer cells[33] (see Figure I.3). LTβR signaling causes expression of the adhesion molecules VCAM1 and ICAM1 by activating the canonical NFκB pathway. It also induces the expression of the chemokines CXCL13, CCL21 and CCL19 by activating the non-canonical NFκB pathway[34, 35]. These chemokines and adhesion molecules attract and retain early LN-forming cells, and thus are key to LN formation and PP development[35, 36].

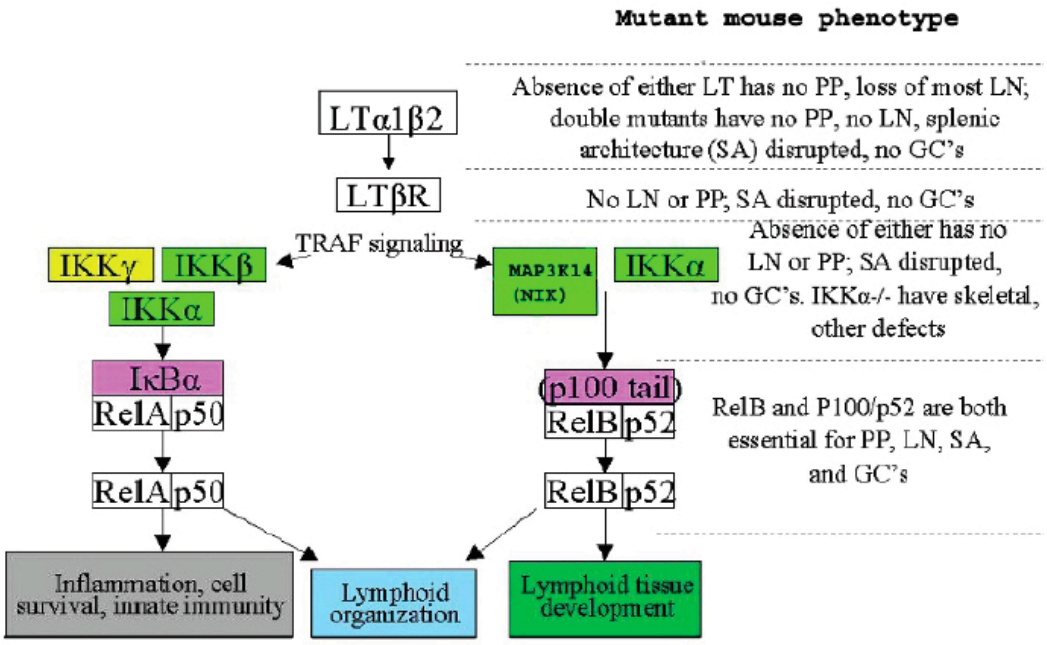

Figure I.3. Signaling through the lymphotoxin β receptor (LTβR). From Seymour et al, 2006[35].

Signaling by both LTβR and TNFR1, which exclusively uses the NFκB canonical pathway, is important for the development of follicular dendritic cells (FDCs) from stromal precursors in the spleen. FDCs are critical for the formation of B cell follicles[35]. Generation of FDCs requires expression of LTβR and TNFR1 on stromal cells and expression of TNFα and $LT\alpha_1\beta_2$ on lymphocytes[37-39]. TNF, TNFR1, LTα, LTβ, and LTβR deficient mice all lack FDCs and splenic follicles[35, 40]. LTα, LTβ, and LTβR deficient mice and p50, p100, RelA and RelB deficient mice also lack marginal zones (MZs)[10, 30, 40-42], since MAdCAM1 expression also depends on $LT\alpha_1\beta_2$ and TNF activity, and is essential for proper MZ formation[43, 44]. MZ B cells must require p50, since $p50^{-/-}$ $Rag2^{-/-}$ chimeras still did not develop MZ B cells. This lack may be due to dysfunctional B cell receptor signaling[45].

NFκB and the antibody response

Immunization results in the formation of germinal centers (GCs) within secondary B cell follicles that serve as sites of B cell proliferation, selection, maturation and death during antibody responses. Disruption of NFκB signaling inhibits GC function, as many NFκB protein knock-out mice lack GCs[10, 28]. FDCs are also essential for the formation of GCs, since FDCs attract B cells by secreting chemokines, and trap immune complexes for presentation to B cells, engaging their BCR and switching off apoptotic machinery[44, 46, 47]. Formation of germinal centers also requires intact CD40, LPS and BCR signaling, which depend on NFκB as well[4, 48-50]. All these ligands activate NFκB via the canonical pathway, with CD40 also activating the non-canonical pathway. Class switch recombination is also reported to require NFκB[27].

In summary, proper antigen responses rely on the presence of FDCs and the formation of an intact GC. Because IκBα S32I mutant mice lack LN and PP and cannot form GCs, it is likely that the same is true for IκBα deficient patients, at least those who carry the S32I mutation. If this is indeed the case, it is unlikely that hematopoietic stem cell transplant would cure their immunodeficiency as donor-derived normal B and T cells would not be able to function without a proper splenic architecture, PP and LN, which depend on intact NFκB signaling in the recipient stromal cells.

REFERENCES

1. Medzhitov R, Janeway C, Jr. Innate immunity. N Engl J Med 2000; 343:338-44.
2. Chaplin DD. 1. Overview of the human immune response. J Allergy Clin Immunol 2006; 117:S430-5.
3. Janeway CA, Jr., Travers P, Walport M, Shlomchik M. Immunobiology: The Immune System in Health and Disease. New York: Garland Publishing; 2001.
4. Pone EJ, Zan H, Zhang J, Al-Qahtani A, Xu Z, Casali P. Toll-like receptors and B-cell receptors synergize to induce immunoglobulin class-switch DNA recombination: relevance to microbial antibody responses. Crit Rev Immunol; 30:1-29.
5. Rajewsky K. Clonal selection and learning in the antibody system. Nature 1996; 381:751-8.
6. Delves PJ, Roitt IM. The immune system. First of two parts. N Engl J Med 2000; 343:37-49.
7. Cambier JC, Gauld SB, Merrell KT, Vilen BJ. B-cell anergy: from transgenic models to naturally occurring anergic B cells? Nat Rev Immunol 2007; 7:633-43.
8. Kracker S, Durandy A. Insights into the B cell specific process of immunoglobulin class switch recombination. Immunol Lett; 138:97-103.
9. Hayden MS, Ghosh S. NF-kappaB, the first quarter-century: remarkable progress and outstanding questions. Genes Dev; 26:203-34.

10. Bonizzi G, Karin M. The two NF-kappaB activation pathways and their role in innate and adaptive immunity. Trends Immunol 2004; 25:280-8.

11. Karin M, Ben-Neriah Y. Phosphorylation meets ubiquitination: the control of NF-[kappa]B activity. Annu Rev Immunol 2000; 18:621-63.

12. Chiao PJ, Miyamoto S, Verma IM. Autoregulation of I kappa B alpha activity. Proc Natl Acad Sci U S A 1994; 91:28-32.

13. Ito CY, Kazantsev AG, Baldwin AS, Jr. Three NF-kappa B sites in the I kappa B-alpha promoter are required for induction of gene expression by TNF alpha. Nucleic Acids Res 1994; 22:3787-92.

14. Shih VF, Tsui R, Caldwell A, Hoffmann A. A single NFkappaB system for both canonical and non-canonical signaling. Cell Res; 21:86-102.

15. Srivastava AK, Durmowicz MC, Hartung AJ, Hudson J, Ouzts LV, Donovan DM, et al. Ectodysplasin-A1 is sufficient to rescue both hair growth and sweat glands in Tabby mice. Hum Mol Genet 2001; 10:2973-81.

16. Zonana J, Elder ME, Schneider LC, Orlow SJ, Moss C, Golabi M, et al. A novel X-linked disorder of immune deficiency and hypohidrotic ectodermal dysplasia is allelic to incontinentia pigmenti and due to mutations in IKK-gamma (NEMO). Am J Hum Genet 2000; 67:1555-62.

17. Hanson EP, Monaco-Shawver L, Solt LA, Madge LA, Banerjee PP, May MJ, et al. Hypomorphic nuclear factor-kappaB essential modulator mutation database and reconstitution system identifies phenotypic and immunologic diversity. J Allergy Clin Immunol 2008; 122:1169-77 e16.

18. Puel A, Picard C, Ku CL, Smahi A, Casanova JL. Inherited disorders of NF-kappaB-mediated immunity in man. Curr Opin Immunol 2004; 16:34-41.

19. Mooster JL, Cancrini C, Simonetti A, Rossi P, Di Matteo G, Romiti ML, et al. Immune deficiency caused by impaired expression of nuclear factor-kappaB essential modifier (NEMO) because of a mutation in the 5' untranslated region of the NEMO gene. J Allergy Clin Immunol; 126:127-32 e7.

20. Courtois G, Smahi A, Reichenbach J, Doffinger R, Cancrini C, Bonnet M, et al. A hypermorphic IkappaBalpha mutation is associated with autosomal dominant anhidrotic ectodermal dysplasia and T cell immunodeficiency. J Clin Invest 2003; 112:1108-15.

21. Janssen R, van Wengen A, Hoeve MA, ten Dam M, van der Burg M, van Dongen J, et al. The same IkappaBalpha mutation in two related individuals leads to completely different clinical syndromes. J Exp Med 2004; 200:559-68.

22. McDonald DR, Mooster JL, Reddy M, Bawle E, Secord E, Geha RS. Heterozygous N-terminal deletion of IkappaBalpha results in functional nuclear factor kappaB haploinsufficiency, ectodermal dysplasia, and immune deficiency. J Allergy Clin Immunol 2007; 120:900-7.

23. Ohnishi H, Miyata R, Suzuki T, Nose T, Kubota K, Kato Z, et al. A rapid screening method to detect autosomal-dominant ectodermal dysplasia with immune deficiency syndrome. J Allergy Clin Immunol; 129:578-80.

24. Lopez-Granados E, Keenan JE, Kinney MC, Leo H, Jain N, Ma CA, et al. A novel mutation in NFKBIA/IKBA results in a degradation-resistant N-truncated

protein and is associated with ectodermal dysplasia with immunodeficiency. Hum Mutat 2008; 29:861-8.

25. Wu S, Walenkamp MJ, Lankester A, Bidlingmaier M, Wit JM, De Luca F. Growth hormone and insulin-like growth factor I insensitivity of fibroblasts isolated from a patient with an I{kappa}B{alpha} mutation. J Clin Endocrinol Metab; 95:1220-8.

26. Dupuis-Girod S, Cancrini C, Le Deist F, Palma P, Bodemer C, Puel A, et al. Successful allogeneic hemopoietic stem cell transplantation in a child who had anhidrotic ectodermal dysplasia with immunodeficiency. Pediatrics 2006; 118:e205-11.

27. Snapper CM, Zelazowski P, Rosas FR, Kehry MR, Tian M, Baltimore D, et al. B cells from p50/NF-kappa B knockout mice have selective defects in proliferation, differentiation, germ-line CH transcription, and Ig class switching. J Immunol 1996; 156:183-91.

28. Gerondakis S, Grumont R, Gugasyan R, Wong L, Isomura I, Ho W, et al. Unravelling the complexities of the NF-kappaB signalling pathway using mouse knockout and transgenic models. Oncogene 2006; 25:6781-99.

29. Beg AA, Sha WC, Bronson RT, Baltimore D. Constitutive NF-kappa B activation, enhanced granulopoiesis, and neonatal lethality in I kappa B alpha-deficient mice. Genes Dev 1995; 9:2736-46.

30. Koni PA, Sacca R, Lawton P, Browning JL, Ruddle NH, Flavell RA. Distinct roles in lymphoid organogenesis for lymphotoxins alpha and beta revealed in lymphotoxin beta-deficient mice. Immunity 1997; 6:491-500.

31. Rennert PD, James D, Mackay F, Browning JL, Hochman PS. Lymph node genesis is induced by signaling through the lymphotoxin beta receptor. Immunity 1998; 9:71-9.

32. Muller JR, Siebenlist U. Lymphotoxin beta receptor induces sequential activation of distinct NF-kappa B factors via separate signaling pathways. J Biol Chem 2003; 278:12006-12.

33. Benezech C, White A, Mader E, Serre K, Parnell S, Pfeffer K, et al. Ontogeny of stromal organizer cells during lymph node development. J Immunol; 184:4521-30.

34. Dejardin E, Droin NM, Delhase M, Haas E, Cao Y, Makris C, et al. The lymphotoxin-beta receptor induces different patterns of gene expression via two NF-kappaB pathways. Immunity 2002; 17:525-35.

35. Seymour R, Sundberg JP, Hogenesch H. Abnormal lymphoid organ development in immunodeficient mutant mice. Vet Pathol 2006; 43:401-23.

36. van de Pavert SA, Mebius RE. New insights into the development of lymphoid tissues. Nat Rev Immunol; 10:664-74.

37. Endres R, Alimzhanov MB, Plitz T, Futterer A, Kosco-Vilbois MH, Nedospasov SA, et al. Mature follicular dendritic cell networks depend on expression of lymphotoxin beta receptor by radioresistant stromal cells and of lymphotoxin beta and tumor necrosis factor by B cells. J Exp Med 1999; 189:159-68.

38. Matsumoto M, Fu YX, Molina H, Huang G, Kim J, Thomas DA, et al. Distinct roles of lymphotoxin alpha and the type I tumor necrosis factor (TNF)

receptor in the establishment of follicular dendritic cells from non-bone marrow-derived cells. J Exp Med 1997; 186:1997-2004.

39. Wang Y, Wang J, Sun Y, Wu Q, Fu YX. Complementary effects of TNF and lymphotoxin on the formation of germinal center and follicular dendritic cells. J Immunol 2001; 166:330-7.

40. Alimzhanov MB, Kuprash DV, Kosco-Vilbois MH, Luz A, Turetskaya RL, Tarakhovsky A, et al. Abnormal development of secondary lymphoid tissues in lymphotoxin beta-deficient mice. Proc Natl Acad Sci U S A 1997; 94:9302-7.

41. Franzoso G, Carlson L, Poljak L, Shores EW, Epstein S, Leonardi A, et al. Mice deficient in nuclear factor (NF)-kappa B/p52 present with defects in humoral responses, germinal center reactions, and splenic microarchitecture. J Exp Med 1998; 187:147-59.

42. Caamano JH, Rizzo CA, Durham SK, Barton DS, Raventos-Suarez C, Snapper CM, et al. Nuclear factor (NF)-kappa B2 (p100/p52) is required for normal splenic microarchitecture and B cell-mediated immune responses. J Exp Med 1998; 187:185-96.

43. Ettinger R, Mebius R, Browning JL, Michie SA, van Tuijl S, Kraal G, et al. Effects of tumor necrosis factor and lymphotoxin on peripheral lymphoid tissue development. Int Immunol 1998; 10:727-41.

44. Zindl CL, Kim TH, Zeng M, Archambault AS, Grayson MH, Choi K, et al. The lymphotoxin LTalpha(1)beta(2) controls postnatal and adult spleen marginal sinus vascular structure and function. Immunity 2009; 30:408-20.

45. Cariappa A, Liou HC, Horwitz BH, Pillai S. Nuclear factor kappa B is required for the development of marginal zone B lymphocytes. J Exp Med 2000; 192:1175-82.

46. Vinuesa CG, Linterman MA, Goodnow CC, Randall KL. T cells and follicular dendritic cells in germinal center B-cell formation and selection. Immunol Rev; 237:72-89.

47. Allen CD, Cyster JG. Follicular dendritic cell networks of primary follicles and germinal centers: phenotype and function. Semin Immunol 2008; 20:14-25.

48. Foy TM, Laman JD, Ledbetter JA, Aruffo A, Claassen E, Noelle RJ. gp39-CD40 interactions are essential for germinal center formation and the development of B cell memory. J Exp Med 1994; 180:157-63.

49. Hsing Y, Hostager BS, Bishop GA. Characterization of CD40 signaling determinants regulating nuclear factor-kappa B activation in B lymphocytes. J Immunol 1997; 159:4898-906.

50. Goetz CA, Baldwin AS. NF-kappaB pathways in the immune system: control of the germinal center reaction. Immunol Res 2008; 41:233-47.

Chapter 1:

Immune deficiency caused by impaired expression of NEMO due to a mutation in the 5' untranslated region of the *NEMO* gene

A version of this chapter was published by in the *Journal of Allergy and Clinical Immunology,* Volume 126, 2010 and has been reproduced with permission.

Note of Clarification:

I performed all of the experiments in this chapter, under the supervision of Dr. Douglas McDonald.

Immune deficiency caused by impaired expression of NEMO due to a mutation in the 5' untranslated region of the NEMO gene

Jana L. Mooster[1], Caterina Cancrini, MD, PhD[2,3], Alessandra Simonetti, MD[2,3], Paolo Rossi, MD, PhD[2,3], Gigliola Di Matteo, PhD[2,3], Maria Luisa Romiti, PhD[2,3], Silvia Di Cesare[2,3], Luigi Notarangelo, MD[1], Raif S. Geha, MD[1]*, Douglas R. McDonald, MD, PhD[1]*

[1]Division of Immunology, Children's Hospital, Boston

[2]Department of Pediatrics, Children's Hospital Bambino Gesù, Rome, Italy

[3]University of Rome Tor Vergata School of Medicine, Rome, Italy

ABSTRACT

Background: Nuclear factor κB (NFκB) is a key transcription factor that regulates both innate and adaptive immunity, as well as ectodermal development. Mutations in the coding region of the IκB kinase γ (IKKγ)/NFκB essential modifier (NEMO) gene cause X-linked ectodermal dysplasia with immunodeficiency.

Objective: To determine the genetic cause of recurrent sinopulmonary infections and dysgammaglobulinemia in a patient with a normal NEMO coding sequence and his affected brother.

Methods: TNFα and IFNα production in response to Toll-like Receptor (TLR) stimulation was analyzed by ELISA, NEMO mRNA levels were measured by qPCR, and NEMO protein expression was measured by Western blotting. NFκB activation was assessed by nuclear translocation of p65 and luciferase reporter gene assays.

Results: TLR-induced TNFα and IFNα production by peripheral blood mononuclear cells was impaired in the patient and his brother. Sequencing of the patient's NEMO gene revealed a novel mutation in the 5' untranslated region, which was also present in the brother, resulting in abnormally spliced transcripts and a 4-fold reduction in mRNA levels. NEMO protein levels in EBV transformed B cells and fibroblasts from the index patient were 8-fold lower than normal controls. NFκB p65 nuclear translocation in the patient's EBV B cells following TLR7 ligation was defective. NFκB dependent luciferase gene expression in IL-1 stimulated fibroblasts from the patient was impaired.

Conclusion: This is the first description of immune deficiency resulting from low expression of a normal NEMO protein.

Clinical Implications: Immune deficiency can result from low expression of a normal NEMO protein. If the index of suspicion is high for defective NFκB function in an immune deficient patient with normal NEMO coding sequence, NEMO mRNA and protein levels must be analyzed and sequencing of the 5' and 3' regions of the NEMO gene should be performed.

Capsule Summary: Two brothers with recurrent sinopulmonary infections were found to have severely reduced levels of NEMO mRNA and protein due to a mutation in the 5' untranslated region of the NEMO gene.

Key Words: NEMO, immune deficiency, recurrent infections, 5' untranslated region mutation

Abbreviations:

EBV: Epstein-Barr virus

ED-ID: Ectodermal dysplasia associated with immune deficiency

ELISA: Enzyme-linked immunosorbent assay

IκBα: Inhibitor of NFκB α

IVIG: Intravenous immunoglobulin

p38 MAPK: p38 mitogen activated protein kinase

NEMO: NFκB essential modifier, also IκB kinase γ (IKKγ)

PBMC: Peripheral blood mononuclear cell

UTR: Untranslated region

INTRODUCTION

The transcription factor Nuclear Factor κB (NFκB) is required for normal development and function of the immune system. Proper functioning of the immune system requires a tightly regulated inflammatory response, which is dependent upon activation of NFκB[1, 2]. In the resting state, NFκB proteins are retained in the cytoplasm by the inhibitor of NFκB (IκB) proteins, which include IκBα. Activation of numerous cell receptors, including pro-inflammatory cytokines (IL-1, TNFα), CD40, and Toll-like receptors, cause activation of the IκB kinase complex (IKK), which leads to phosphorylation of IκB proteins. Phosphorylated IκB proteins are subsequently ubiquitinated and degraded, allowing nuclear translocation of NFκB and activation of gene transcription[3, 4].

Proper function of the IKK complex is dependent upon IκB kinase γ/NFκB essential modifier (IKKγ/NEMO), which is encoded by a gene (*IKBKG*) located on the X chromosome. NEMO functions as a scaffolding protein and links upstream signaling pathways to activation of the IKK complex[3]. Numerous mutations in *NEMO* that result in the production of a dysfunctional NEMO protein have been described in male patients with the syndrome of ectodermal dysplasia associated with immune deficiency (ED-ID). ED-ID arises because normal ectodermal development (hair, teeth, and sweat glands), as well as effective innate and adaptive immune responses, require NEMO-dependent NFκB activation downstream of both the ectodysplasin A receptor (EDAR) and several receptors of the immune system[1, 2, 5]. Mutations in *NEMO* that result in ED-ID are termed hypomorphic because they result in reduced, but not absent, function of NEMO.

Absence of NEMO function (amorphic mutations) in males is lethal *in utero*, whereas heterozygosity for null NEMO mutations results in incontinentia pigmenti in females[6, 7].

Impaired NFκB activation is detrimental to both innate and adaptive immune function. TLRs, nucleotide-binding oligomerization domain (NOD)-like receptors (NLRs), and retinoic acid inducible gene I (RIG-I)-like helicases (RLHs) are pathogen recognition receptors that signal through NFκB to indicate detection of invading pathogens, including bacteria, mycobacteria, fungi, and viruses[2, 8]. Therefore, defects in NFκB activation can result in impaired inflammatory responses to invading pathogens, resulting in decreased production of pro-inflammatory cytokines and type 1 interferons[1,2]. Because T and B cell receptors also signal through NFκB, impaired NFκB function can result in defective antigen-specific immunity[3]. As a result, patients with ED-ID can be susceptible to a wide variety of bacterial, mycobacterial, viral, and fungal infections. Immunologic evaluation of these patients commonly reveals hypogammaglobulinemia with variably increased IgM and IgA levels, variable defects in specific antibody responses to protein and polysaccharide antigens, and variably impaired T cell proliferation to antigens[6, 7, 9, 10]. Some immunodeficient patients with mutations in the NEMO gene have normal ectodermal development, suggesting a less stringent requirement for NEMO dependent NFκB activation for normal ectodermal development[10-13].

In this report, we describe an 11-year-old boy with immune deficiency but not ectodermal dysplasia, and a normal NEMO coding sequence but low levels of NEMO mRNA and protein. Sequencing of the 5' untranslated region of the patient's *NEMO* gene revealed a G to T mutation at position +1 of the donor splice site of the

untranslated exon 1B. This results in destruction of the normal exon 1B to exon 2 splice site, generation of two abnormally-sized NEMO mRNA species with intact coding sequences, reduced levels of NEMO mRNA overall, and production of 8-fold less NEMO protein relative to normal controls. A brother of the patient with similar clinical manifestations and low NEMO expression also had an identical mutation in the 5'-untranslated region of the NEMO gene.

METHODS

Reagents

Toll-like receptor ligands used in this study were as previously described[14]. Antiphospho-NFκB inhibitor α (IκBα) and antiphospho-p38 mitogen-activated protein kinase (MAPK) were from Cell Signaling (Danvers, MA), anti-IκBα and anti-NEMO/IKKγ were from Santa Cruz Biotechnology (Santa Cruz, CA). Recombinant human IL-1β and the ELISA kits for human TNFα and human IFNα were obtained from Biosource (Camarillo, CA).

Cell isolation, and stimulation

Informed consent for blood and dermal biopsy samples was obtained from the patient and healthy control subjects in accord with the institutional review board at Children's Hospital, Boston. Peripheral blood mononuclear cells (PBMCs) were isolated by centrifugation through Ficoll-Paque PLUS (Amersham Biosciences, Uppsala, Sweden). PBMCs were cultured in RPMI plus 10% FCS, with L-glutamine and penicillin/streptomycin (Invitrogen, Carlsbad, CA). Cell stimulations (4×10^5 PBMCs/condition) were performed in 96-well plates in a volume of 200 μL medium with the following concentrations of TLR ligands: PAM3CSK4 (0.1 μg/mL), Poly I:C (50 μg/mL), LPS (0.1 μg/mL), Flagellin (1 μg/mL), 3M-002 and 3M-013 (20 μM), and CpG ODN2216 (5 μM). PBMCs were also stimulated with PMA (7.5 ng/mL) plus ionomycin (7.5 ng/mL), and IFNβ (1×10^5 U/mL) as positive controls. TNFα and IFNα were measured after 24 hours stimulation by ELISA.

Western blotting

Fibroblasts, EBV transformed B cells or PBMCs from patients and controls were lysed in sample buffer (62.5 mM TRIS, pH 6.8, 2% SDS, 10% glycerol, 2% b-mercaptoethanol, 0.01% bromophenol blue). Fibroblasts (40,000/condition) or PBMCs (5×10^5/condition) were stimulated with IL-1β (10 ng/ml) for the indicated times before lysis. Nuclear and cytoplasmic fractions were isolated using a kit from Active Motif (Carlsbad, CA). Proteins were resolved by 10% SDS-PAGE (Bio-rad, Hercules, CA) and transferred to nitrocellulose membranes (Invitrogen, Carlsbad, CA). Western blotting was performed according to the manufacturer's recommendations.

NEMO sequencing and expression analysis

Sequencing of genomic DNA was performed at the Children's Hospital Core facility. PCR primers and sequencing primers are available in the Supplemental Materials and Methods. The PCR products were cloned into the pCR2.1-TOPO vector (Invitrogen, Carlsbad, CA) for ease in sequencing. RNA was isolated from fibroblast lines or EBV lines and reverse transcribed using iScript (Bio-rad, Hercules, CA). NEMO cDNA using exons 1A, 1B and 1C were amplified and cloned from cDNA isolated from normal fibroblasts (Supplemental Materials and Methods). The misspliced 1B isoforms were amplified from cDNA isolated from patient fibroblasts. The PCR products were also cloned into the pCMV-Tag4a vector (Invitrogen, Carlsbad, CA) for expression studies. TaqMan gene expression assays were performed using human NEMO (Hs99999905_m1) and GAPDH (Hs00175318_m1) probes from Applied Biosystems (Roche, Branchburg, NJ).

NFκB reporter assays

NFκB-luciferase reporter plasmids containing four NFκB binding sites in the promoter, and Renilla control plasmids were both kindly provided by Dr. Laurie Glimcher, Harvard Medical School, Boston, MA. The plasmids were transfected into patient and normal fibroblasts using Lipofectamine LTX with Plus reagent (Invitrogen, Carlsbad, CA). After 24 hours, the cells were stimulated for 6 hours with 10-15 ng/ml recombinant IL-1β. The cells were lysed in passive lysis buffer and luciferase activity was analyzed using the Dual Luciferase Reporter Assay System (Promega, Madison, WI).

SUPPLEMENTAL MATERIALS AND METHODS

Primer pairs used to amplify NEMO coding region cDNA for sequencing, including the 3' UTR:

Forward	Reverse
TCACCAAACTTGACTGCGCTCT	CCAGAGCCTGGCATTCCTTAG
AGGACAAGGCCTCTGTGAAA	GACAGCTGGCCTTCAGTTTGC
GCCGAGCAGCACAAGATT	GGAGAGGAAAGCGCAGACT

Primer pairs used for 5' upstream genomic PCR for sequencing:

Forward	Reverse
AACGGATACTACTCAGCAACACTG	CTGGAAGGGGGCAGTAAGTAC
CCAGAAATGTTCTGAGGAAAGG	CGTGTAATTTGAGATGAAGCCCTT
CGCACGATGTGGAAGAACTAACTA	AGACAACATCTGCCTATCGTCA
TTTCTACTCCTCCCTCCTCCTC	GAAGAGCCAACTGTGTGAGATGG

Sequencing primers for 5' upstream genomic sequencing:

GGAGTCTCACTCTGTCGGCC
GCCAGGCAGTTAGGAAGC
CACAAGGTGACTTAGTAGA
CTAGGTCATGCTGAGCTTGT
TCAGAGTCCTGGCTGTTAAG
CTCTTCTGAGGGGACCAG
GGTGGCTCATGCCTGTCA
CCTGGAGCATGGGAGATG
CCCACAGCTATGACACCG
CATTCACAGCTACCAACTTC
GTGGATTTGCCTGTTGTAGA
CGTGTCACCACACTCTGC
TTCCAGCCTGGAGCTAGG

CATGGTGAGACCCCGTTTC
GACTGGTCTGCTGAGTCAC
CCATCATTGGGATGCGTCC
CGAGGCTCTTCAGAGAGAGG
AGTGCTGGGATTACAGACGT
AGTCTCACTGCCCCATGG
CCCATGATGATGAATATGTG
TGCTCTGCATCCCCAATT
ATCGTTCTAGCAGTGGTGG
CTCACCGCAACCTCCATC
ATGGATTCGCCATCAGCT
GGAGACTAGAAGTCCAAAACC

Primers for cDNA transcript PCR (adds BamHI site in forward primers and HindIII site on reverse):
Exon 1A Forward: 5' ATGGATCCCATGGCCCTTGTGATCCAG 3'
Exon 1B Forward: 5' ATGGATCCGACACCGGAAGCCGGAAG 3'
Exon 1C Forward: 5' ATGGATCCAGCCCGTTCCTGCTCCG 3'
Exon 10 Reverse: 5' ATAAGCTTCTCAATGCACTCCATGACATGTATC 3'

RESULTS

Case Report

The index patient is an 11-year-old boy who was healthy until three years of age when he began experiencing recurrent upper and lower respiratory infections (otitis requiring placement of tympanostomy tubes, lymphadenitis, bronchitis/bronchopneumonia), recurrent diarrhea and hematuria. Causative pathogens for the diarrhea and hematuria were not identified and these conditions have resolved. A chest CT scan revealed bronchiectasis. There was no hepatosplenomegaly. The patient has no features of ectodermal dysplasia (Fig. 1.1). His immune evaluation at 4 years of age revealed normal total white blood count, lymphocyte count and normal T and B cell subsets, but a low percentage of $CD27^{+}IgD^{-}IgM^{-}$ switched memory B cells (Table 1.1). The patient had an elevated IgA level (901 mg/dl) with normal IgG (653 mg/dl) and low IgM (31mg/dl). IgM levels have remained low (Table 1.2). Specific antibodies against tetanus toxoid, rubella, and pneumococccal polysaccharide antigens were detected, but the patient had rapidly waning antibody titers to tetanus and pneumococcus over time. There was no specific antibody response to hepatitis B virus, measles or mumps immunization (Table 1.3). He had normal *in vitro* T cell proliferation responses to phytohemagglutinin (PHA), pokeweed mitogen (PWM), and anti-CD3, but decreased responses to tetanus toxoid antigen (Table 1.4). The patient was started on intravenous immunoglobulin (IVIG) therapy at the age of 10 years. He is currently healthy, with improved and stable pulmonary status and no active gastrointestinal complaints. The patient's younger brother, age 5, also suffered from recurrent

Figure 1.1 Normal ectodermal development in the patient. The index patient at 11 years of age. Notice normal dentition and hairline.

Table 1.1. Lymphocyte counts of the index patient

Cell counts per mm^3	11/2001	Normal range
Absolute lymphocyte count	5140	1700-6900
CD3	3084	900-4500
CD4	596	500-2400
CD8	709	300-1600
CD16/CD56	1182	100-1000
CD19	668	200-2100
$CD27^+IgD^+IgM^+$ (non-switched memory)	29 (4.4% of $CD19^+$)	30-98 (7-14%)
$CD27^+IgD^-IgM^-$ (switched memory)	10 (1.5% of $CD19^+$)	22-76 (5-12.3%)
$CD27^-IgD^+IgM^+$ (naive)	625 (93.6% of $CD19^+$)	260-716 (70.7-85%)

These measurements were taken when the patient was first seen at 4 years of age. Similar numbers have been obtained on subsequent evaluations.

Reference range values (10^{th}-90^{th} percentile) for B cell subsets:
Huck K, Feyen O, Ghosh S, Beltz K, Bellert S, Niehues T. Memory B-cells in healthy and antibody-deficient children. Clin Immunol. 2009; 131:50-9.

Table 1.2. Serum Immunoglobulin levels from the index patient

Serum Immunoglobulins (mg/dL)	11/2001	Normal range
IgG	653	441-1135
IgG1	369	360-810
IgG2	248	60-310
IgG3	38	9-160
IgG4	8	9-160
IgA	901	22-159
IgM	31	47-200

This table shows immunoglobulin levels measured when the patient was first seen at age 4, before intravenous immunoglobulin therapy was initiated.

Table 1.3. Antibody response to immunization

Serum Titers	6/2003	5/2004	1/2005	9/2006	6/2008
Tetanus (IU/mL)	0.2	-	-	0.09	0.1
Measles (IU/mL)	-	absent	-	absent	absent
Mumps (AU/mL)		absent		absent	absent
Pneumococcus (mg/L)	40		150	90	30
Hepatitis B Virus sAb (mIU/mL)	-	absent	-	absent	absent

The patient received MMR vaccinations 8/1999 and 9/2005, Tetanus 7/1998, 9/1998, 3/1999, 8/1999, 6/2003, and 12/2005, Pneumococcus (Pneumovax) 6/2003 and 12/2005, Hepatitis B Virus 7/1998, 9/1998, 3/1999 and 3/2007. Protective titers after immunization with tetanus toxoid and pneumococcus are >0.1 IU/mL and >60 mg/L, respectively.

Table 1.4. Proliferation of PBMCs, ^{3}H counts per minute

Stimulus	Patient	Healthy Control
Medium, day 3	455	316
PHA	33376	34506
PWM	25564	36794
Anti-CD3 (OKT3)	25267	34111
Medium, day 6	282	187
Tetanus	2165	9601

Measured 5/2006, blood sample was taken before IVIG infusion. Cells were examined for proliferation to PHA, PWM and anti-CD3 after 3 days of culture, and to tetanus after 6 days of culture.

respiratory infections, and had no features of ectodermal dysplasia. His immunologic analysis revealed normal lymphocyte counts, normal T cell subset distribution, decreased percentage of $CD27^{+}IgD^{-}IgM^{-}$ switched memory B cells (3.8% of $CD19^{+}$ cells, normal 10^{th} to 90^{th} percentile range 5-12.3%), an IgG of 653 mg/dL (normal range 441-1135 mg/dL), an IgA of 65 mg/dL (normal range 22-159 mg/dL), a borderline IgM of 47 mg/dL (normal range 47-200 mg/dL), and failure to respond to immunization with pneumococcus vaccine (pre-immunization titer 3 mg/L, post immunization titer 3 mg/L, normal response >60 mg/L).

Family history is also significant for an older male maternal cousin of the patient who presented with recurrent upper respiratory infections (pharyngitis, tonsillitis) and hypogammaglobulinemia from early childhood. He did not have ectodermal dysplasia and was diagnosed with common variable immune deficiency. In his late teens he was diagnosed with widespread *Mycobacterium avium intracellulare* infection, and had multiple pneumonias, chronic diarrhea, and malnutrition. He died of infection at the age of 19 years.

Impaired cytokine production in response to TLR ligands

The index patient's history of recurrent infections, low IgM, elevated IgA, and a family history of a maternal cousin with recurrent infections, including infection with a poorly virulent mycobacterium, was consistent with impaired NFκB activation due to a defect in NEMO. To test NFκB function, we measured cytokine production by peripheral blood mononuclear cells (PBMCs) in response to TLR ligands. Stimulation of the index patient's PBMCs with PAM3CSK4 (TLR1,2), polyI:C (TLR3), LPS (TLR4),

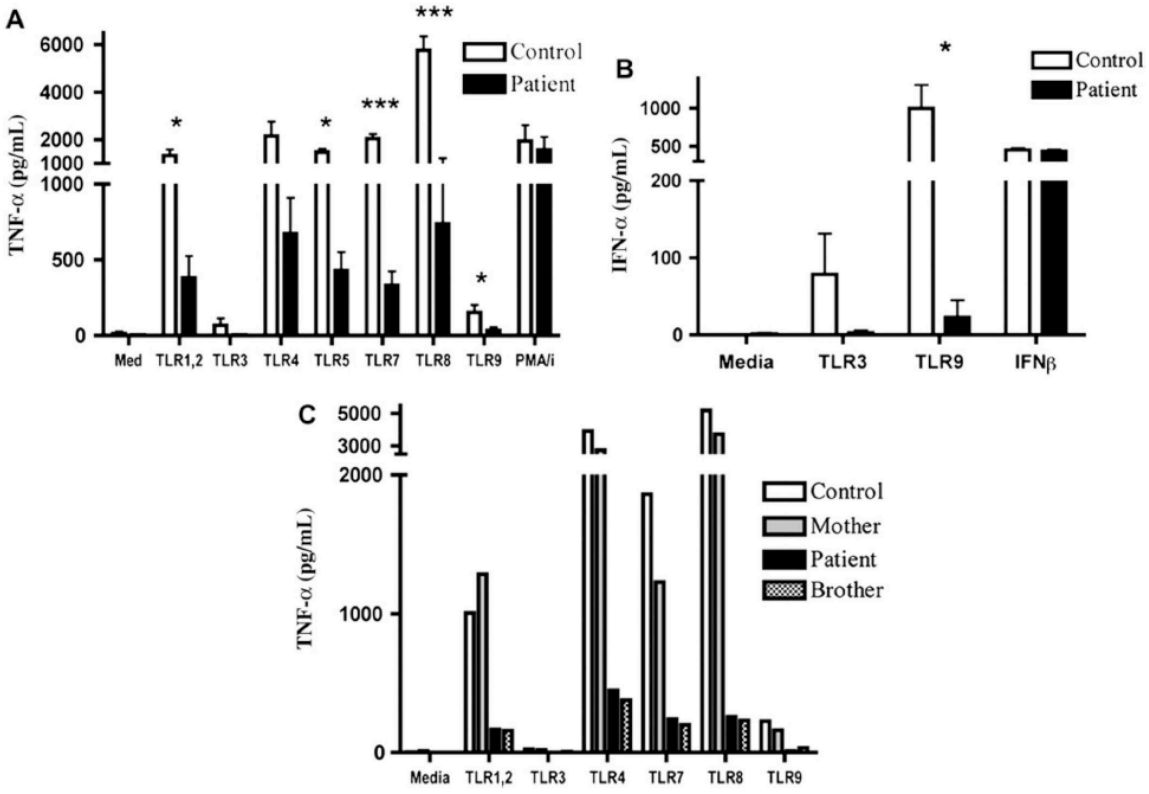

Figure 1.2. Impaired TLR-induced NFκB–dependent cytokine production by patient PBMCs. PBMCs were incubated with medium or TLR ligands for 24 hours and (**A)** TNFα and **(B)** IFNα were quantified. Graphs show the mean and SD of 4 independent experiments using PBMCs from the index patient and healthy controls (n=4). *p<0.05, ***p<0.001. **(C)** TNFα production in PBMCs from the patient's affected brother.

flagellin (TLR5), 3M-013 (TLR7), 3M-002 (TLR8), and ODN2216 (TLR9) revealed significant impairment of TNFα production compared to the mean of 4 normal healthy controls (Fig. 1.2A). Stimulation of the index patient's PBMCs with TLR3 and 9 ligands also revealed significant impairment of IFNα production compared to the mean of 4 normal healthy controls (Fig. 1.2B). TLR-induced TNFα production by the patient's affected younger brother was similarly impaired (Fig. 1.2C). In contrast, TLR-induced cytokine production in PBMCS from the patient's mother was normal (Fig. 1.2C). Studies on the mother and brother of the index patient were performed only once due to limited availability of blood from them. Technical reasons precluded measurement of IFNα production in response to TLR stimulation of their PBMCs.

Levels of NEMO protein and mRNA are significantly decreased in the patient

Impaired TLR functions in the patient and his brother are consistent with a defect in IKKγ/NEMO. A Western blot of lysates of PBMCs from the patient and his brother showed severely reduced NEMO protein levels compared to a normal control (Fig. 1.3A). In contrast, the NEMO protein level in the mother's PBMCs was comparable to that of the normal control. Decreased NEMO protein levels in the patient were confirmed by comparing NEMO levels in lysates from EBV transformed B cells from the patient and five healthy controls (Fig. 1.3B). Scanning densitometry revealed an 8-fold decrease in relative NEMO protein levels (normalized to actin) compared to the mean of five normal controls (Fig. 1.3C).

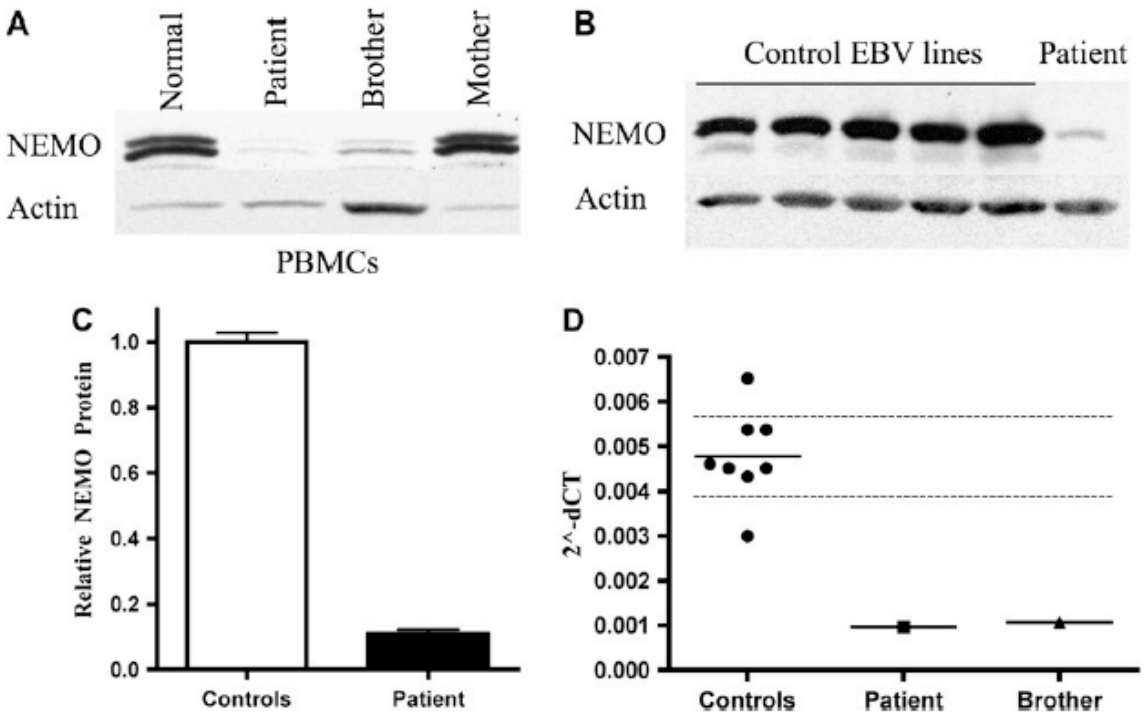

Figure 1.3. Decreased NEMO protein and mRNA levels in the patient. Western blots from **(A)** PBMC lysates from control, index patient, affected brother, and unaffected mother, **(B)** EBV B cell lysates. **(C)** Scanning densitometry of NEMO protein levels for each EBV B cell line, normalized to actin. Controls arbitrarily set to 1. **(D)** qPCR analysis of NEMO mRNA levels, normalized to GAPDH, in EBV B cell lines from index patient, brother, and 8 controls. Bar represents the mean, dashed lines span the 95% confidence interval.

This decrease was confirmed in fibroblasts from the index patient, which exhibited an 8-fold decrease in NEMO protein levels compared to the mean of fibroblasts from 4 normal controls (data not shown).

Given the reduced NEMO protein levels in the patient and his brother, cDNA was generated from patient fibroblasts and sequenced. No mutations were found within the coding region. NEMO mRNA levels were then quantified by qPCR in EBV B cells from the patient, his brother, and 8 normal controls. GAPDH mRNA levels were used as an internal control. The patient's and his brother's EBV transformed B cell lines had 4-5 fold lower NEMO mRNA levels than EBV B cell lines from healthy controls (Fig. 1.3D).

Sequencing reveals a splice site mutation in the 5' untranslated region of the patient's NEMO gene

Since NEMO mRNA levels were significantly decreased in the patient, the 5' and 3' untranslated (UTR) regions of his NEMO gene were analyzed. No mutations were detected in the 3'UTR, or in the polyA tail signal region. The four first exons (1A-D) of the NEMO gene are alternatively spliced to the ATG-containing second exon, resulting in mRNAs that are translated into an identical protein product (Fig. 1.4A). Lymphocytes express NEMO transcripts containing exons 1A, 1B and 1C, but not 1D, spliced to exon 2. Exon 1B transcripts are much more abundant than transcripts starting at exon 1A or exon 1C[15]. We found a similar pattern in normal fibroblasts (data not shown). We sequenced an approximately 20 Kb region of genomic DNA upstream of the NEMO translation initiation site, including exons 1A, 1B, 1C and 1D. Two previously described polymorphisms were found in the intron between exon 1A and 1B (-4875 bp and -4858 bp from the translation initiation site). A novel G to T mutation was found 4257 bp

upstream of the translation initiation site, at position +1 of the donor splice-site of exon 1B (Fig. 1.4A). This mutation destroys the normal exon 1B to exon 2 splice site. The mutation was present in the patient's affected younger brother. The patient's mother and maternal aunt were confirmed to be carriers.

The splice site mutation results in two alternatively spliced mRNA products in the patient

The splice site mutation in the patient and his brother would be expected to result in aberrant splicing. To test this hypothesis, we amplified the three potential PCR products arising from the splicing of exons 1A, 1B and 1C to exon 2. Oligonucleotides corresponding to the extreme 18 bp at the 5' end of each of exons 1A, 1B and 1C were used as forward primers. The common reverse primer corresponded to the last 25 bp before the stop codon in exon 10 (Fig. 1.4A). Transcripts from exon 1D are liver-specific[15] and were not analyzed. PCR products were amplified from cDNA isolated from EBV B cell lines from the patient and a healthy control. When the exon 1A and 1C specific primers were used, both patient and control template cDNA produced the normally sized transcripts (Fig. 1.4B). When the exon 1B specific primer was used, a normally sized exon 1B-containing transcript of 1404 bp was amplified from the control cDNA. However, the patient cDNA instead gave rise to two aberrantly spliced transcripts 1748 bp and 1294 bp in size respectively (Fig. 1.4B). The larger 1748 bp transcript starts at exon 1B, reads through the 1B-1C intron and exon 1C, then splices to exon 2. The smaller 1294 bp transcript uses an alternative splice site within exon 1B that splices to exon 2, resulting in an mRNA product with an internal deletion (Fig. 1.4C). Similar results were obtained using cDNA from fibroblasts (data not shown).

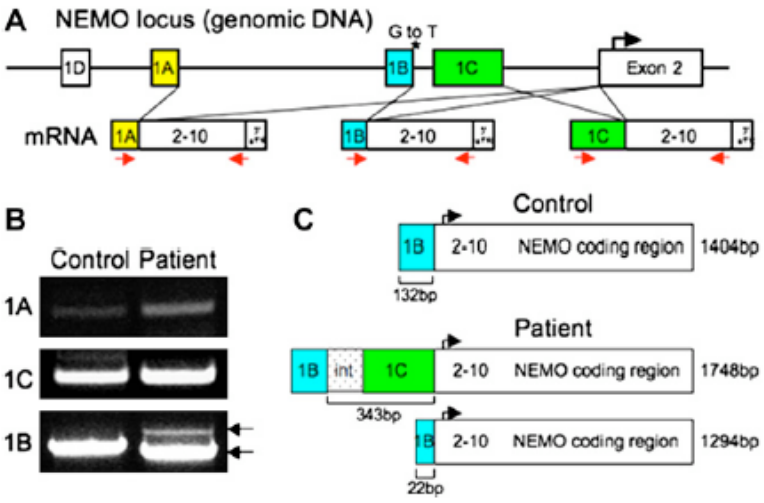

Figure 1.4. The patients' NEMO mutation results in two aberrant mRNA products. **(A)** Representation of normal NEMO splicing. Patient's mutation shown as asterisk. mRNA splicing using exon 1A, 1B or 1C is depicted, arrows represent PCR primers used. **(B)** Agarose gel showing control and patient NEMO RT-PCR products containing exons 1A, 1C and 1B. **(C)** Schematic of aberrant NEMO exon 1B transcripts in the patient.

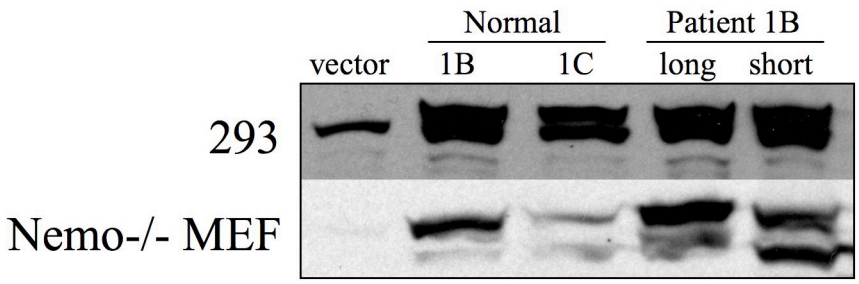

Figure 1.5 Western blot showing expression of NEMO cDNA isoforms amplified from normal and patient cells. NEMO cDNA using exons 1B and 1C were amplified from cDNA isolated from normal fibroblasts and the misspliced 1B isoforms were amplified from cDNA isolated from patient fibroblasts. The PCR products were cloned into the pCMV-Tag4a vector and expressed in T293 HEK cells (top) or in Nemo$^{-/-}$ mouse embryonic fibroblasts (bottom). Note the presence of the endogenous NEMO band in T293 cells but not in NEMO deficient MEFs.

Introduction in 293 T cells and NEMO$^{-/-}$ mouse embryonic fibroblasts of constructs that encoded cDNA corresponding to the 1748 bp and 1294 bp transcripts under the control of the pCMV promoter resulted in the expression of normal sized NEMO protein Fig. 1.5), demonstrating that these transcripts were potentially translated in the patient's cells.

Impaired phosphorylation and degradation of IκBα in response to IL-1 and reduced NFκB activation in patient cells

To assess the level of impairment of NFκB signaling, primary fibroblasts from the patient were treated with IL-1β and IκBα phosphorylation and degradation were analyzed by Western blot (Fig. 1.6A). In normal fibroblasts, the majority of IκBα protein was phosphorylated after 5 minutes of IL-1β stimulation and IκBα protein was completely degraded by 15 minutes. In contrast, in the patient's fibroblasts, only about half of the IκBα was phosphorylated after 5 minutes of IL-1β stimulation and there was still residual IκBα protein detected 15 and 30 minutes after stimulation. Western blotting with anti-phospho-p38 MAPK demonstrates a comparable response of normal and patient fibroblasts to IL-1β stimulation.

Incomplete IκBα degradation in response to receptor stimulation would lead to reduced NFκB nuclear translocation. To assess NFκB nuclear translocation, patient and control EBV B cell lines were stimulated with the TLR7 ligand 3M-013, and nuclear extracts were prepared 30, 60 and 90 minutes after stimulation and Western blotted with an anti-p65 antibody. Western blot with anti-PARP was used as a protein loading control for nuclear extracts. The results demonstrated reduced p65 nuclear

translocation in the patient EBV cells in response to stimulation with TLR7 ligand (Fig. 1.6B).

In order to measure NFκB activity, NFκB luciferase assays were performed on normal and patient fibroblasts. Fibroblasts were transfected with NFκB luciferase reporter plasmids and control Renilla plasmids. Cells were lysed following a 6-hour stimulation with IL-1β. Patient fibroblasts had 2.4 times less NFκB activity following IL-1β stimulation compared to control fibroblasts, $p = 0.0126$ (Fig. 1.6C).

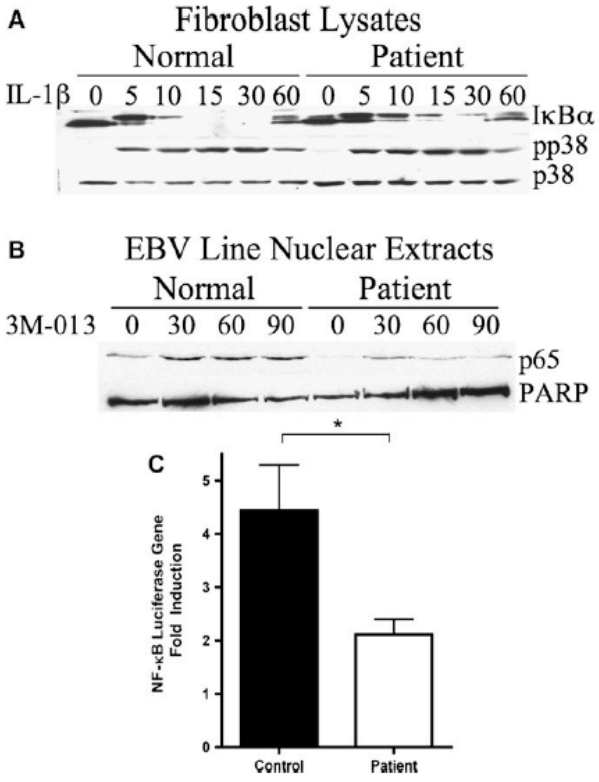

Figure 1.6. NFκB signaling is reduced in the patient. **(A)** WB of lysates from fibroblasts stimulated with IL-1β. **(B)** Western blot of p65 nuclear translocation in TLR7 stimulated EBV B cells. **(C)** NFκB-luciferase reporter assay in fibroblasts treated 6 hours with IL-1β. Fold activation represents mean and SD of 8 experiments using patient fibroblasts and three healthy controls.

DISCUSSION

We present a male patient with immunodeficiency without ectodermal dysplasia associated with a novel splice site mutation in the 5'UTR of the NEMO transcript. This mutation results in abnormally spliced NEMO mRNA species, a 4-fold decreased level of NEMO mRNA levels and an 8-fold lower expression level of NEMO protein than in normal controls. To our knowledge, this is the first description of an immunodeficiency due to inadequate levels of a normal NEMO protein, as opposed to a mutation that results in an altered protein with hypomorphic function.

The low NEMO protein levels in the patient lead to reduced IκBα phosphorylation and degradation, resulting in decreased NFκB function after IL-1 stimulation. Although the reduced NEMO expression and reduced NFκB activation allowed normal ectodermal development, they resulted in impaired innate and adaptive immune functions, including low IgM and high IgA, typical of patients with hypomorphic NEMO mutations[10, 16]. Antibody production to protein and polysaccharide antigens was variably impaired. Importantly, specific antibody titers waned rapidly over time. B and T cell total numbers were normal, although the absolute number of memory B cells was low. The patient's younger brother is also affected and has the same NEMO mutation. Additionally, a male cousin of the patient had recurrent infections and died from atypical mycobacterial pneumonia. Although his NEMO gene was never sequenced, his mother (the patient's maternal aunt) is a carrier of the mutation in the 5'UTR of NEMO. Thus, most likely he had the same mutation as the index patient and suffered from NEMO deficiency.

The mutation in the 5'UTR of NEMO that we have described is unique because it results in the generation of abnormally sized NEMO message, with low total NEMO mRNA, resulting in protein levels significantly lower than normal controls. Importantly, the reduction in NEMO protein levels appears greater than the reduction in the level of NEMO message, suggesting that translation of the abnormally sized NEMO message may be relatively inefficient. The reduction in NEMO protein expression was associated with a 2.4-fold (60%) reduction in NFκB activation, as measured by luciferase assay. This case demonstrates that a residual NFκB activity of ~40% might be sufficient for ectodermal development; however, it results in both innate and adaptive immune dysfunction. This is consistent with the notion that immune function has a more stringent requirement for NFκB function than does ectodermal development. We have demonstrated that NEMO expression is low in ectodermally-derived cells (e.g. fibroblasts) and mesenchymally-derived cells (e.g. PBMCs and EBV transformed B cells) in our index patient. However, it is presently not known which NEMO transcripts are used during ectodermal development. It remains possible that other isoforms may be utilized, that would circumvent the aberrant 1B transcripts and allow normal ectodermal development.

The 8-fold reduction in expression of a normal NEMO protein resulted in a reproducible, modestly reduced degradation of IκBα in IL-1 stimulated fibroblasts, likely due to inefficient activation of the IKK complex, relative to normal fibroblasts (Fig. 1.4A). The modestly reduced degradation of IκBα, however, resulted in significant impairment in TLR induced TNFα production (Fig. 1.1). Although we did not examine the effects of reduced NEMO expression on IL-1 induced degradation of IκBβ and IκBε, degradation

of these inhibitors of NFκB would be expected to be similarly impaired. Therefore, the effect of reduced NEMO expression on NFκB-dependent functions would be due to impaired disinhibition of IκBα, IκBβ, and IκBε.

The case we present indicates that in male patients with dysgammaglobulinemia and recurrent sinopulmonary infections, but with normal ectodermal development and a normal NEMO coding sequence, evaluation of NEMO mRNA and protein levels and of NFκB-dependent immune responses (e.g. TLR function) is essential. Abnormal expression of NEMO should then be followed by analysis of the 5' and 3' untranslated regions.

Acknowledgements: The authors thank Dr. Michel Masaad for useful discussions.

References

1. Ghosh S, May MJ, Kopp EB. NF-kappa B and Rel proteins: evolutionarily conserved mediators of immune responses. Annu Rev Immunol 1998; 16:225-60.
2. Ghosh S, Karin M. Missing pieces in the NF-kappaB puzzle. Cell 2002; 109 Suppl:S81-96.
3. Vallabhapurapu S, Karin M. Regulation and function of NF-kappaB transcription factors in the immune system. Annu Rev Immunol 2009; 27:693-733.
4. Karin M, Ben-Neriah Y. Phosphorylation meets ubiquitination: the control of NF-[kappa]B activity. Annu Rev Immunol 2000; 18:621-63.
5. Cui CY, Schlessinger D. EDA signaling and skin appendage development. Cell Cycle 2006; 5:2477-83.
6. Puel A, Picard C, Ku CL, Smahi A, Casanova JL. Inherited disorders of NF-kappaB-mediated immunity in man. Curr Opin Immunol 2004; 16:34-41.
7. Smahi A, Courtois G, Rabia SH, Doffinger R, Bodemer C, Munnich A, et al. The NF-kappaB signalling pathway in human diseases: from incontinentia pigmenti to ectodermal dysplasias and immune-deficiency syndromes. Hum Mol Genet 2002; 11:2371-5.
8. Kumar H, Kawai T, Akira S. Pathogen recognition in the innate immune response. Biochem J 2009; 420:1-16.
9. Ku CL, Yang K, Bustamante J, Puel A, von Bernuth H, Santos OF, et al. Inherited disorders of human Toll-like receptor signaling: immunological implications. Immunol Rev 2005; 203:10-20.

10. Hanson EP, Monaco-Shawver L, Solt LA, Madge LA, Banerjee PP, May MJ, et al. Hypomorphic nuclear factor-kappaB essential modulator mutation database and reconstitution system identifies phenotypic and immunologic diversity. J Allergy Clin Immunol 2008; 122:1169-77 e16.
11. Niehues T, Reichenbach J, Neubert J, Gudowius S, Puel A, Horneff G, et al. Nuclear factor kappaB essential modulator-deficient child with immunodeficiency yet without anhidrotic ectodermal dysplasia. J Allergy Clin Immunol 2004; 114:1456-62.
12. Puel A, Reichenbach J, Bustamante J, Ku CL, Feinberg J, Doffinger R, et al. The NEMO mutation creating the most-upstream premature stop codon is hypomorphic because of a reinitiation of translation. Am J Hum Genet 2006; 78:691-701.
13. Orange JS, Levy O, Brodeur SR, Krzewski K, Roy RM, Niemela JE, et al. Human nuclear factor kappa B essential modulator mutation can result in immunodeficiency without ectodermal dysplasia. J Allergy Clin Immunol 2004; 114:650-6.
14. McDonald DR, Brown D, Bonilla FA, Geha RS. Interleukin receptor-associated kinase-4 deficiency impairs Toll-like receptor-dependent innate antiviral immune responses. J Allergy Clin Immunol 2006; 118:1357-62.
15. Fusco F, Mercadante V, Miano MG, Ursini MV. Multiple regulatory regions and tissue-specific transcription initiation mediate the expression of NEMO/IKKgamma gene. Gene 2006; 383:99-107.

16. Orange JS, Levy O, Geha RS. Human disease resulting from gene mutations that interfere with appropriate nuclear factor-kappaB activation. Immunol Rev 2003; 203:21-37.

Chapter 2:

Heterozygous N-terminal deletion of IκBα results in NFκB Haploinsufficency, Ectodermal Dysplasia and Immune Deficiency

A version of this chapter was published by in the *Journal of Allergy and Clinical Immunology,* Volume 120, 2007 and has been reproduced with permission.

Note of Clarification:

This chapter was a collaboration between myself and Douglas McDonald. I performed the Western blots and inhibition experiments.

Heterozygous N-terminal deletion of IκBα results in NFκB haploinsufficency, Ectodermal Dysplasia and Immune Deficiency

Douglas R. McDonald[1], Jana L. Mooster[1], Malathi Reddy[2], Erawati Bawle[2], Elizabeth Secord[2], and Raif S. Geha[1]

[1]Division of Immunology, Children's Hospital and the Department of Pediatrics, Harvard Medical School, Boston, MA

[2]Division of Genetics and Metabolic Disorders, Children's Hospital of Michigan, and the Department of Pediatrics, Wayne State University, Detroit, MI

ABSTRACT

Background: Nuclear factor κB (NFκB) is a master transcriptional regulator critical for ectodermal development and normal innate and adaptive immune function. Mutations in the IκB kinase γ/NFκB essential modifier have been described in male subjects with the syndrome of X-linked ectodermal dysplasia with immune deficiency that results from impaired activation of NFκB.

Objectives: We sought to determine the genetic cause of ectodermal dysplasia with immune deficiency in a female patient.

Methods: Toll-like receptor-induced production of the NFκB-dependent cytokines TNFα and IFNα was examined by means of ELISA, the patient's IκBα gene was sequenced, and NFκB activation was evaluated by means of electrophoretic mobility shift assay and NFκB–luciferase assays in transfectants.

Results: Toll-like receptor function was impaired in the patient. Sequencing of the patient's IκBα gene revealed a novel heterozygous mutation at amino acid 11 (W11X). The mutant IkBaW11X protein did not undergo ligand-induced phosphorylation or degradation and retained NFκB in the cytoplasm. This led to roughly a 50% decrease in NFκB DNA-binding activity, leading to functional haploinsufficiency of NFκB activation. Unlike the only other reported IκBα mutant associated with ectodermal dysplasia associated with immune deficiency (ED-ID), S32I, IκBαW11X exerted no dominant-negative effect.

Conclusions: Functional NFκB haploinsufficiency was associated with ED-ID, and this strongly suggests that normal ectodermal development and immune

function are stringently dependent on NFκB in that they might require more than half of normal NFκB activity.

Clinical implications: Although ED-ID is well described in male subjects, female subjects can present with a similar syndrome of ectodermal dysplasia with immune deficiency resulting from mutations in autosomal genes within the NFκB pathway.

INTRODUCTION

Nuclear factor of kappa B (NFκB) is a master transcription factor required for the normal development and function of the immune system. Effective host defense against invading pathogens requires an effective inflammatory response that is dependent upon appropriate activation of NFκB. Five NFκB proteins have been described, including p65 (RelA), p105/p50, p100/p52, c-Rel, and RelB[1, 2]. The NFκB proteins form numerous homo- and heterodimers that mediate specific biological responses. In resting cells, NFκB proteins are retained in the cytoplasm by the IκB (inhibitor of NFκB) family of proteins, which includes IκBα, IκBβ, and IκBε[3]. The prototypic IκB, IκBα, is abundant in white blood cells. Activation of a wide variety of cell surface receptors results in NFκB activation. Stimuli including proinflammatory cytokines (TNFα and IL-1) and pathogen associated molecular patterns (i.e. Toll-like receptor ligands) cause activation of the IκB kinase (IKK) complex, which phosphorylates IκBα on serine residues 32 and 36, leading to ubiquitination of lysines 21 and 22 and the subsequent degradation of IκBα[4]. Serines 32 and 36 as well as lysines 21 and 22 are contained within an N-terminal 73-amino-acid sequence designated the signal response domain because this region regulates the degradation of IκBα. Inflammation-induced degradation of IκBα releases NFκB, primarily p50/p65 heterodimers, uncovering a nuclear localization signal that allows NFκB to translocate to the nucleus where it binds to consensus sequences in the promoters of a wide variety of genes and results in their transcription[2].

Importantly, transcription of IκBα is regulated by NFκB[5, 6]. In this manner, NFκB-induced transcription of IκBα leads to a feedback inhibition of NFκB activity.

To date, mutations in two genes, IκB kinase γ/NFκB essential modifer (IKKγ/NEMO) and IκBα, have been found to result in impaired activation of NFκB in human subjects and in ectodermal dysplasia associated with immune deficiency (ED-ID)[7]. This combination of clinical manifestations arises because normal ectodermal development (hair, teeth, and sweat glands), as well as effective innate and adaptive immune responses, depends on NFκB activation[8]. IKKγ/NEMO is the scaffolding subunit of the IKK complex that links upstream receptor signaling components to the protein kinases IKKα and IKKβ[3]. Because IKKγ/NEMO is encoded on the X chromosome, IKKγ/NEMO deficiency affects only boys who suffer from X-linked ED-ID. Numerous mutations in IKKγ/NEMO have been described[9]. They are all hypomorphic, because total loss of IKK activity and, therefore, of NFκB activity is lethal. A single mutation in one of the two *IκBα* alleles has been identified to date as a cause of autosomal dominant ED-ID in two male patients[10, 11]. The mutation substitutes Ser32 with isoleucine (S32I). Since Ser32 is one of the two serines phosphorylated by IKKβ, IκBαS32I cannot be phosphorylated nor degraded, resulting in impaired NFκB activation. The IκBαS32I mutation was termed a hypermorphic mutation, since IκBαS32I cannot be "disinhibited" and thereby exaggerates its function. In addition, the IκBαS32I mutant was shown to exert a dominant-negative effect because the IκBαS32I mutant was a significantly more potent inhibitor of NFκB activity than WT IκBα in an NFκB luciferase reporter assay[10].

Impaired activation of NFκB has deleterious effects on both innate and adaptive immune function[12]. TLRs and nucleotide-binding oligomerization domain (NOD) proteins are pathogen recognition receptors within the innate immune system that detect invading pathogens, including bacteria, mycobacteria, fungi, and viruses[13, 14]. Because TLRs and NOD proteins signal through NFκB, defects in NFκB activation can cause impaired inflammatory responses to invading pathogens, resulting in decreased production of proinflammatory cytokines and type I interferons[7, 15, 16]. Since the T cell receptor and B cell receptor signaling pathways also converge on NFκB, impaired NFκB function leads to deficits in antigen specific immunity[17]. As a result, patients with X-linked ED-ID demonstrate increased susceptibility to a wide variety of bacterial, mycobacterial, fungal, and viral infections[18]. Analysis of immunoglobulins in these patients commonly reveals hypogammaglobulinemia with variably elevated IgM or IgA levels. Specific antibody responses to protein and polysaccharide antigens are variably impaired. T cell proliferation to mitogens (phytohemagglutinin, pokeweed mitogen, concanavalin A) is intact; however, T cell proliferation to antigens is variably diminished[18].

Two boys with ED-ID but normal sequence of IKKγ/NEMO have been found to have a heterozygous IκBαS32I mutation. In both patients, bone marrow transplantation was performed within 1 to 3 years of life due to severe, recurrent infections. Immunologic analysis revealed highly elevated serum IgM levels, low levels of serum IgG and IgA levels and absent specific antibody titers. Cellular analysis revealed normal percentages of B and T lymphocytes; however, there

was a polyclonal lymphocytosis and an absence of memory T cells. T cell proliferation to mitogens (PHA) was normal; however T cell proliferation to antigens (candida, tetanus) was absent. The IκBαS32I mutation was shown to prevent ligand-induced phosphorylation of IκBα, and its subsequent degradation. NFκB activation was severely impaired in the patient's cells and the mutant was shown to exert a dominant negative effect.

In this report we describe a ten-year-old female with ED-ID and a novel heterozygous nonsense mutation in IκBα (IκBαW11X), resulting in a persistence-of-function mutant that cannot be degraded. Unlike IκBαS32I, the only previously described human IκBα mutant associated with ED-ID, IκBαW11X does not exert a dominant negative effect and results in functional NFκB haploinsufficiency. The association of ED-ID with the IκBαW11X mutant suggests a stringent requirement for NFκB activation in ectodermal development and immune function.

MATERIALS and METHODS

Production of cytokines in response to TLR ligands

Informed consent for blood and dermal biopsy samples was obtained from the patient and heatlthy control subjects in accord with with institutional review board at Children's Hospital Boston. PBMCs were obtained by means of centrifugation through Ficoll-Paque PLUS (Ammersham Biosciences). PBMCs (300,000 cells/200 μl) were stimulated in media, as previously described[19]. Cell stimulations were 12 hours for TNFα ELISA and 48 hours for IFNα ELISA (Invitrogen).

Sequencing of IκBα

RNA was isolated from PBMCs as previously described[19]. cDNA was generated random-primed reverse transcription using Superscript II (Invitrogen). The IκBα transcript was amplified using the forward primer 5'-CCAGCGAGGAAGCAGCG-3' and the reverse primer 5'-CTAGGCAGTGTGCAGTGTGG-3' with an annealing temperature of 61^{o}C. The internal forward primer 5-CATCCTGAAGGCTACCAACTAC-3' and the reverse primer 5'-GAGGCTAAGTGTAGACACG-5' were also used for sequencing. Genomic DNA was generated from the patient's fibroblasts using the phenol:chloroform method. Exon 1 of IκBα was sequenced using the forward primer 5'-GCAGAGGACGAAGCCAGTTC-3' and reverse primer 5'-CCACTTACGAGTCCCGTC-3'. Sequencing of IκBα was performed at the Molecular Biology Core Facility at Children's Hospital, Boston.

Western blotting

Primary dermal fibroblast cultures were grown in RPMI media plus 10% fetal calf serum (Hyclone, Logan UT) plus L-glutamine and penicillin and streptomycin (Invitrogen, Carlsbad, CA). Fibroblasts were stimulated with media or 25 ng/ml IL-1 (Invitrogen, Carlsbad, CA) for the indicated times, followed by lysis in Sample buffer (62.5 mmol/l TRIS, pH 6.8, 2% wt./vol. SDS, 10% glycerol, 2% β-mercaptoethanol, 0.01% bromophenol blue). Lysates were resolved by 12% SDS-PAGE (BioRad, Hercules, CA) and proteins were transferred to polyvinylidene fluoride (PVDF) membranes (Milipore, Billerica, MA). Western blotting was performed with anti-phospho-IκBα (Cell Signaling, Danvers, MA), anti-full length (FL) IκBα (Upstate, Charlottsville, VA), anti-N-terminal IκBα (Santa Cruz Biotechnology, Santa Cruz, CA), anti-phospho- p38MAPK and anti-p38MAPK (Cell Signaling, Danvers, MA), and anti-p65 (Santa Cruz Biotechnology) according to manufacturer recommendations. Sheep anti-mouse HRP conjugated and sheep anti-rabbit HRP conjugated secondary antibodies were obtained from GE Healthcare (Piscataway, NJ).

Immunoprecipitation

Fibroblasts or HEK293T cells were lysed in 1 ml Triton buffer (20 mM TRIS pH 7.4, 1% Triton X-100 (Sigma, St. Louis, MO.), 100 mM NaCl, 10 mM NaF, 2 mM sodium orthovanadate, 1 mM EGTA, protease inhibitor cocktail (Sigma, St. Louis, MO.). Lysates were incubated at 4^{o}C for 3 hours with 1 μg anti-FL-IκBα, anti-Flag (Sigma, St. Louis, MO), or non specific antibody (Ctrl IgG) and protein G-Sepharose (Calbiochem, La Jolla, CA). Immunopreciptates were

washed three times in 1 ml Triton buffer, followed by boiling in Sample buffer. Immunoprecipitates were resolved by SDS-PAGE as above.

Electrophoretic mobility shift assay

Equal numbers of primary fibroblasts were removed from flasks by trypsinization and plated in 6 well tissue culture plates. Fibroblasts were stimulated with 25 ng/ml IL-1 over a 1-hour time course. Media was removed and cells were scraped off in 1 ml ice cold PBS plus phosphatase inhibitors (Active Motif, Carlsbad, CA). Cytosolic and nuclear fractions were generated using a nuclear extract kit (Active Motif). Protein content was measured using Bradford reagent (Pierce, Rockford, IL). EMSA for NFκB was performed as previously described[20] using the oligonucleotide 5'-TCGCTGGGGACTTTCCAGGGA-3' and 2 μg of nuclear extract per condition. Supershift of NFκB complexes was performed using anti-p65 antibodies (Santa Cruz Biotechnology) included in one sample to demonstrate the specificity of the probe. In addition, Western blot with anti-PARP (Santa Cruz Biotechnology) and anti-p50 (Santa Cruz Biotechnology) was performed as described above using 10 μg of nuclear extract per condition.

Constructs

Full length wild type (WT) human IκBα was cloned from cDNA generated from normal control blood cells using the forward primer containing a BamH1 overhang 5'-ATGGATCCGTCCGCGCCATGTTCC-3' and the reverse primer containing a Sal1 overhang 5'-ATGTCGACTAACGTCAGACGCTGGCC-3'. The BamH1-IκBα-Sal1 product was inserted into the expression vector pCMV-Tag4a,

which contains a C-terminal Flag tag. The mutant human IκBα (IκBαW11X Mut 1) construct was cloned from the cDNA derived from the mutant IκBα allele of the patient using the forward primer containing a BamH1 overhang 5'-ATGGATCCGTCCGCGCCATGTTCC-3' and the reverse primer containing an EcoRV overhang 5'-ATGATATCTAACGTCAGACGCTGGCC-3'. The mutant human IκBα (IκBαW11X, Mut 2) construct was cloned from cDNA using the forward primer containing a BamH1 overhang 5'-ATGGATCCCCAGGAGTAGGCCATGG-3', which contains the coding sequence encompassing the second ATG within the *IKBα* gene (Fig. 2.4A), and the reverse primer containing am EcoRV overhang 5'-ATGATATCTAACGTCAGACGCTGGCC-3'. The IκBα sequence was verified by sequencing in the Molecular Biology Core Facility at Children's Hospital, Boston. The BamH1-IκBαW11X-EcoRV products of Mut 1 and Mut 2 were initially inserted into the expression vector pcDNA6. IκBαW11X Mut 1 and Mut 2 were then cut from pcDNA6 using BamH1 and Sal1 and then inserted into pCMV-Tag4a. The sequence of all IκBα constructs was verified by sequencing in the Molecular Biology Core Facility at Children's Hospital, Boston.

Luciferase assays

HEK293T cells were grown in DMEM media plus 10% FCS (Hyclone, Logan, UT) plus L-glutamine and penicillin and streptomycin (Invitrogen, Carlsbad, CA). HEK293T cells were plated on poly-L-lysine coated plates and co-transfected with Fugene reagent (Roche, Indianapolis, IN) overnight with the indicated quantities of vector, WT IκBα, or IκBαW11X and 100 ng NFκB-

luciferase reporter construct plus 10 ng pRL TK-Renilla reporter construct. Transfected HEK293T cells were stimulated with media or 20 ng/ml human TNFα (Invitrogen, Carlsbad, CA) for 6 hours. Luciferase activity was measured using the Dual Luciferase Reporter Assay System (Promega, Madison, WI) according to the manufacturer's recommendations. Luciferase activity was normalized using Renilla.

RESULTS

Case Report. A ten-year girl presented with a history of 15 episodes of pneumonia since 2 months of age and evidence of bronchiectasis by means of computed tomographic scanning. To date, the patient has not had any documented episodes of bacteremia and no mycobacterial infections. She was born to unrelated parents, both of whom are healthy. Physical exam was significant for slightly thin hair, pegged teeth, and coarse skin (Fig. 2.1). Additionally, she was noted to be heat intolerant and unable to sweat. She was subsequently given a diagnosis of ectodermal dysplasia.

Immunological analysis was significant for a markedly elevated serum IgA level and a low serum IgM level. Serum levels of IgG and IgG subclasses were normal except for a modestly decreased IgG2 level. IgE level was normal (Table 1). The patient developed protective titers to immunization with tetanus toxoid; however, she had no specific antibody response to any of the polysaccharide antigens analysed that were contained in the pneumococcal polysaccharide vaccine Pneumovax (data not shown). Analysis of lymphocytes revealed a lymphocytosis with normal percentages of T and B lymphocytes and natural killer cells (Table 1). T cell proliferation in response to PHA-P, anti-CD3, anti-CD3 plus anti-CD28, phorbol 12-myristate 13-acetate plus ionomycin, tetanus, and diptheria was normal (Fig. 2.2). Oxidative burst was normal, as determined by dihydrorhodamine assay (data not shown).

Figure 2.1: Photograph of patient with ED-ID

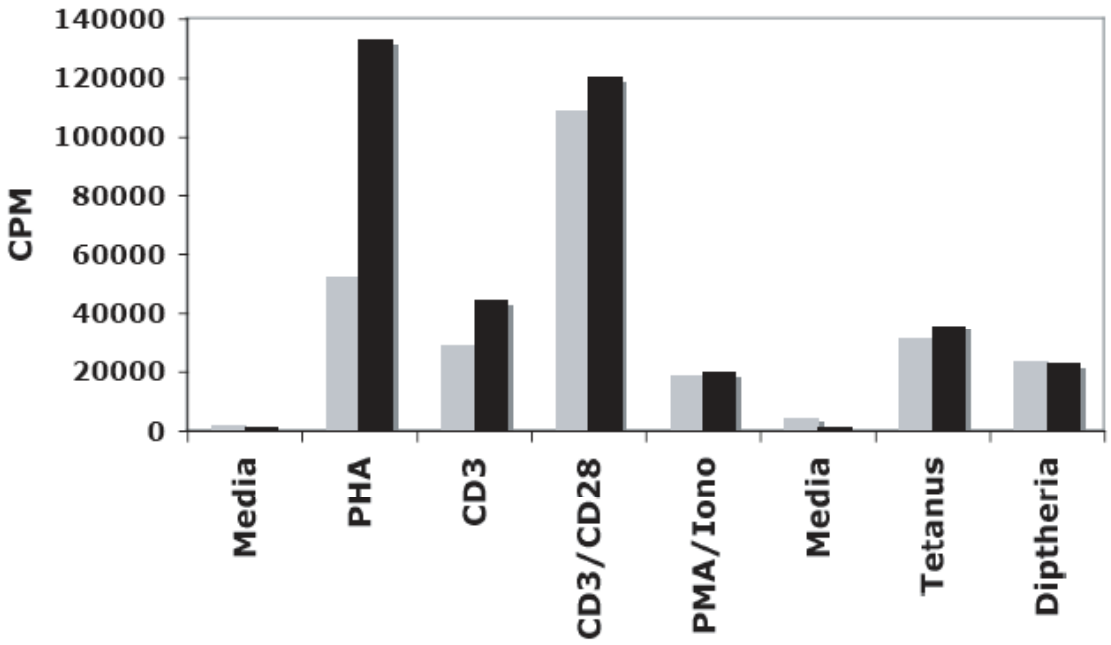

Figure 2.2: Evaluation of T cell proliferation. PBMCs (200,000/condition) from a normal healthy control and the patient were incubated in triplicate with media, phytohemagglutinin (PHA), anti-CD3, anti-CD3 plus anti-CD28, and phorbol-myristate-acetate plus ionomycin for 3 days, followed by incubation overnight with ^{3}H-thymidine (0.8 mCi/well). Also, PBMCs were incubated in triplicate with media (control), tetanus toxoid, or diptheria for 5 days in the Clinical Immunology laboratory at Children's Hospital, Boston. Data is representative of two experiments.

Impaired cytokine production in response to TLR ligands. The presence of ectodermal dysplasia and recurrent infections is consistent with defective activation of NFκB[7]. In order to assess the patient's NFκB function, we evaluated her ability to produce NFκB-dependent cytokines in response to TLR ligands[21]. Stimulation of the patient's blood cells with Poly I:C (TLR3), lipopolysaccharide (TLR4), flagellin (TLR5), and ODN2216 (TLR9) demonstrated significant impairment in TNFα production, whereas 3M-13 (TLR7) stimulation induced normal TNFα production (Fig. 2.3A). Engagement of TLR3, TLR7, TLR8 and TLR9 stimulates production of type I interferons, which is also dependent upon NFκB activation. Stimulation of the patient's blood cells with TLR3 and TLR9 ligands demonstrated markedly impaired production of IFNα, whereas IFNα production in response to TLR7 ligand was less impaired (Fig. 2.3B). Thus, the patient's blood cells demonstrate defects in the production of the NFκB-dependent cytokines TNFα and IFNα.

Heterozygous mutation in IκBα results in the expression of an N-terminally truncated IkBaW11X protein. To our knowledge this is the first known female patient with ED-ID with clinical and laboratory findings similar to those found in male patients with X-linked ED-ID due to mutations in IKKγ (NEMO). We therefore sequenced her IκBα gene, an autosomally encoded gene, from cDNA obtained from her blood cells. The results revealed a heterozygous nonsense mutation at codon 32 of IκBα (G32A; Fig. 2.4A), which was confirmed by sequencing exon 1 of IκBα from the patient's genomic DNA obtained from

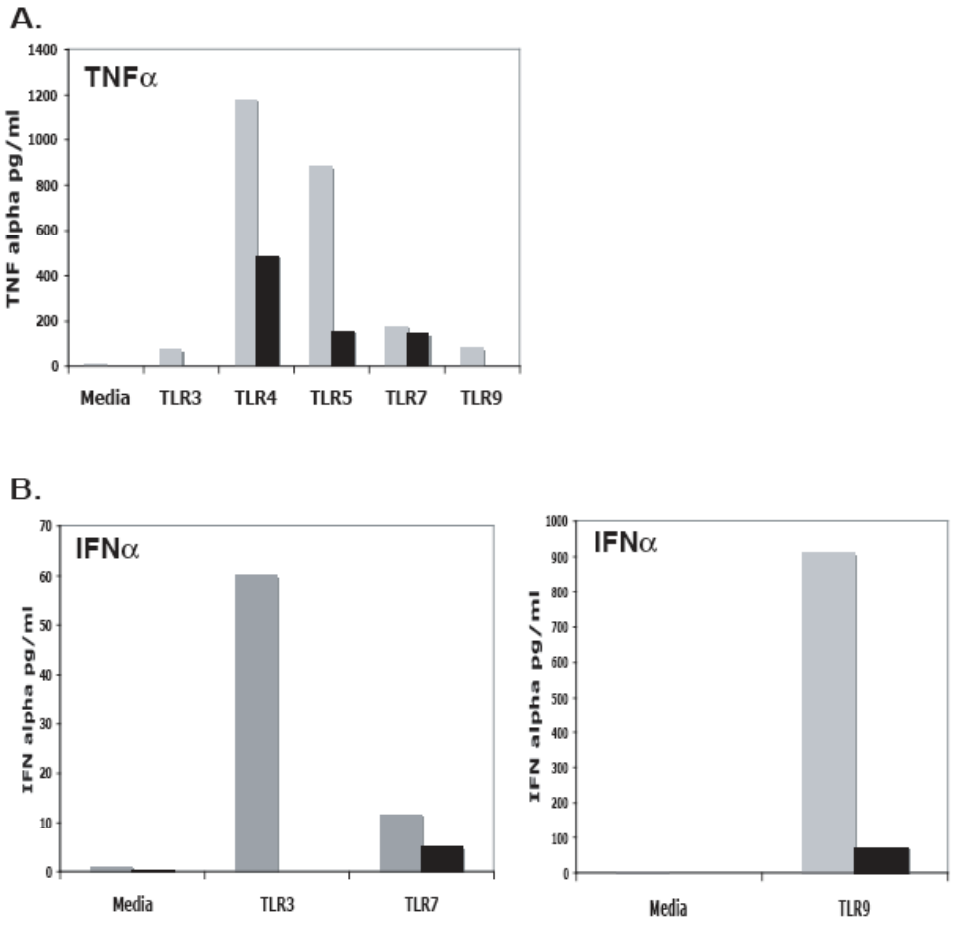

Figure 2.3: Impaired TLR-induced NFκB-dependent cytokine production by patient PBMCs. A) PBMCs (300,000/condition) were incubated with media, Poly I:C (TLR3), LPS (TLR4), Flagellin (TLR5), 3M-13 (TLR7), or ODN2216 (TLR9) for 12 hours, followed by collection of cell culture supernatants and quantitation of TNFα production by ELISA. B) PBMCs (300,000/condition) were incubated with media, Poly I:C (TLR3), 3M-13 (TLR7), or ODN2216 (TLR9) for 48 hours, followed by collection of cell culture supernatants and quantitation of IFNα production by ELISA Note that TLR 9 induced IFNα production is shown on a separate graph due to the large quantities of IFNα induced by TLR9. Data is representative of two experiments.

fibroblasts. Sequencing of cDNA derived from the patient's mother's blood cells was normal (data not shown). Unfortunately, the patient's father is not available for analysis. The G32A mutation results in a W11X nonsense mutation in the translated protein (Fig. 2.4B).

Examination of the coding sequence of IκBα reveals the presence of 2 ATG codons (Met13 and Met45 in the native IκBα) downstream from the nonsense mutation that are flanked by a consensus Kozak translation initiaion sequence[22]. This might allow the in-frame translation of a truncated IκBα that lacks the N-terminal 12 and 44 amino acids, respectively.

Patient fibroblasts express a mutant IκBαW11X protein that fails to be phosphorylated and degraded after IL-1 stimulation. To determine whether a protein product is translated from the mutant IκBα allele, cell lysates were prepared from unstimulated and IL-1-stimulated primary dermal fibroblasts of the patient and a healthy control subject and elecrophoresed on 12% polyacrylamide gels to resolve proteins close in molecular weight. The gels were Western blotted for IκBα using 2 different antibodies, one directed against full length IκBα, and another directed against an N-terminal peptide of IκBα (amino acids 1-30). Western blot of unstimulated normal fibroblast lysates with both antibodies revealed a single band that corresponded to WT IκBα. In contrast, Western blotting of lysates from the patient with antibody to full-length IκBα revealed 2 species of IκBα, a band of normal size that corresponded to WT IκBα and a smaller-sized species (Fig. 2.4C). The N- terminus antibody failed to recognize the smaller-sized IκBα band in the lysates from the patient's cells,

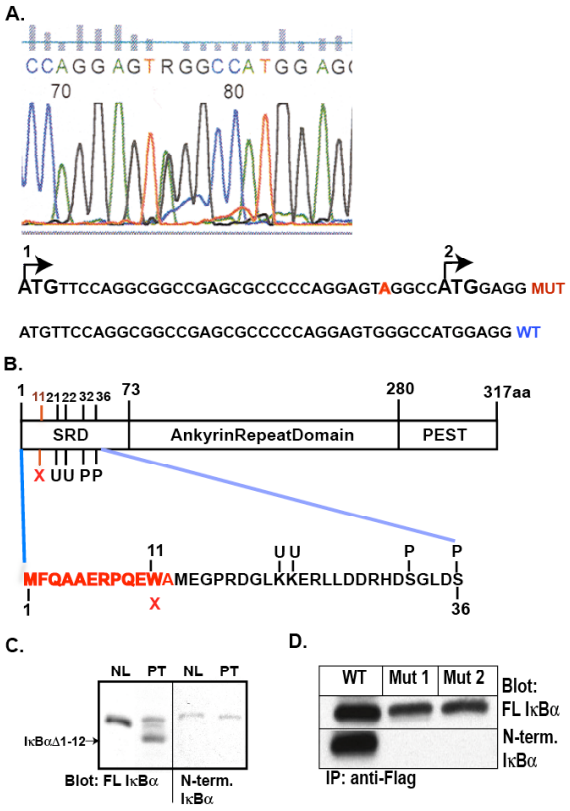

Figure 2.4: Sequencing and Western blot of IκBα from the patient. A) IκBα was amplified from cDNA generated from the patient's PBMCs. Sequence analysis reveals a heterozygous G to A transition at codon 32 of IκBα. The G32A mutation is shown in red. The wild type start codon is shown by arrow 1 and a second putative start codon is shown by arrow 2. Sequencing was performed two times. B) The putative translated mutant IκBα protein is shown. The W11X mutation within the signal response domain (SRD) is in red and the deleted N terminal 12 amino acids of IκBα is shown in red. The position of the putative secondary translation initiation start site relative to lysines 21 and 22 and serines 32 and 36 is shown. C) Anti-full length IκBα Western blot of fibroblast lysates from a normal control and the patient reveals a smaller protein product from the mutant IκBα allele (IκBαW11X) from the patient. Western blot with anti-N terminal IκBα antibody does not detect IκBαW11X. D) HEK293T cells were transfected overnight with 1 μg Flag-WT IκBα, 1 μg Flag- IκBαW11X (Mut 1), or 1 μg Flag-IκBαW11X (Mut 2). IκBα was immunoprecipitated with anti-Flag antibodies and Western blotted with anti-FL IκBα or with anti-N-terminal IκBα.

which is consistent with N-terminal truncation of the mutant. These results indicate that the heterozygous mutation in the patient results in the expression of an N-terminally truncated IκBαW11X protein.

Activation of NFκB requires the phosphorylation of IκBα on serines 32 and 36, followed by ubiquitination of IκBα on lysines 21 and 22 and its degradation by the proteasome. This allows NFκB to translocate to the nucleus and activate gene transcription[4]. Because the IκBαW11X mutant might contain serines 32 and 36, as well as lysines 21 and 22, we evaluated whether IκBαW11X undergoes normal phosphorylation and degradation. Control and patient fibroblasts were stimulated with IL-1, and cell lysates were Western blotted with anti-phospho-IκBα antibody and anti-IκBα against the full-length protein. Western blot with anti-phospho-IκBα antibody demonstrated that WT IκBα protein was phosphorylated within 5 minutes of stimulation in control fibroblasts. This was accompanied by a shift in molecular weight in blots with anti-full length IκBα antibodies (Fig. 2.5, lane 2). Similarly, in the patient's cells, the product of the normal allele full-length WT IκBα was also phosphorylated and underwent a molecular weight shift at the 5 minute time point, confirming the intact activation of the IKK complex in the patient's cells. In contrast, there was no evidence of phosphorylation of IκBαW11X mutant, as indicated by the absence of a lower molecular weight band in the phospho-IκBα blot (Fig. 2.5, lane 7). Lysates were probed with anti-phosphop38 MAPK antibodies to demonstrate that IL-1 activated control and patient fibroblasts equivalently. Stimulation of control and

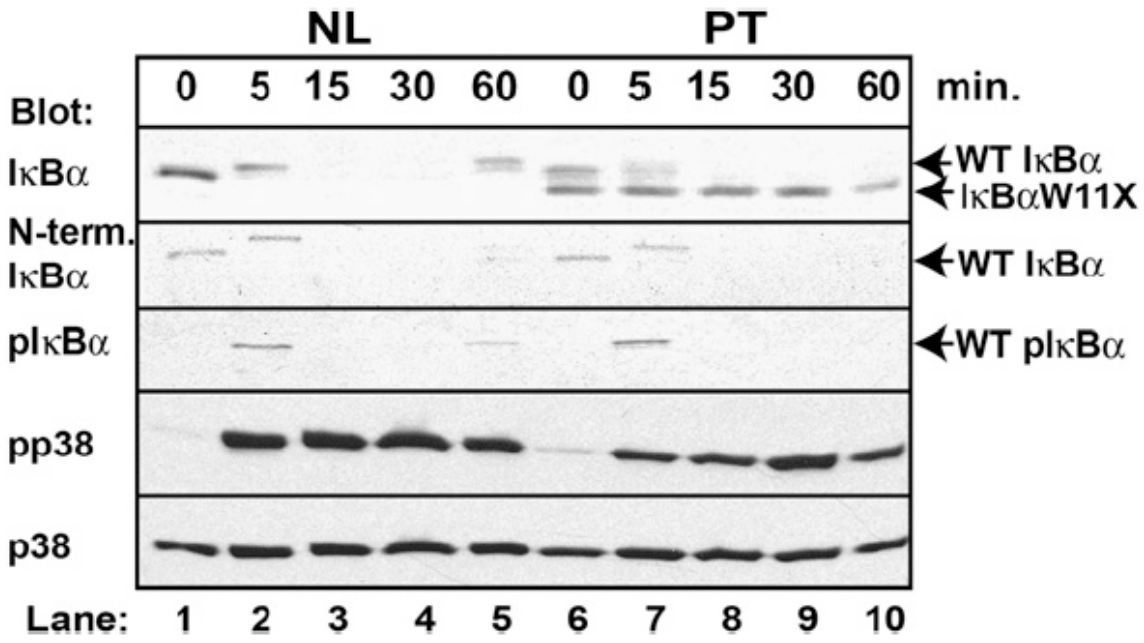

Figure 2.5: Patient fibroblasts express a mutant IκBαW11X protein that does not undergo IL-1 induced phosphorylation and degradation. Western blotting of lysates from control and patient fibroblasts after stimulation with IL-1 is shown. The blot was first probed with with anti-phopsho IκBα and then stripped and re-probed sequentiall with anti-full length (FL) IκBα, anti-N-terminal IκBα, anti-phospho-p38MAPK, and anti-p38MAPK as a protein loading control. The experiment is representative of three independent experiments. NL: healthy control; PT: patient.

patient fibroblasts with IL-1 resulted in equivalent activation of p38 MAPK (Fig. 2.5).

Western blotting of IκBα demonstrated that WT IκBα was completely degraded within 15 minutes in both control and patient fibroblasts. In contrast, the IκBαW11X protein was not significantly degraded over the course of 1 hour, as evidenced by the persistence of the lower molecular weight band recognized by the anti-full length IκBα antibody. Degradation of WT IκBα in IL-1-stimulated control fibroblasts was followed by its synthesis, as indicated by its reappearance and phosphorylation at 1 hour (Fig. 2.5, lane 5). In contrast, one hour after IL-1 stimulation reappearance of WT IκBα was not evident in the patient's fibroblasts (Fig. 2.5, lane 10). Because the synthesis of IκBα is NFκB dependent, these results are consistent with impaired activation of NFκB.

The IκBαW11X mutatnt retains p65 in the cytoplasm after activation of the patient's cells. Because the IκBαW11X mutant does not undergo normal IL-1-induced phosphorylation and degradation, we examined whether it retains NFκB following activation with IL-1. Control and patient's fibroblasts were stimulated with IL-1, then IκBα was immunoprecipitated with an anti-full length IκBα antibody and the IκBα immunopreciptates were probed with anti-p65 antibodies to detect co-precipitating p65. In unstimulated fibroblasts from the healthy control subjects and the patient, p65 coprecipitated with IκBα. Following stimulation of normal fibroblasts with IL-1, p65 was no longer detected in IκBα precipitates, consistent with complete degradation of IκBα and release of p65. In contrast, a sizeable fraction of p65 remained associated with IκBαW11X

following stimulation of the patient's fibroblasts with IL-1, which is consistent with the persistence of the IκBαW11X mutant (Fig. 2.6A). Because of the IκBα degradation, signal transducer and activator of transcription1 (STAT1) Western blotting was performed on equal aliquots of fibroblast lysates to demonstrate equal protein content of the lysates used in the immunoprecipitation.

The persistent association of p65 with the IκBαW11X mutant after IL-1 activation suggests that a portion of p65 remains retained in the cytoplasm in the patient's cells. Cytosolic fractions of control and patient fibroblasts were prepared following IL-1 stimulation and probed for p65 to confirm this (Fig. 2.6B). As expected, p65 virtually disappeared from the cytosolic fractions of control fibroblasts stimulated with IL-1. Twenty minutes after stimulation only 18% ± 3% of total cellular p65 was retained in the cytoplasm. In contrast, 55% ± 10% of total cellular p65 remained in the cytosolic fractions of the patient's fibroblasts after IL-1 stimulation for 20 minutes ($p = .004$). These results suggest that IκBαW11X is a persistence-of-function mutant that sequesters NFκB in the cytoplasm after receptor stimulation.

Impaired nuclear translocation of NFκB in patient's cells. Because the IκBαW11X mutant retains NFκB, we predicted that translocation of NFκB to the nucleus and binding to DNA would be reduced in the patient's fibroblasts following activation with IL-1. Control and patient fibroblasts were stimulated with IL-1 over a 1-hour time course and nuclear extracts were examined for the presence of p50 and p65 (Fig. 2.7A). Western blot of nuclear extracts with an antibody against the p65 subunit of NFκB demonstrated that the nuclear

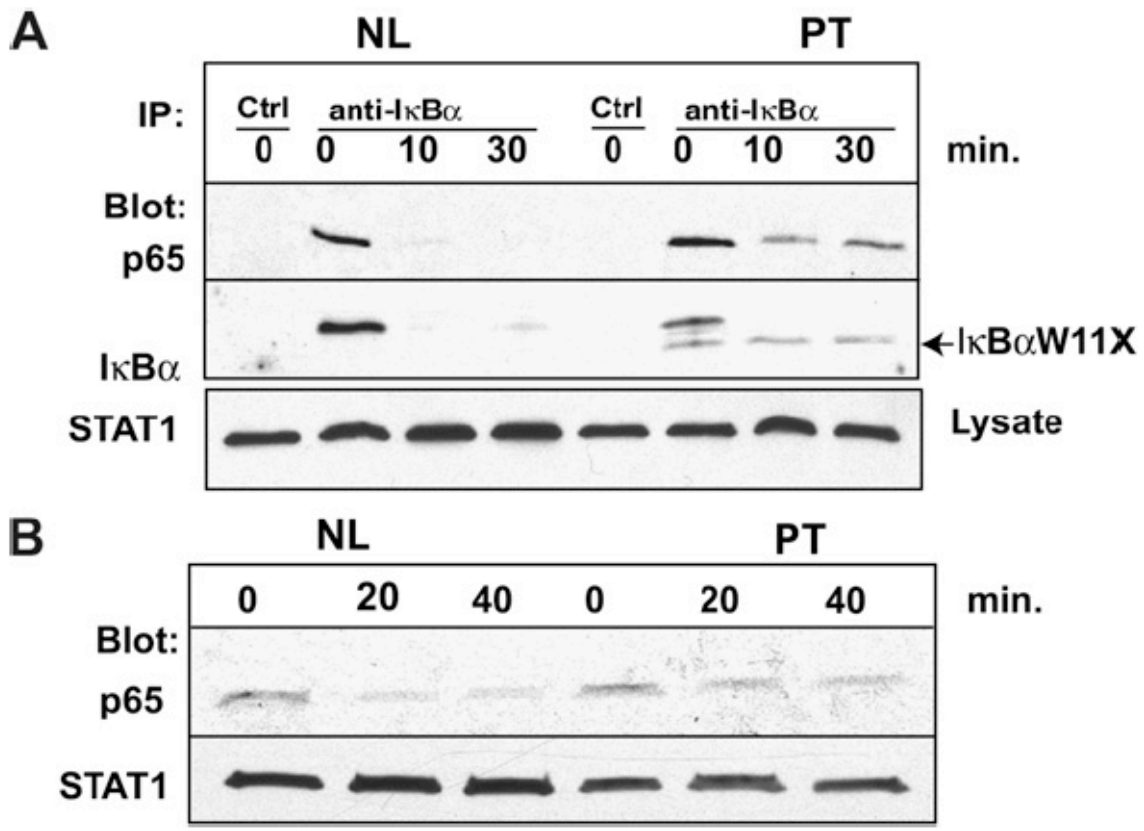

Figure 2.6: NFκB p65 is persistently bound by IκBαW11X in patient fibroblasts. A) Lysates of fibroblasts stimulated with media or 25 ng/ml IL-1 for the indicated times were immunoprecipitated with non-specific rabbit IgG (ctrl IgG) or anti-IκBα and were Western blotted with mouse anti-p65 and anti-IκBα antibodies. 15 μl of each lysate was Western blotted with anti-signal transducer and activator of transcripton1 (STAT1) to verify the presence of equal amounts of protein. B) Western blotting of cytosolic fractions with anti-p65 and anti-STAT1. Data is representative of three independent experiments.

translocation of NFκB was reduced in the patient's cells. Densitometric analysis of the intensity of the p65 and p50 bands at the 20-minute time point in control and patient fibroblasts showed that nuclear accumulation of p65 and p50 in the patient's cells was reduced by 40% ± 5% and 50% ± 10%, respectively, compared with that seen in control cells. These results are consistent with impaired nuclear translocation of NFκB in the patient's cells after stimulation.

The binding of NFκB to DNA in nuclear extracts from normal and patient's fibroblasts was evaluated by electrophoretic mobility shift assay (EMSA). Figure 2.7B shows that stimulation with IL-1 resulted in an increase in the capacity of nuclear extracts from control fibroblasts to bind an NFκB-specific oligonucleotide probe, as evidenced by an increase in the intensity of the two retarded bands present in unstimulated cells and by the appearance of a new retarded third band. Addition of anti-65 antibody to the nuclear extracts supershifted the upper band in the retarded complexes. Consistent with the impaired nuclear translocation of NFκB in the patient's fibroblasts, binding of nuclear extracts from IL-1-stimulated patient's fibroblasts to the NFκB-specific oligonucleotide probe was reduced by approximately 47% ± 6% compared with that seen in control cells, as determined by means of densitometric analysis of the supershifted bands (Fig. 2.7B).

The IκBαW11X mutant does not exert a dominant negative effect on NFκB activation. HEK 293T cells were cotransfected with an NFκB-Luciferase expression construct and with increasing quantities of Flag-tagged WT IκBα or Flag-tagged IκBαW11X mutant to test whether the IκBαW11X mutant acts as a

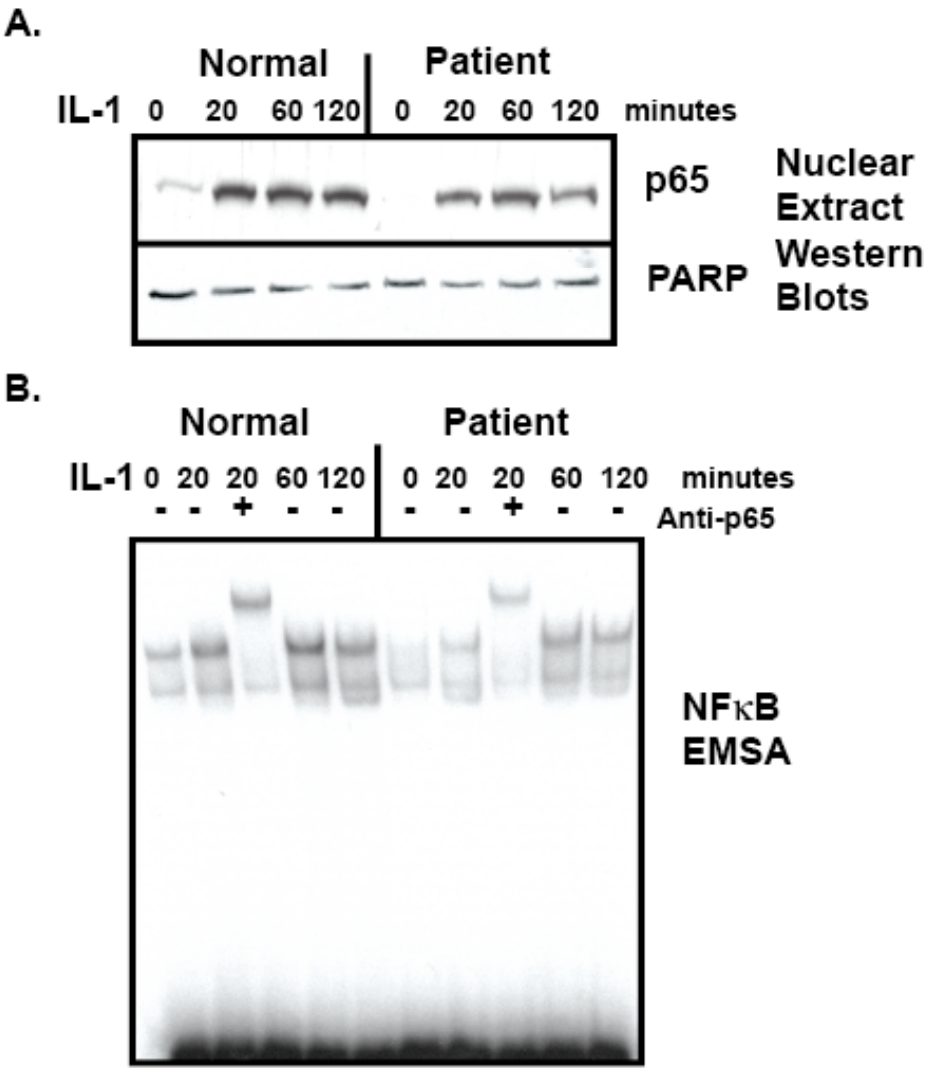

Figure 2.7: Reduced NFκB nuclear translocation and binding to ^{32}P-labeled NFκB-specific oligonucleotide in nuclear extracts from patient fibroblasts. Fibroblasts were stimulated with media or 25 ng/ml IL-1 for the indicated times. A) 10 μg of each nuclear extract was resolved by 10% SDS-PAGE and transferred to Immobilon. Western blot with anti-NFκB p65 (p65) was performed to evaluate nuclear translocation. Blot was stripped and re-probed with Anti-PARP as a protein loading control. B) Nuclear extracts were generated and 2 μg of protein from each nuclear extract was used for NFκB EMSA. Anti-p65 antibodies were used in one reaction to demonstrate specificity of the assay. Data is representative of three independent experiments.

dominant negative mutant, as has been reported for the IκBαS32I mutant. Consistent with the function of IκBα as an inhibitor of NFκB activity, transfection with increasing amounts of WT IκBα led to a dose-dependent inhibition of NFκB-luciferase activity. Transfection of IκBαW11X mutant resulted in a comparable dose-dependent inhibition curve (Fig. 2.8A). Western blotting of cell lysates with anti-Flag antibody demonstrates that WT IκBα and IκBαW11X were expressed comparably (Fig. 2.8B). Note that expression of IκBα in 293T cells transfected with 30ng of the constructs was less than the limit of detection of by means of Western blotting with anti-Flag. Taken together, these data indicate that IκBαW11X is not a dominant negative mutant but rather a persistence-of-function mutant that results in functional NFκB haploinsufficiency.

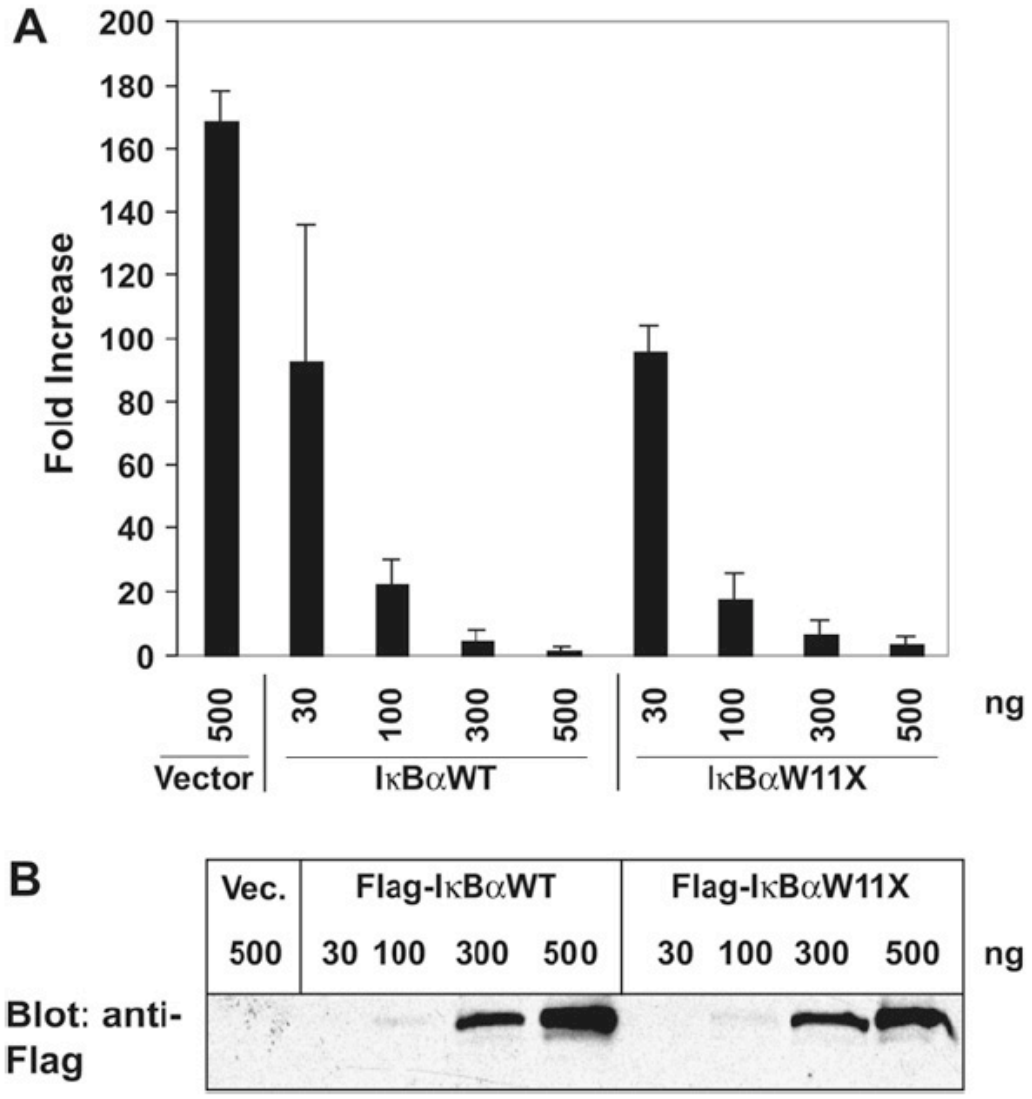

Figure 2.8: IκBαW11X does not exert a dominant negative effect. A) HEK293T cells were co-transfected Flag-WT IκBα, or Flag IκBαW11X and 100 ng NFκB-luciferase reporter construct and TK-Renilla reporter construct and then stimulated with media or 20 ng/ml TNFα for 6 hours. Fold activation of luciferase activity was calculated relative to unstimulated HEK293T cells transfected with 500 mg vector DNA. Transfection efficiency was normalized using Renilla. B) Anti-Flag Western blot of cellular lysates.

DISCUSSION

We describe a female patient with ED-ID associated with a novel heterozygous nonsense mutation in the *IκBα* gene that gives rise to a truncated protein that lacks the N-terminus of IκBα. The mutant protein is not phosphorylated or degraded following IL-1 receptor signaling. As a result, it sequesters NFκB and results in functional NFκB haploinsudfficiency.

To our knowledge, the patient we have described is the first reported female with ED-ID. She has several of the classical features of ED including teeth abnormalities, receding hairline (Fig. 2.1) and inability to sweat[23]. She suffered from recurrent infections and exhibited immunological defects common to other described ED-ID patients, which included lymphocytosis, impaired specific antibody responses to polysaccharide antigens, and elevated IgA levels. Her PBMCs showed impaired response to Toll receptor ligands, characteristic of patients with ED-ID (Fig. 2.2)[10, 18].

A heterozygous missense mutation (G32A) in IκBα introduced a stop codon at position 11 in the patient (Fig. 2.3A and B). This might have allowed translation initiation at the second or fourth methionine codons. We indeed demonstrated the presence of an N-terminally truncated protein in the pateint's cells. The exact start site that is used to generate this protein remains to be determined. The mutant IκBαW11X protein is not phosphorylated nor degraded following of IL-1 receptor engagement. This resulted in retention in the cytosol of

approximately half of p65 after stimulation and in a corresponding reduction in the nuclear translocation of p65 (Fig. 2.5 and 2.6).

The immunodeficiency in our patient is less severe than that in the 2 patients previously described with an S32I mutation in IκBα. These two patients had a hyper-IgM syndrome with high serum IgM and low serum IgG levels, absent specific antibody responses to both protein and polysaccharide antigens and absent antigen-stimulated T cell proliferation. Both patients underwent bone marrow transplantation due to the severity of their recurrent infections[10, 11]. In contrast, our patient has normal serum IgG levels, good antibody responses to the protein antigen tetanus toxoid and normal T cell proliferation to antigens. More importantly, she has been in relatively good health while receiving intravenous immunoglobulin infusions, and to date has not suffered from mycobacterial infections that commonly occur in patients with ED-ID,

The milder clinical phenotype of the patient compared to the two patients with the S32I mutation in IκBα is likely explained by the milder impairment of NFκB activation in this patient, although differences in the genetic background may have also contributed. Both the IκBαS32I and IκBαW11X mutations prevent ligand-induced phosphorylation and degradation of the mutant IκBα and there for are persisitence-of-function mutants. However, in the case of the S32I mutation, TNFα-induced phosphorylation and degradation of the product of the normal IκBα allele is barely detectable[10]. In contrast, IL-1 induced phosphorylation and degradation of the product of the normal IκBα allele is intact in our patient. Consistent with these observations, TNFα stimulated activation of NFκB in

fibroblasts from the patient with the S32I mutation was barely detectable, whereas IL-1 stimulated activation of NFκB in fibroblasts from our patient was roughly half that of the healthy control, as determined by means of scanning densitometry of NFκB nuclear translocation and EMSA data.

A dominant negative effect of the S32I mutation was confirmed in transfection studies in which the capacity of IκBαS32I and WT IκBα to inhibit TNFα-driven NFκB-luciferase reporter gene expression was compared. The S32I mutant exerted a dominant negative effect because it was much more potent than WT IκBα in inhibiting reporter gene expression[10]. These results suggest that in addition to being a persistence-of-function mutant, the S32I mutant functions as a dominant-negative mutant. This is possibly because the S32I mutant, which has an intact signal response domain, might compete with WT IκBα for IKK and perhaps function as an irreversible inhibitor of IKK. In contrast, IκBαW11X exerted no detectable dominant-negative effect because its effect was comparable with that of WT IκBα. Because this mutant lacks a portion of the N-terminus of IκBα, it might not effectively compete for IKK. In future experiments we plan to transfect IκBα$^{-/-}$ murine embryonic fibroblasts with WT IκBα and IκBαW11X to confirm that IκBαW11X functions as a persistence-of-function mutant. This will have the advantage of using cells without endogenous IκBα.

In summary, the novel IκBαW11X mutant we describe in this report, which does not undergo normal ligand-induced degradation and which impairs NFκB activation through persistence of function (eg, retention of NFκB), simply results in functional NFκB haploinsufficiency. The fact that functional NFκB

haploinsufficiency was associated with ED-ID strongly suggests that normal ectodermal development and immune function are stringently dependent on NFκB, in that they might require more than half of normal NFκB activity.

REFERENCES

1. Ghosh S, May MJ, Kopp EB. NF-kappa B and Rel proteins: evolutionarily conserved mediators of immune responses. Annu Rev Immunol 1998; 16:225-60.
2. Ghosh S, Karin M. Missing pieces in the NF-kappaB puzzle. Cell 2002; 109 Suppl:S81-96.
3. Bonizzi G, Karin M. The two NF-kappaB activation pathways and their role in innate and adaptive immunity. Trends Immunol 2004; 25:280-8.
4. Karin M, Ben-Neriah Y. Phosphorylation meets ubiquitination: the control of NF-[kappa]B activity. Annu Rev Immunol 2000; 18:621-63.
5. Chiao PJ, Miyamoto S, Verma IM. Autoregulation of I kappa B alpha activity. Proc Natl Acad Sci U S A 1994; 91:28-32.
6. Ito CY, Kazantsev AG, Baldwin AS, Jr. Three NF-kappa B sites in the I kappa B-alpha promoter are required for induction of gene expression by TNF alpha. Nucleic Acids Res 1994; 22:3787-92.
7. Puel A, Picard C, Ku CL, Smahi A, Casanova JL. Inherited disorders of NF-kappaB-mediated immunity in man. Curr Opin Immunol 2004; 16:34-41.
8. Smahi A, Courtois G, Rabia SH, Doffinger R, Bodemer C, Munnich A, et al. The NF-kappaB signalling pathway in human diseases: from incontinentia pigmenti to ectodermal dysplasias and immune-deficiency syndromes. Hum Mol Genet 2002; 11:2371-5.

9. Orange JS, Levy O, Geha RS. Human disease resulting from gene mutations that interfere with appropriate nuclear factor-kappaB activation. Immunol Rev 2005; 203:21-37.

10. Courtois G, Smahi A, Reichenbach J, Doffinger R, Cancrini C, Bonnet M, et al. A hypermorphic IkappaBalpha mutation is associated with autosomal dominant anhidrotic ectodermal dysplasia and T cell immunodeficiency. J Clin Invest 2003; 112:1108-15.

11. Janssen R, van Wengen A, Hoeve MA, ten Dam M, van der Burg M, van Dongen J, et al. The same IkappaBalpha mutation in two related individuals leads to completely different clinical syndromes. J Exp Med 2004; 200:559-68.

12. McDonald DR, Janssen R, Geha R. Lessons learned from molecular defects in nuclear factor kappaB dependent signaling. Microbes Infect 2006; 8:1151-6.

13. Athman R, Philpott D. Innate immunity via Toll-like receptors and Nod proteins. Curr Opin Microbiol 2004; 7:25-32.

14. Ku CL, Yang K, Bustamante J, Puel A, von Bernuth H, Santos OF, et al. Inherited disorders of human Toll-like receptor signaling: immunological implications. Immunol Rev 2005; 203:10-20.

15. Takeuchi O, Akira S. Toll-like receptors; their physiological role and signal transduction system. Int Immunopharmacol 2001; 1:625-35.

16. Lemaitre B. The road to Toll. Nat Rev Immunol 2004; 4:521-7.

17. Schulze-Luehrmann J, Ghosh S. Antigen-receptor signaling to nuclear factor kappa B. Immunity 2006; 25:701-15.

18. Orange JS, Jain A, Ballas ZK, Schneider LC, Geha RS, Bonilla FA. The presentation and natural history of immunodeficiency caused by nuclear factor kappaB essential modulator mutation. J Allergy Clin Immunol 2004; 113:725-33.

19. McDonald DR, Brown D, Bonilla FA, Geha RS. Interleukin receptor-associated kinase-4 deficiency impairs Toll-like receptor-dependent innate antiviral immune responses. J Allergy Clin Immunol 2006; 118:1357-62.

20. Tsitsikov EN, Laouini D, Dunn IF, Sannikova TY, Davidson L, Alt FW, et al. TRAF1 is a negative regulator of TNF signaling. enhanced TNF signaling in TRAF1-deficient mice. Immunity 2001; 15:647-57.

21. Karin M. Signal transduction and gene control. Curr Opin Cell Biol 1991; 3:467-73.

22. Kozak M. Regulation of translation via mRNA structure in prokaryotes and eukaryotes. Gene 2005; 361:13-37.

23. Zonana J, Elder ME, Schneider LC, Orlow SJ, Moss C, Golabi M, et al. A novel X-linked disorder of immune deficiency and hypohidrotic ectodermal dysplasia is allelic to incontinentia pigmenti and due to mutations in IKK-gamma (NEMO). Am J Hum Genet 2000; 67:1555-62.

Chapter 3:

Heterozygous S32I mutation in IκBα that causes ectodermal dysplasia with immunodeficiency results in defective development of lymphoid organs and impaired B cell function

Note of clarification:

I performed all experiments in this chapter.

Heterozygous S32I mutation in IκBα that causes ectodermal dysplasia with immunodeficiency results in defective development of lymphoid organs and impaired B cell function

Jana L. Mooster[1], Severine Le Bras[1], John Manis[2] and Raif S. Geha, MD[1],

[1]Division of Immunology and [2]Division of Transfusion, Children's Hospital, [1]Department of Pediatrics and [2]Department of Pathology, Harvard Medical School, Boston, MA,

ABSTRACT

Autosomal ectodermal dysplasia with immunodeficiency (ED-ID) is caused by mutations in the inhibitor of NFκB α (IκBα), which is phosphorylated and degraded in response to immune signaling pathways. We generated a mouse model of ED-ID by replacing one IκBα allele with a non-phosphorylatable IκBα, IκBα S32I, which resulted in decreased NFκB signaling. These mice have dysmorphic hair and teeth, as well as decreased serum immunoglobulins, and a severe decrease in their specific antibody response to T-dependent and T-independent antigens. The mice lack lymph nodes (LN) and Peyer's patches (PP), have a disrupted splenic architecture with no marginal zone, and fail to develop germinal centers (GCs). T cell function is intact but B cell function is deficient *in vitro*. Rag2$^{-/-}$ bone marrow chimeras formed proper lymphoid organs and had normal cutaneous hapten sensitivity but did not produce specific antibodies. This mouse model shows that autosomal dominant ED-ID results in failure to develop LN and PP, disorganized splenic architecture, failure to develop GCs and an intrinsic B cell defect.

INTRODUCTION

Both innate and adaptive immune responses depend on activation of nuclear factor κB (NFκB), a transcription factor that is induced upon ligation of Toll-like receptors (TLRs), TNF-family cytokine receptors and antigen receptors. Stimulation through these receptors causes activation of the IκB kinase (IKK) complex, which contains the catalytic subunits IKKα and IKKβ, and the regulatory subunit IKKγ, also called NFκB essential modulator (NEMO). NFκB dimers are retained in the cytoplasm by the inhibitors of NFκB (IκB) family, including IκBα, IκBβ and IκBε, which prevent the nuclear translocation of NFκB[1]. In the canonical NFκB signaling pathway, the activated IKK complex phosphorylates IκBα at Ser 32 and Ser 36, which targets its polyubiquitination, and subsequent degradation by the 26S proteasome. The released NFκB dimers (primarily p50/p65) translocate to the nucleus and activate transcription of genes encoding chemokines, cytokines, adhesion molecules and inhibitors of apoptosis[2, 3].

There is a growing understanding of the family of diseases resulting from mutations in the NFκB signaling pathway[4-6]. Patients with hypomorphic mutations in NEMO have X-linked ectodermal dysplasia associated with immune deficiency (ED-ID), characterized by recurrent pyogenic infections; hypogammaglobulinemia with low IgG and variable serum IgM and IgA; specific antibody deficiency, particularly to polysaccharide antigens; and decreased cytokine and type I interferon production[6]. The ectodermal dysplasia is caused by defective NFκB signaling downstream of ectodysplasin A (EDA) and its receptor,

which regulate ectodermal development. ED is characterized by abnormal development of the ectoderm, including sparse hair, conical teeth and reduced sweat glands[4, 7, 8].

Autosomal dominant ED-ID is caused by mutations in the IκBα gene. Four heterozygous mutations in five patients have been described. Two patients had a heterozygous serine to isoleucine at position 32 in IκBα (IκBαS32I) and the other three had a nonsense mutation (W11X, E14X and Q9X), which resulted in the expression of an N-terminally truncated IκBα protein. In each case, the mutation impaired IKK phosphorylation and degradation of the mutant protein[9-13]. These mutations caused sequestration of NFκB in the cytoplasm by the product of the mutant allele, which resulted in the attenuation of NFκB activation. The two patients with the S32I mutation had severe recurrent pyogenic infections, low IgG, high IgM and low IgA levels in the serum, made no specific antibodies to immunization, and had an impaired T cell response to anti-CD3. They also had a profound deficiency in memory T cells and γδ T cells[9, 10]. Both patients with the S32I mutations and the patient with the E14X mutation received bone marrow transplantation. Only one of the three survived. This patient has 100% chimerism and normal T cell proliferation, but continues to have impaired immune function and requires intravenous gammaglobulin replacement and trimethoprim/ sulfamethoxazole prophylaxis against opportunistic infections[14]. The fourth patient with the W11X mutation also had recurrent infections but had a milder clinical course and is doing relatively well on gammaglobulin and

trimethoprim/sulfamethoxazole prophylaxis[11]. Treatment for the fifth patient with the Q9X mutation is unknown.

The rarity of patients with ED-ID, as well as logistical considerations, makes it difficult to investigate their immune function in detail. We have created an IκBα S32I knock-in mouse model of ED-ID in order to gain insights into the disease. IκBα S32I knock-in mutant mouse recapitulates many of the ectodermal and immune abnormalities found in patients with ED-ID due to IκBα mutation, including poor responses to TLR and poor antibody responses due to an intrinsic defect in B cell function. In contrast, these mice had no intrinsic T cell defect. However, they lack lymph nodes (LN) and Peyer's patches (PP), follicular dendritic cells (FDCs) and germinal centers (GCs). These abnormalities were not due to intrinsic defects in hematopoietic cells, and may have resulted from defective NFκB signaling in stromal cells.

MATERIALS AND METHODS

Generation of Heterozygous IκBα S32I Knock-in Mice

The arms of the IκBα S32I targeting vector were amplified by PCR from genomic DNA of the CJ7 ES cell line derived from the 129Sv mouse strain. The 2.8-kb 5′ and 3.1-kb 3′ arms were cloned into the pKS-neo-DTAIII vector (a gift from the lab of Dr. Michael Greenberg) and the nucleic acid G94T mutation was introduced by site-directed mutagenesis (Stratagene) into exon 1 in the 5′ arm resulting in the amino acid S32I mutation (Fig. 3.1A). The linearized targeting construct was electroporated into CJ7 ES cells, which were then selected in 0.4 mg/ml G418 and 10 mg/ml gancyclovir. An ES cell clone containing a disrupted allele and no random integration of the neo gene was confirmed by PCR and Southern blotting (Fig. 3.1B), then injected into 3.5-day-old C57BL/6 blastocysts, and IκBα S32I heterozygous neo mice were obtained by standard methods[15]. Presence of mutant RNA was confirmed by amplifying cDNA with the primers CAGGACTGGGCCATGGAG and ATCTCCCGCAGCTCCTTC, followed by a digest with MwoI.

Mice were back-crossed six generations to C57Bl6 mice from Charles River Labs. All mice were kept in a specific pathogen-free environment, in autoclaved cages with trimethoprim and sulfamethoxazole added to the water. Procedures were performed in accordance with the Animal Care and Use Committee of the Children's Hospital Boston.

Western Blotting

Primary dermal fibroblast cultures were grown in RPMI media plus 10% FCS (Hyclone, Logan, UT) plus L-glutamine, penicillin and streptomycin (Invitrogen). Fibroblasts were stimulated with media, 10ng/ml IL-1, 10ng/ml TNFα (R&D systems), or 1mg/ml LPS (Sigma) for the indicated times. Western blotting was performed as previously described[11] using anti-phospho IκBα (Cell Signaling), anti-mouse full-length IκBα (Abcam) and anti-actin (Sigma), according to the manufacturer's recommendations.

Sheep anti-mouse horseradish peroxidase–conjugated and sheep anti-rabbit horseradish peroxidase–conjugated secondary antibodies were obtained from GE Healthcare (Piscataway, NJ). Quantification was performed using the public domain ImageJ software from the National Institutes of Health.

FACS Analysis

Single-cell suspensions from 4 to 6 wk old mice were stained with FITC, PE, PE-Cy7, APC, PerCP-Cy5.5, AlexaFluor 700, or APC-eFluor 780-labeled monoclonal antibodies and analyzed on a FACS Canto (BD). Antibodies to B220, CD3, IgM, CD21, CD23, CD93, CD43, CD4, CD8, GL-7, Mac-1, CD11b, and Ly6G were from eBioscience, Fas was from BD Pharmingen and FITC-conjugated PNA was from Sigma.

Murine embryonic fibroblasts were treated for 24 hours with 2μg/ml anti-LTβR agonist antibody AFH6 (a gift from Jeff Browning, Biogen) or 10ng/ml TNFα, dissociated with trypsin/EDTA, and stained with anti-VCAM1

(eBioscience).

Immunohistochemistry

IHC was performed as described in Cariappa, et al[16] and Kranich, et al[17].

Purification and Stimulation of Splenic T and B cells

Assays for proliferation, cytokine production, and GC formation were performed as previously described[18]. Briefly, B cells were purified from spleen suspensions using anti-CD43 microbeads (Miltenyi) resuspended in RPMI supplemented with penicillin/streptomycin, HEPES (GIbco), sodium pyruvate and β-mercaptoethanol (Sigma). 200,000 cells in 96-well plates were plated for proliferation assays, and 250,000 per 24-well for *in vitro* Ig analysis. Cells were stimulated with 10μg/ml anti-μ (Jackson ImmunoResearch), 500ng/ml anti-CD40 (eBioscience), 10μg/ml LPS (Sigma), and 40ng/ml IL-4 (R&D Systems) alone or in combination. Tritiated thymidine (PerkinElmer) was added at day 3, and incorporation was assayed after 15 to 18 hours. Supernatants from *in vitro* Ig experiments were analyzed by ELISA on day 6.

T cells were purified from spleen suspensions using the pan-T cell isolation kit from Miltenyi, and 100,000 per 96-well were plated, along with 300,000 irradiated (3000 rad) non-T cell (CD90.2 kit from Miltenyi) APCs. For anti-CD3 experiments, plates were coated with 0.25μg/ml anti-CD3 (eBioscience, clone 145-2C11) at 37C for 1 hour and washed with PBS. Cells were also stimulated with 200μg/ml Ovalbumin (OVA) (Sigma). Tritiated thymidine was

added on day 3 and incorporation was assayed after 15 to 18 hours. IL-2 production was assayed from day 2 supernatants by ELISA (BD Bioscience).

Serum Ig Levels and Antibody Responses

4 to 6 week old mice were immunized i.p. with 50μg of OVA with Alum (Sigma) in PBS at day 0, boosted at day 14, and bled at days 0 and 21. Mice were immunized i.p. with 25 μg TNP-LPS (Biosearch Technologies) in PBS or with 25 μg TNP–Ficoll (Biosearch Technologies) at day 0 and bled at days 0 and 14. Antigen-specific antibody responses were analyzed by OVA-specific or TNP-specific ELISA using 96-well plates coated with either OVA or TNP-conjugated BSA (Biosearch Technologies) at 10μg/mL in PBS. For serum immunoglobulin levels, plates were coated with isotype-specific antibodies (Southern Biotech). AP-conjugated secondary antibodies(Southern Biotech) and PNPP (Sigma) were used for ELISA.

Contact Hypersensitivity to Oxazolone

Mice were sensitized by the application of 100 μL of 2% oxazolone (Sigma) in ethanol on day 1 to shaved abdominal skin. On day 5, the left ear was challenged with 10 μL of 1% oxazolone and the right ear was challenged with vehicle (ethanol) on dorsal and ventral surfaces. Ear thickness was measured after 24 hours with a micrometer (Mitutoyo).

Bone Marrow Reconstitution of Rag2$^{-/-}$ Mice

Bone marrow was collected from 6 week old mutant mice or their WT littermates. Flow cytometry was performed to assure the $CD34^-$ population was comparable between the WT and mutant bone marrow. Adult $Rag2^{-/-}$ recipient mice received a single 250 cGy dose of total body γ irradiation (^{137}Cesium source). Viability of the bone marrow cells was examined by trypan blue dye exclusion and 1×10^5 viable bone marrow cells were injected i.v. into the $Rag2^{-/-}$ mice.

Statistical Analysis

Statistical Analysis of data was performed with Prism software using the Student's *t* test or ANOVA.

RESULTS

Heterozygous IκBα S32I mutant mice have ectodermal dysplasia, failure to thrive and increased postnatal mortality. We generated mice with a G94T misense mutation in exon 1 of IκBα, which results in the substitution of serine at a.a. position 32 by isoleucine (S32I). The strategy for the generation of these mice is shown in Figure 3.1. Heterozygous pups were born at Mendelian ratios, indicating no embryonic lethality.

Heterozygous IκBα S32I mutant mice, hereafter referred to as IκBα mutant mice, were found to have missing third molars and a lack of guard hair types (Fig. 3.2A). This phenotype is similar to that of mice with ectodermal dysplasia caused by disruption of the EDA gene[8]. IκBα mutant mice were significantly smaller in size and in weight than their WT littermates (Fig. 3.2B,C). IκBα mutant mice survived poorly with a 50% survival at 8 weeks (Fig. 3.2D).

Impaired IκBα phosphorylation and degradation in IκBα mutant mice. It is difficult to distinguish between the WT and mutant proteins by Western blot, since the proteins are of the same size and there are no antibodies available that differentially bind to one or the other. We tested indirectly for the presence of the mutant protein by examining the resistance of IκBα to phosphorylation and degradation. Skin fibroblasts were stimulated with IL-1, a known activator of the canonical NFκB pathway, and cell lysates were Western blotted with anti-phospho-IκBα (S32/S36) and anti-IκBα antibodies. WT fibroblasts exhibited robust IκBα phosphorylation 5 minutes after IL-1 stimulation phosphorylation (Fig.

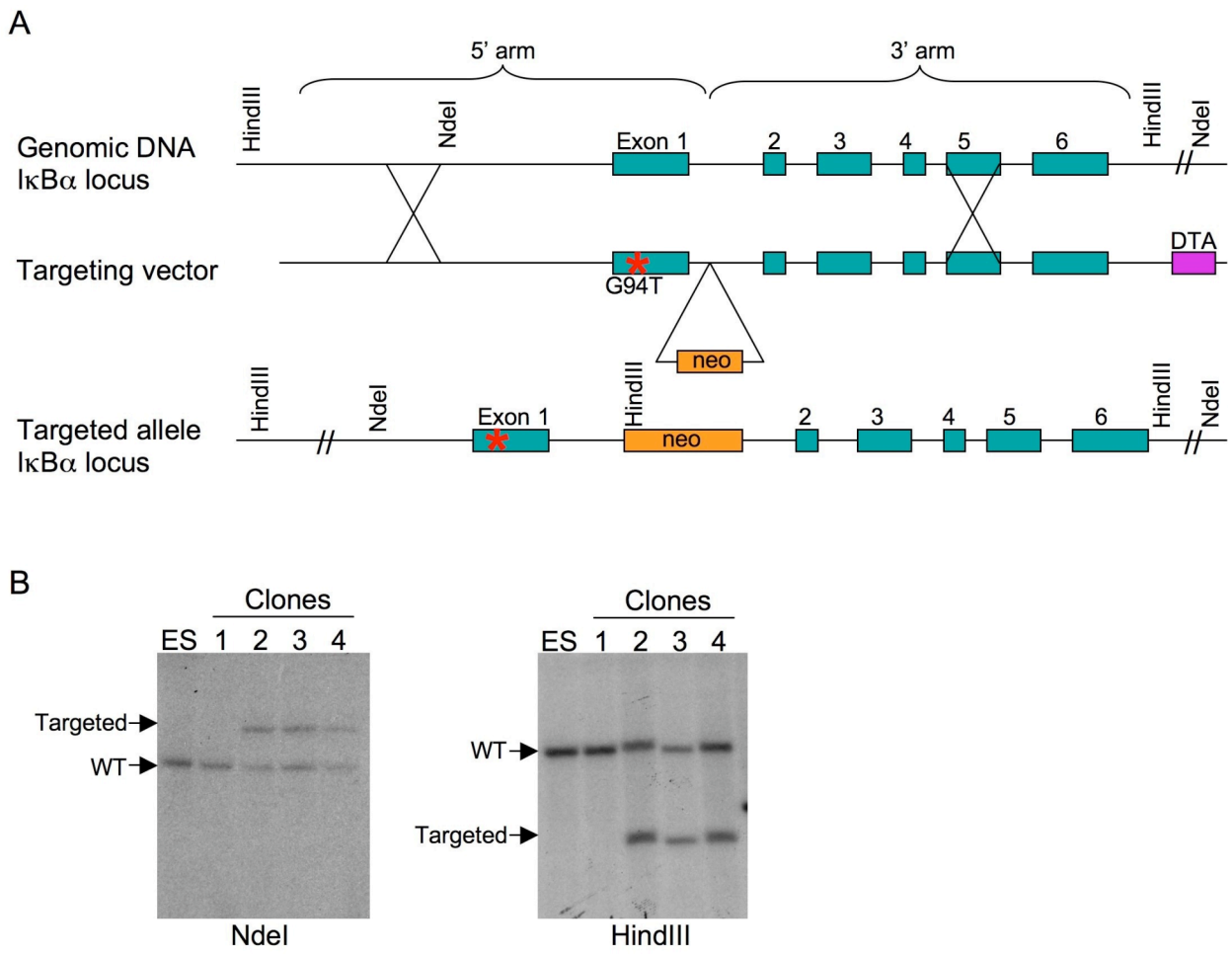

Figure 3.1. Generation of IκBα S32I mutant mice

A. IκBα S32I targeting vector scheme. The arms of the IκBα S32I targeting vector were amplified by PCR from genomic DNA of the CJ7 ES cell line derived from the 129Sv mouse strain. The 2.8-kb 5' and 3.1-kb 3' arms were cloned into the pKS-neo-DTAIII vector and the nucleic acid G94T mutation (red asterisk) was introduced into exon 1 in the 5' arm resulting in the amino acid S32I mutation. **B**. Southern blot confirmed PCR genotyping (not shown). The neo cassette is approximately 1.7kb. Using the restriction enzyme NdeI, the WT allele DNA gives a band at 5.5kb, and the targeted allele 7.2kb. The neo cassette contains a HindIII site, so the targeted band is smaller, 3.7kb, and the WT allele is 6.9 kb. ES cell DNA and clone 1 (negative by PCR) were used as negative controls. After confirmation by sequencing, clone 4 was chosen for blastocyst injection.

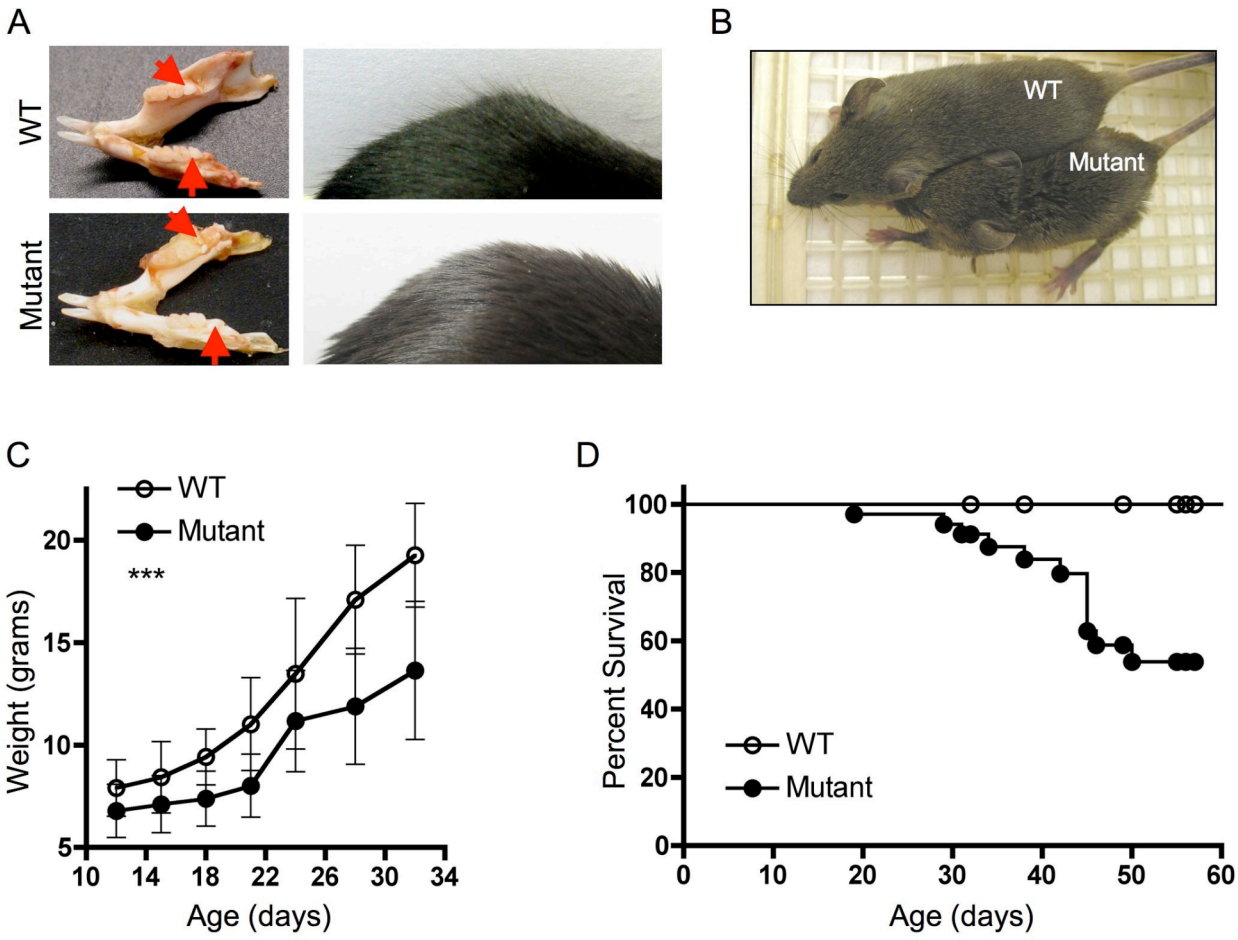

Figure 3.2. Mutant mice have ectodermal dysplasia and failure to thrive

A. The third molars (red arrows) are missing in mutant mice (left panel), and guard/tylotrich hairs are missing in the mutant (right panel). **B**. Photo and **C**. growth chart showing mutant mice are significantly smaller than their littermates. **D**. Survival is decreased in mutant mice.

3.3A). IκBα phosphorylation was distinctly weaker in fibroblasts from mutant mice. Densitometry scanning showed that the ratio of pIκBα:IκBα bands, as determined at 5 minutes, was 3.6±0.7-fold lower in the mutant fibroblasts than in the WT fibroblasts (Fig. 3.3B). Following IL-1 stimulation IκBα was mostly degraded by 15 minutes and completely degraded by 30 minutes in WT fibroblasts. In contrast, the ratio of the IκBα:actin bands showed markedly less degradation (27.8±5.5% of 0 minute timepoint) of IκBα in IL-1 mutant fibroblasts at all time points examined (Fig. 3.3C). Similar results to those obtained with IL-1 stimulation were found when the cells were stimulated with TNFα and LPS, two other well-known activators of the canonical NFκB pathway (data not shown). These results demonstrate that the mutant IκBα protein is expressed in cells from IκBα mutant mice and is resistant to phosphorylation and degradation.

IκBα mutant mice lack lymph nodes. Gross examination revealed a lack of detectable lymph nodes (LN) in IκBα mutant mice, including mesenteric, popliteal, paraaortic, inguinal, axial, and cervical LN, all of which were easily detected in WT littermates (Fig. 3.4A-C). Following the injection of Evan's blue dye in the footpad, lymphatic vessels were readily apparent and were comparable in mutant and WT mice. In contrast, no LN could be detected in the popliteal, inguinal or para-aortic area in the mutant, but were present in the WT control (Fig. 3.4B, C, and data not shown). No LN tissue could be detected in H&E stained serial sections of the inguinal fat pad in IκBα mutant mice (data not shown). Peyer's patches (PP) were readily visible in H&E stained sections of the small intestine of WT mice, but none could be detected in the mutants (Fig.

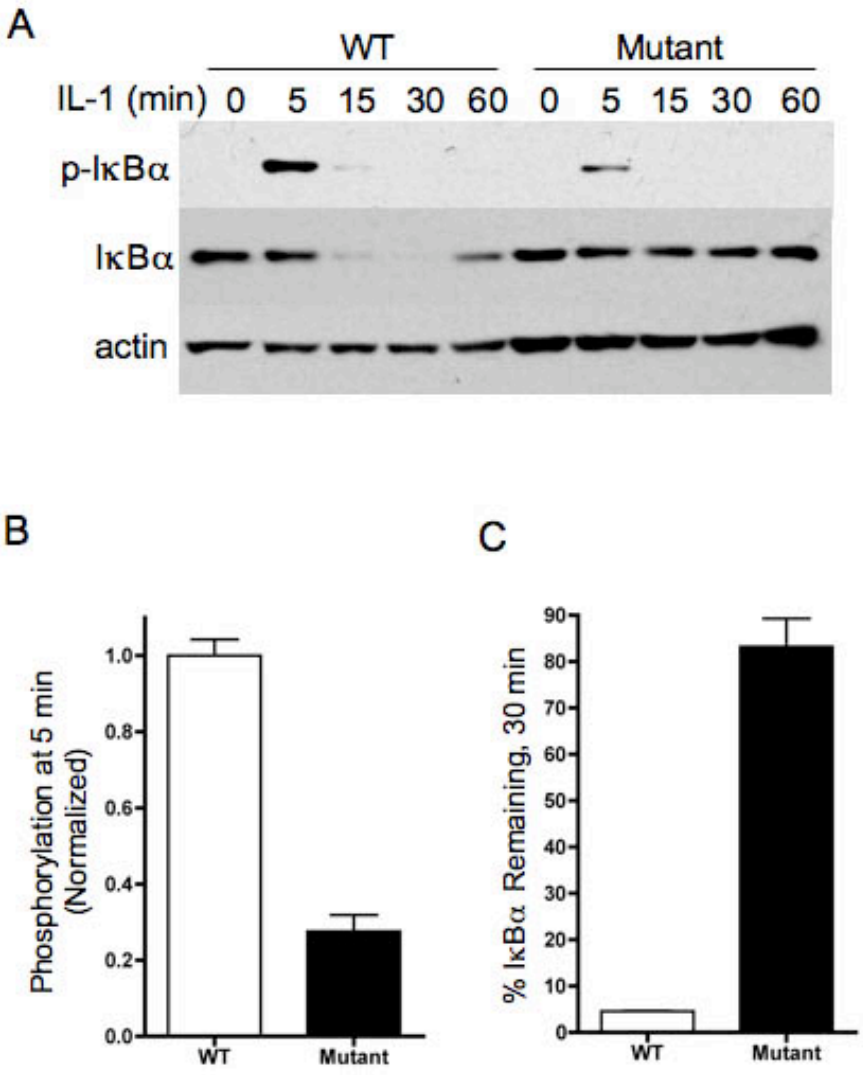

Figure 3.3. Mutant IκBα protein results in decreased NFκB activation

A. Western blot showing phosphorylation and degradation of IκBα following stimulation with 10ng/ml IL-1. **B**. Graph of phosphorylated IκBα/IκBα ratio, normalized to WT. **C**. Graph of IκBα/actin ratio comparing 0 and 30 min.

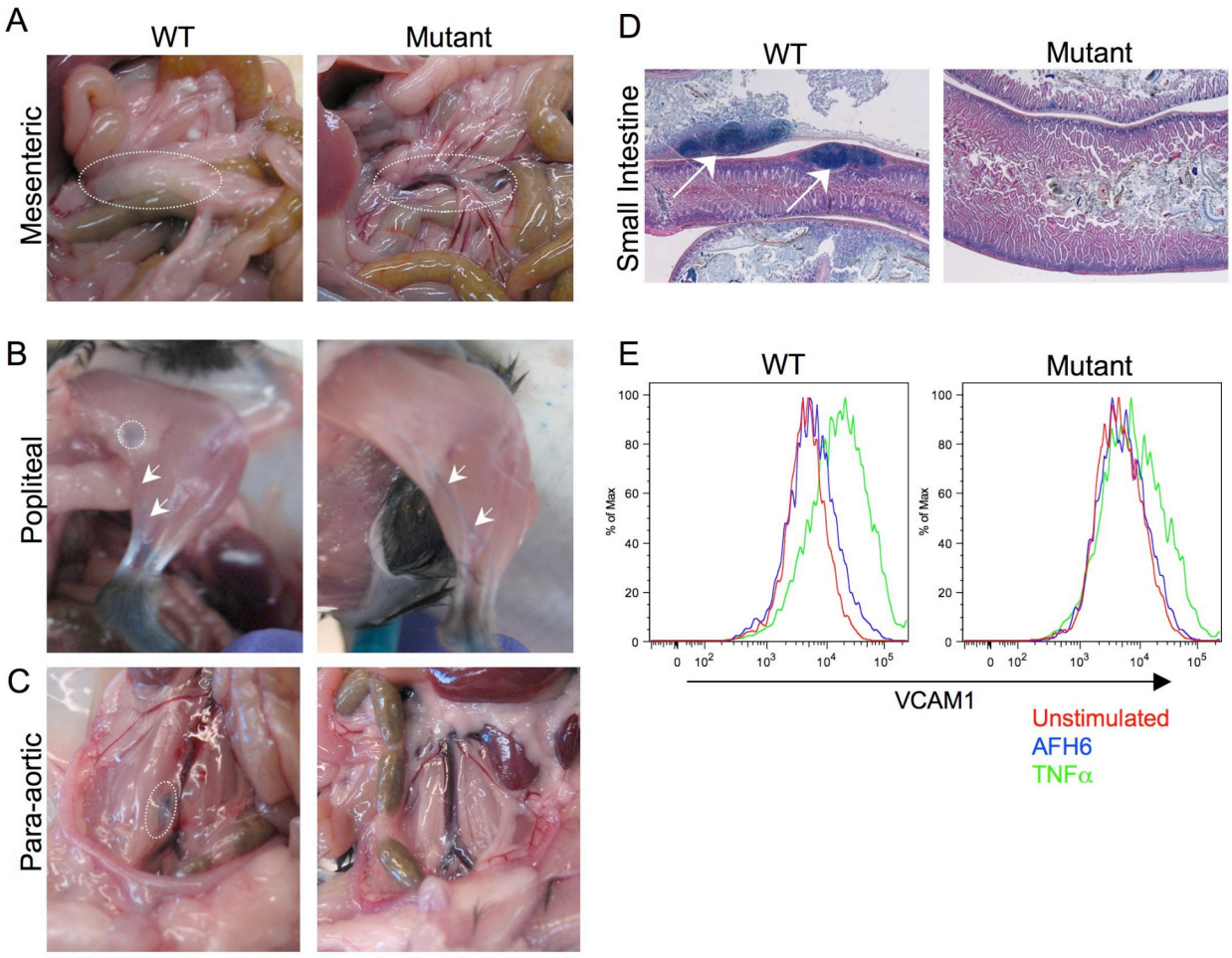

Figure 3.4. IκBα mutant mice lack lymph nodes.

A. Mesenteric lymph nodes (white ovals) are missing in mutant mice. **B**. Evan's blue dye was injected into the foot pad of freshly sacrificed mice in order to view the lymphatic vessels (white arrows) and inguinal lymph nodes (white circle). **C**. Evan's blue dye was injected into the foot pad of freshly sacrificed mice in order to view the para-aortic lymph nodes (white oval). **D**. H&E staining of mouse intestine showing Peyer's patches (white arrows). **E**. MEF from WT or mutant mice were stimulated with 2μg/ml AFH6 or 10ng/ml TNFα for 24 hours and VCAM1 surface expression was analyzed by flow cytometry.

3.4D). LN organogenesis requires the lymphotoxin β receptor (LTβR) signaling in stromal cells mediated by contact with lymphoid tissue inducer (LTi) cells that express the LTβR ligand $LT\alpha_1\beta_2$ on their surface[19, 20] (Fig. 3.5). LTβR, as well as TNFR, signaling in endothelial cells causes the expression of the adhesion molecule VCAM1 by activation of the canonical NFκB pathway[21]. As previously reported, stimulation with the agonistic LTβR mAb AFH6 or TNFα upregulated VCAM1 expression by WT mouse embryonic fibroblasts (MEFs)[21] (Fig. 3.4E). In contrast, AFH6 failed to upregulate VCAM1 expression in MEFs from IκBα mutant mice and TNFα weakly upregulated it. This suggests that defective LTβR signaling may account, at least in part, for the lack of LN and PPs in IκBα mutant mice.

Disrupted architecture of lymphoid organs and absent marginal zone (MZ) B cells in IκBα mutant mice. The size and cellularity of the thymus was comparable in WT and IκBα mutant mice (Fig. 3.6A). The distribution of thymocyte subsets into $CD4^-CD8^-$ double negative (DN) cells, $CD4^+CD8^+$ double positive (DP) cells and $CD4^+$ or $CD8^+$ single positive (SP) cells were comparable in IκBα mutant mice and WT littermates (Fig. 3.6B). However, thymic architecture was disrupted in the IκBα mutant mice. They had a smaller medulla with a greater density of lymphocytes, and a lesser density of lymphocytes in the cortex than in WT littermates (Fig. 3.6C).

Bone marrow cellularity and distribution of ($B220^+IgM^-CD43^+$) pro-B, ($B220^+IgM^-CD43^-$) pre-B, ($B220^+IgM^+$) immature and ($B220^{++}IgM^+$) mature B cell subsets were comparable in IκBα mutant mice and WT littermates (Fig. 3.6D).

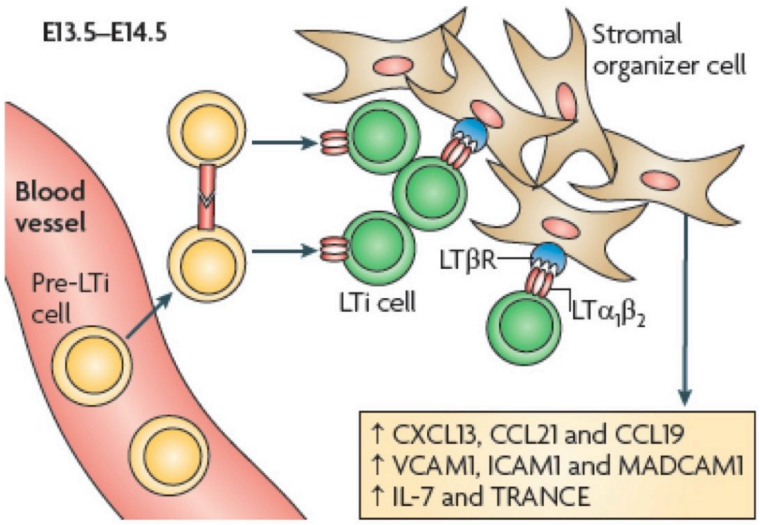

Figure 3.5. Schematic of LN formation from van de Pavert and Mebius, 2010[19].

Clustering of pre-LTi cells facilitates signaling through tumor necrosis factor related activation-induced cytokine receptor (TRANCER) which leads to the induction of $LT\alpha_1\beta_2$, and differentiation into mature LTi cells. Interaction of $LT\alpha_1\beta_2$-expressing LTi cells with LTβR-expressing stromal cells results in their differentiation into stromal organizer cells, which express chemokines, adhesion molecules and cytokines. These factors support attraction and retention of more hematopoietic cells, leading to LN growth.

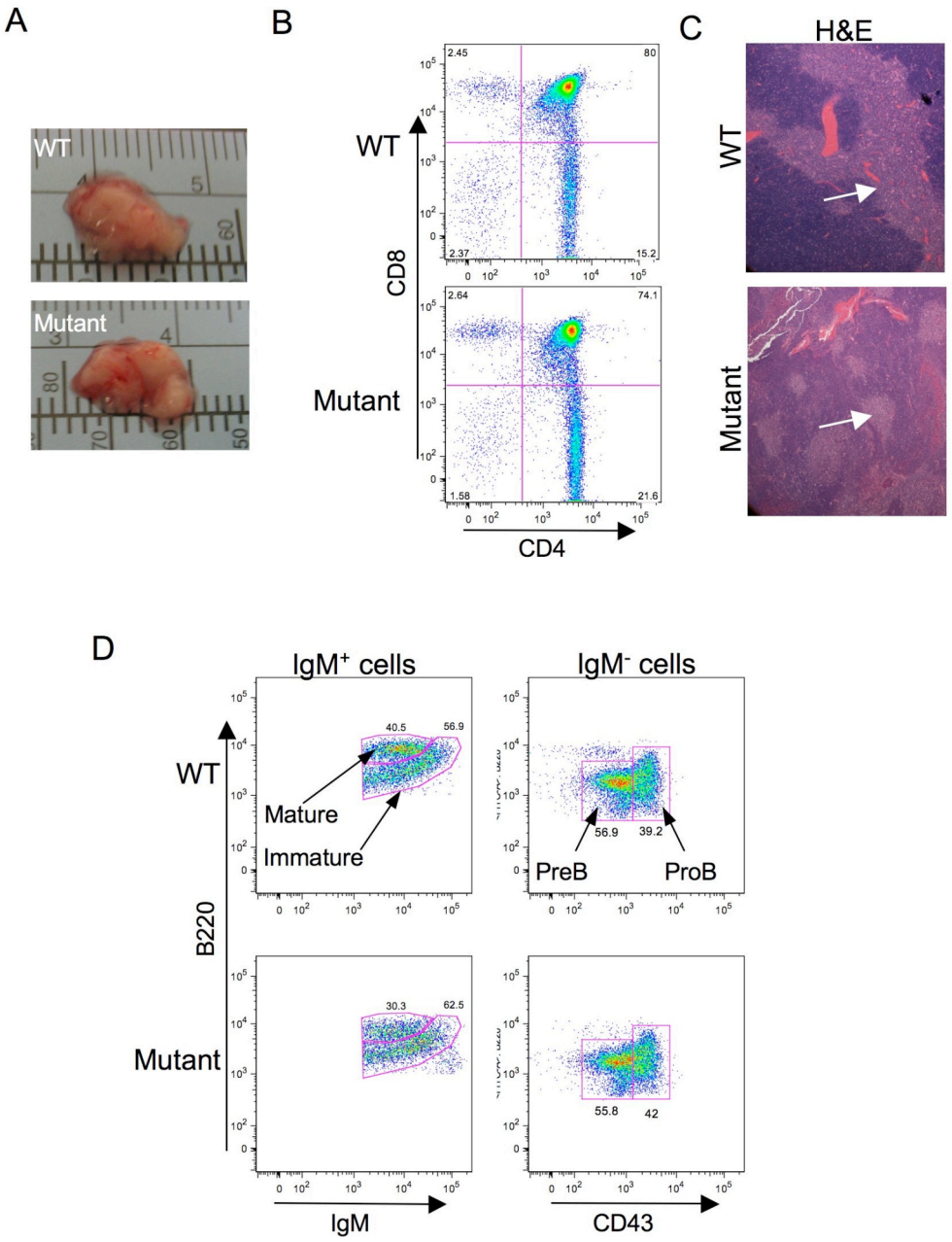

Figure 3.6. Size and cellularity of thymus and bone marrow are normal in IκBα mutant mice

A. Photo of thymus from WT and mutant mice. **B**. Flow cytometric analysis of thymocytes showing CD4 and CD8 double negative, double positive and single positive populations. **C**. H&E staining of thymus from WT and mutant mice. **D**. Flow cytometric analysis of $B220^+$ B cells from bone marrow of WT and mutant mice showing IgM^+B220^{high} mature cells, IgM^+B220^+ immature B cells, IgM^- $B220^+$ $CD43^-$ preB cells and $IgM^-B220^+CD43^+$ proB cells.

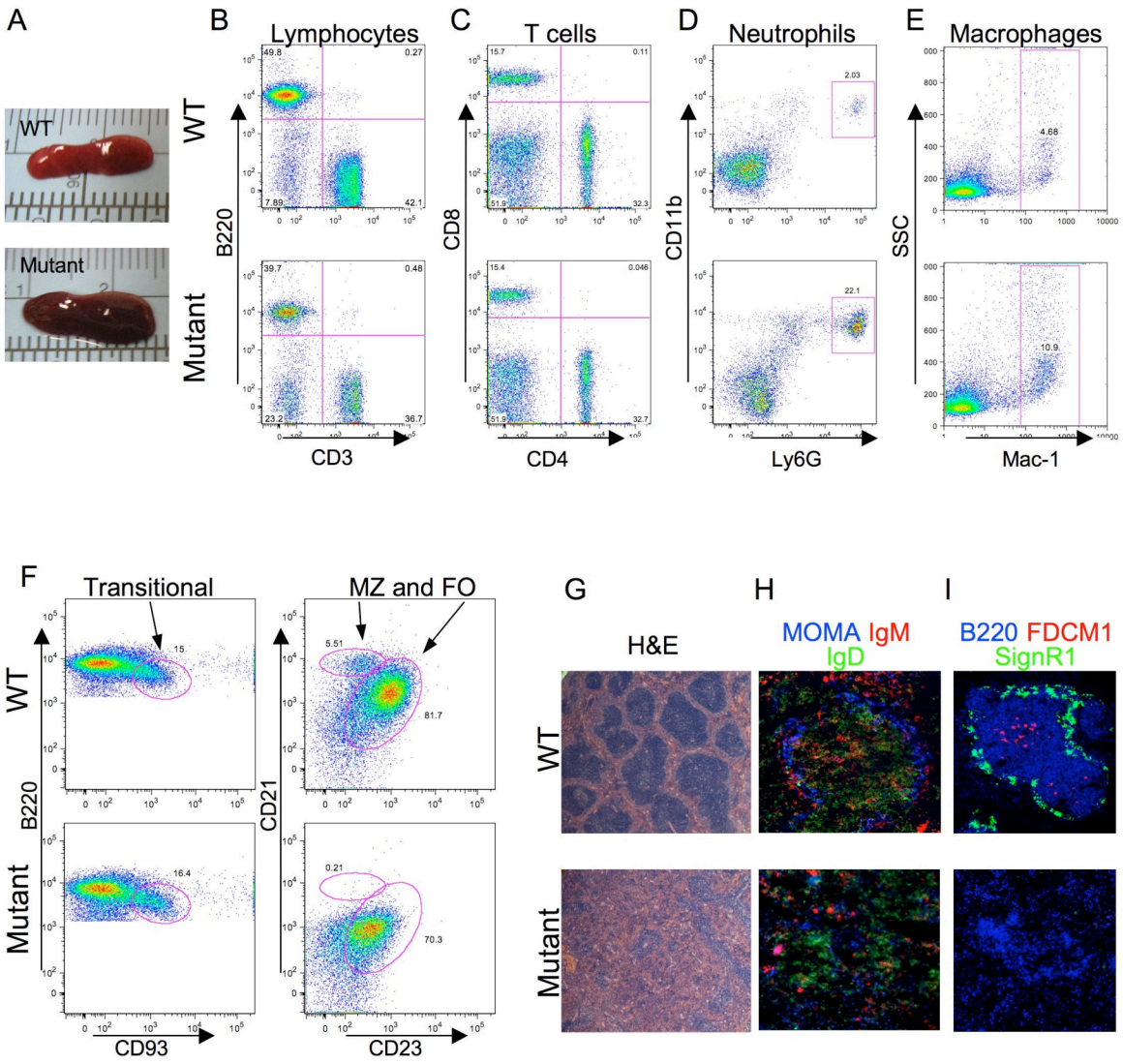

Figure 3.7. Splenic architecture in IκBα mutant mice is impaired.

A. Photo of spleen showing splenomegaly in the mutant. **B**. Flow cytometric analysis of $B220^+$ and $CD3^+$ cells in the spleen. **C**. Flow cytometric analysis of $CD4^+$ and $CD8^+$ cells in the spleen. **D**. Flow cytometric analysis of $CD11b^+Ly6G^+$ neutrophils and **E**. Mac-1^+ macrophages. **F**. Flow cytometric analysis of $B220^+$ splenocytes stained with anti-CD93 to identify transitional B cells, or anti-CD21 and anti-CD23 to identify follicular (FO) and marginal zone (MZ) B cells. **G**. H&E staining of spleen sections. **H**. Immunofluorescent staining of spleen sections stained with anti-MOMA (blue), anti-IgM (red) and anti-IgD (green) in order to show marginal zone structure. **I**. Immunofluorescent staining of spleen stroma for FDCs, red: FDCM1, blue: B220, green: SIGNR1 to identify B cell follicles and FDCs, respectively.

The size and cellularity of the spleen were greater in IκBα mutant mice than WT littermates (Fig. 3.7A). The ratio of $B220^+$ to $CD3^+$ cells was similar between the two groups (Fig. 3.7B), although there was a larger non-lymphocyte population in the IκBα mutant spleens. The distribution of $CD4^+$ and $CD8^+$ subsets were comparable in the two groups (Fig. 3.7C). There was an increased percentage of $CD11b^+$ cells including $Ly6G^+$ neutrophils and of Mac-1^+ macrophages (Fig. 3.7D, E). Analysis of B cell subsets showed a virtual loss of MZ B cells in IκBα mutant mice (0.30±0.03% of $B220^+$ cells in IκBα mutant mice versus 5.23±0.18% in WT littermates, $p<.001$), but the percentages of transitional B cells and follicular B cells were normal in these mice (Fig. 3.7F). Histological examination revealed poor demarcation of the white and red pulps and poorly developed follicles in spleens of IκBα mutant mice (Fig. 3.7G). Immunofluorescence analyses revealed that although $MOMA^+$ macrophages were present in IκBα mutant mice, they failed to form the ring structure typical of a MZ (Fig. 3.7H). Immunofluorescence analysis also showed that $FDCM1^+$ or $CD35^+$ follicular dendritic cells (FDCs) were absent from the spleens of IκBα mutant mice (Fig. 3.7I). Thus, even though T and B cell subsets, except for MZ B cells, were present at comparable numbers, the architecture of the spleen was severely disorganized.

Normal T cell response *in vitro*, but impaired delayed contact hypersensitivity (CHS) in IκBα mutant mice. Purified splenic T cells from IκBα mutant mice and WT littermates, proliferated and secreted IL-2 to a comparable extent in response to immobilized anti-CD3 mAb (Fig. 3.8A). Furthermore purified

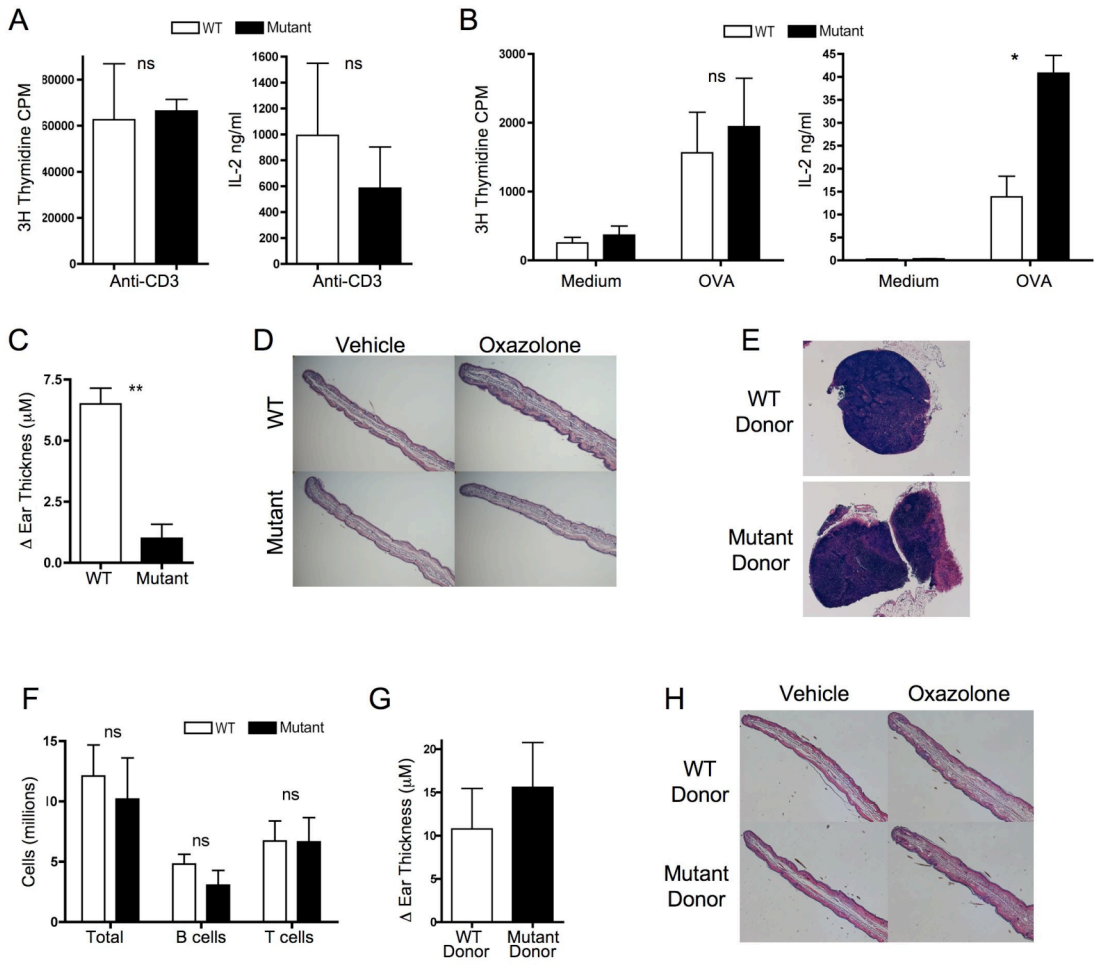

Figure 3.8. Response to TCR stimulation is intact, but *in vivo* responses involving T cells are impaired.

A. Proliferation and IL-2 production from purified splenic T cells stimulated with coated anti-CD3 mAb. WT or mutant cells stimulated with medium alone were <300 CPM, with negligible IL-2 production. **B**. Proliferation and IL-2 production to OVA from splenic T cells purified from OVA-immunized mice. **C**. Difference in thickness between oxazolone- and vehicle-challenged ears at 24 hours post-challenge. **D**. H&E staining of oxazolone- and vehicle-challenged ears at 24 hours. **E**. H&E staining of LN from $Rag2^{-/-}$ mice reconstituted with WT or mutant BM. **F**. Cellularity of one axillary and one inguinal LN from each chimeric mouse. B cells were defined as $B220^{+}$ and T cells as $CD3^{+}$. **G**. Difference in thickness between oxazolone- and vehicle-challenged ears from chimeric mice at 24 hours post-challenge. **H**. H&E staining of oxazolone- and vehicle-challenged ears from chimeric mice at 24 hours.

splenic T cells from IκBα mutant mice and WT littermates immunized intraperitoneally (i.p.) with ovalbumin (OVA) were comparable in their ability to proliferate and secrete IL-2 in response to OVA presented by WT irradiated splenic non-T cells (Fig. 3.8B).

The T cell response to cutaneously introduced antigen depends on the interaction in skin draining LN between recirculating antigen-specific T cells and DCs that have captured antigen. We investigated the ability of IκBα mutant mice to mount a CHS response to the hapten oxazolone. IκBα mutant mice sensitized with oxazolone developed significantly less ear swelling, markedly less cellular infiltration and edema than WT controls (Fig. 3.8C, D). These data indicate that T cells from IκBα mutant mice have no intrinsic defect in responding to antigen receptor ligation, and can be educated *in vivo* to respond to antigen delivered intraperitoneally. However they fail to be educated to cutaneously introduced antigen, likely because they lack LN.

To demonstrate that the lack of LN rather than an intrinsic T cell defect is responsible for the inability of IκBα mutant mice to mount a CHS response, we reconstituted irradiated $Rag2^{-/-}$ mice with bone marrow (BM) from these mice and WT littermates. $Rag2^{-/-}$ mice possess LTi cells and the crosstalk between LTi cells and stromal cell is intact in these mice[20]. Thus they develop LN populated with T and B cells following transplantation of WT normal BM cells. LN from $Rag2^{-/-}$ mice reconstituted with BM from IκBα mutant mice (hereafter referred to as IκBα mutant chimeras) were comparable in size and content to LN from $Rag2^{-/-}$ mice

reconstituted with BM from WT littermates (hereafter referred to as WT chimeras) (Fig. 3.8E, F).

IκBα mutant chimeras mounted a CHS response to oxazolone comparable to that of WT chimeras, as evidenced by ear swelling, cellular infiltration and edema (Fig. 3.8G, H). These findings indicate that the lack of CHS in IκBα mutant is not due to an intrinsic defect in hematopoietically derived cells and that the reduced CHS in these mice is likely due to their lack of LN.

Impaired *in vitro* and *in vivo* B cell function in IκBα mutant mice. Purified splenic B cells from IκBα mutant mice proliferated significantly less in response to stimulation with anti-CD40+IL-4 or LPS+IL-4, compared to B cells purified from WT littermates (Fig. 3.9A). CFSE dilution studies showed both delayed and reduced proliferation in the IκBα mutant B cells (Fig. 3.9B). Purified IκBα mutant B cells produced significantly less IgM than WT B cells after stimulation with anti-CD40+IL-4 and LPS+
IL-4, while IgG production was not statistically different between the two groups (Fig. 3.9C). Serum IgM levels were comparable in IκBα mutant mice and WT littermates but serum IgG levels were significantly decreased in the mutants (Fig. 3.9D). Serum IgA level was nearly absent in IκBα mutant mice.

Antibody responses to the type I T-independent (TI) antigen TNP-LPS, the type II TI antigen TNP-Ficoll, and the T-dependent (TD) antigen OVA were severely diminished in IκBα mutant mice (Fig. 3.10A-C). The specific antibody response to TD antigens requires germinal center (GC) formation[22]. OVA immunization resulted in the robust development of GCs in the spleens of WT

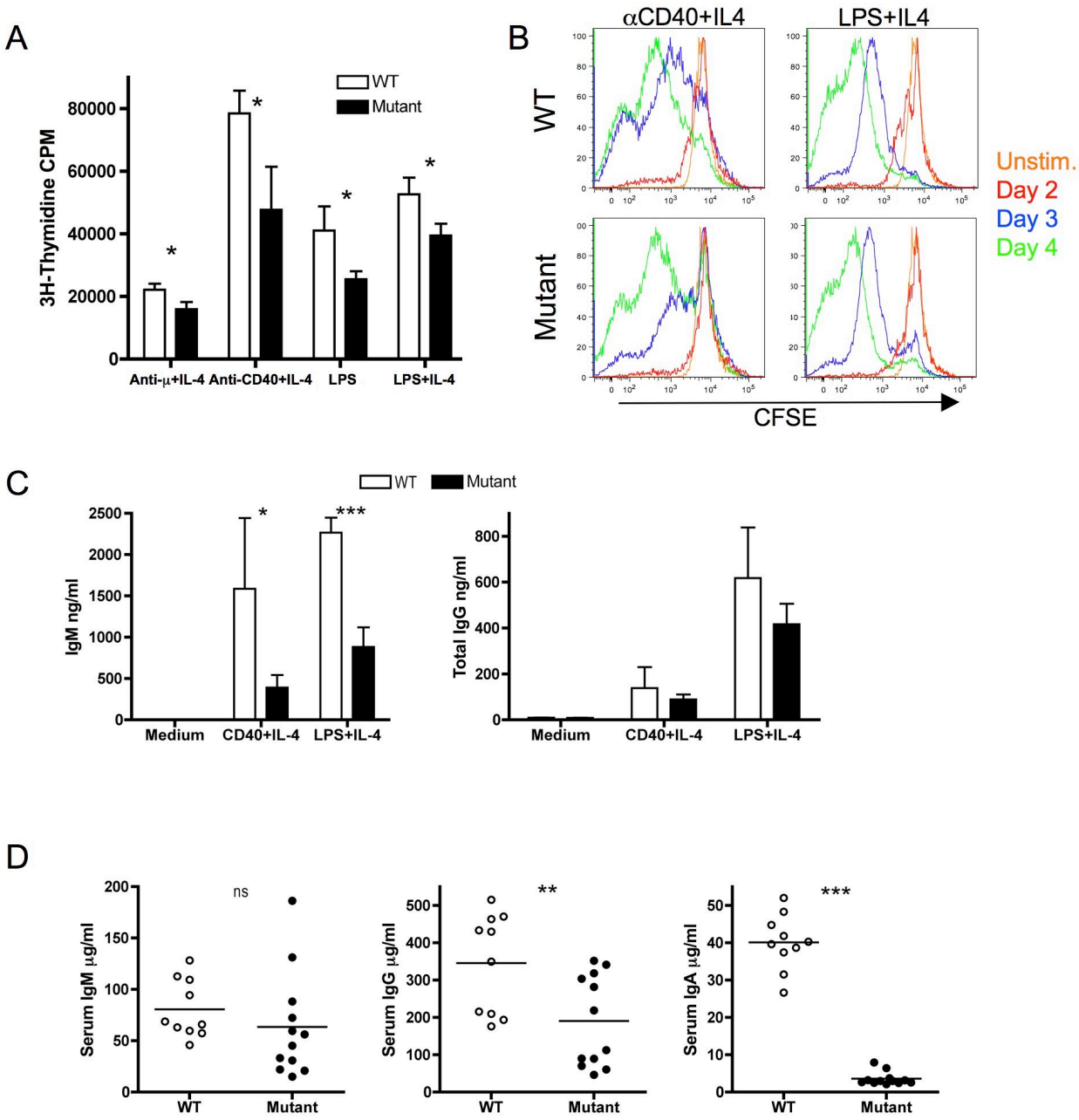

Figure 3.9. B cell function is reduced *in vitro* and IκBα mutant mice have low serum IgM and IgA

A. *In vitro* proliferation of purified splenic B cells to several antigens. **B**. CFSE dilution experiment showing proliferation of purified splenic B cells. **C**. *In vitro* immunoglobulin production to anti-CD40+IL-4 and LPS+IL-4. **D**. Baseline serum antibody concentrations as determined by ELISA.

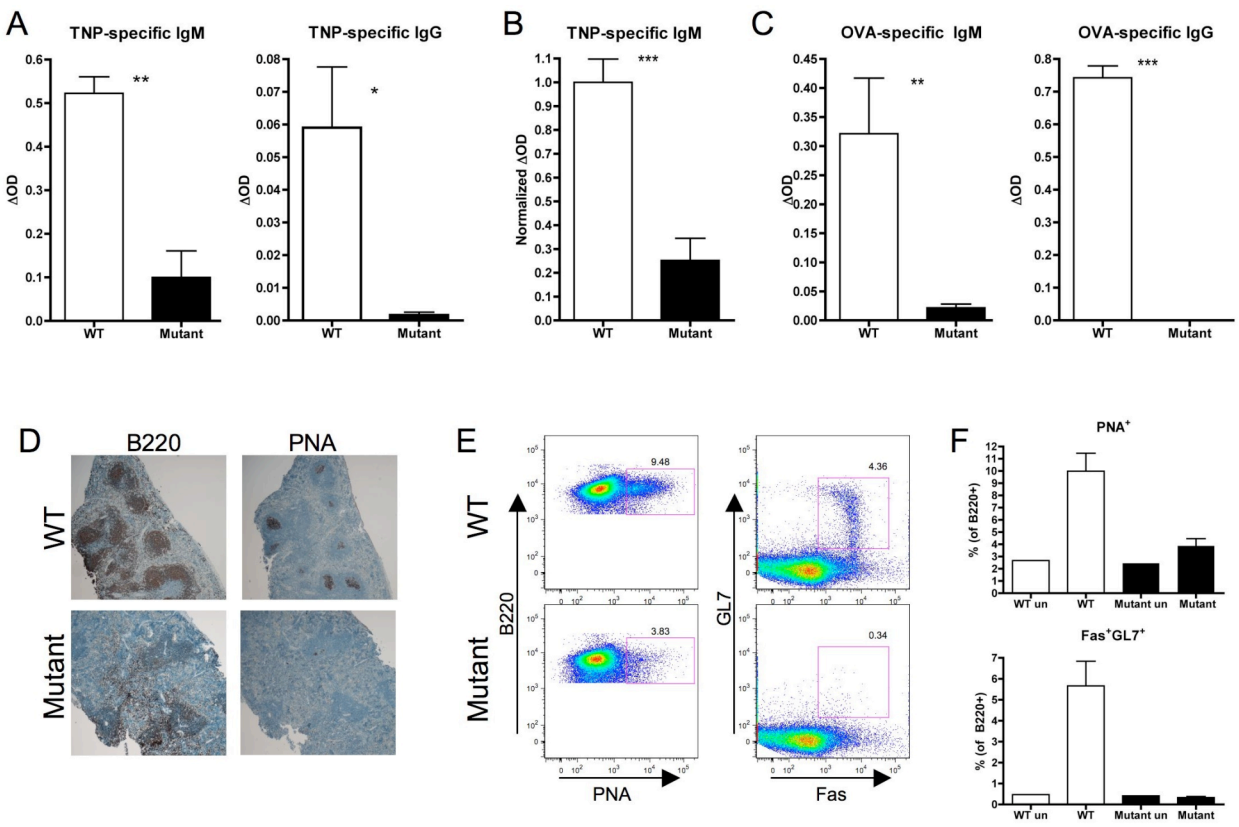

Figure 3.10. Specific antigen formation and GC formation *in vivo* are severely impaired

A. TNP-specific serum Igs after immunization with TNP-LPS, reported as the difference in absorbance between day 14 and day 0 for each mouse. **B**. TNP-specific serum Ig after immunization with TNP-Ficoll, reported as the difference in absorbance between day 14 and day 0 for each mouse. **C**. OVA-specific serum Igs after immunization with OVA, reported as the difference in absorbance between day 21 and day 0 for each mouse. **D**. B220 and PNA IHC of spleen sections from WT and mutant mice after 10-day immunization with OVA. **E**. Representative flow cytometric analysis after 10-day immunization with OVA (gated on $B220^+$). GC B cells were identified at $B220^+PNA^+$or $B220^+GL7^+Fas^+$. Unimmunized mice (un) were included as controls. **F**. Quantification of flow cytometric analysis on GC B cells.

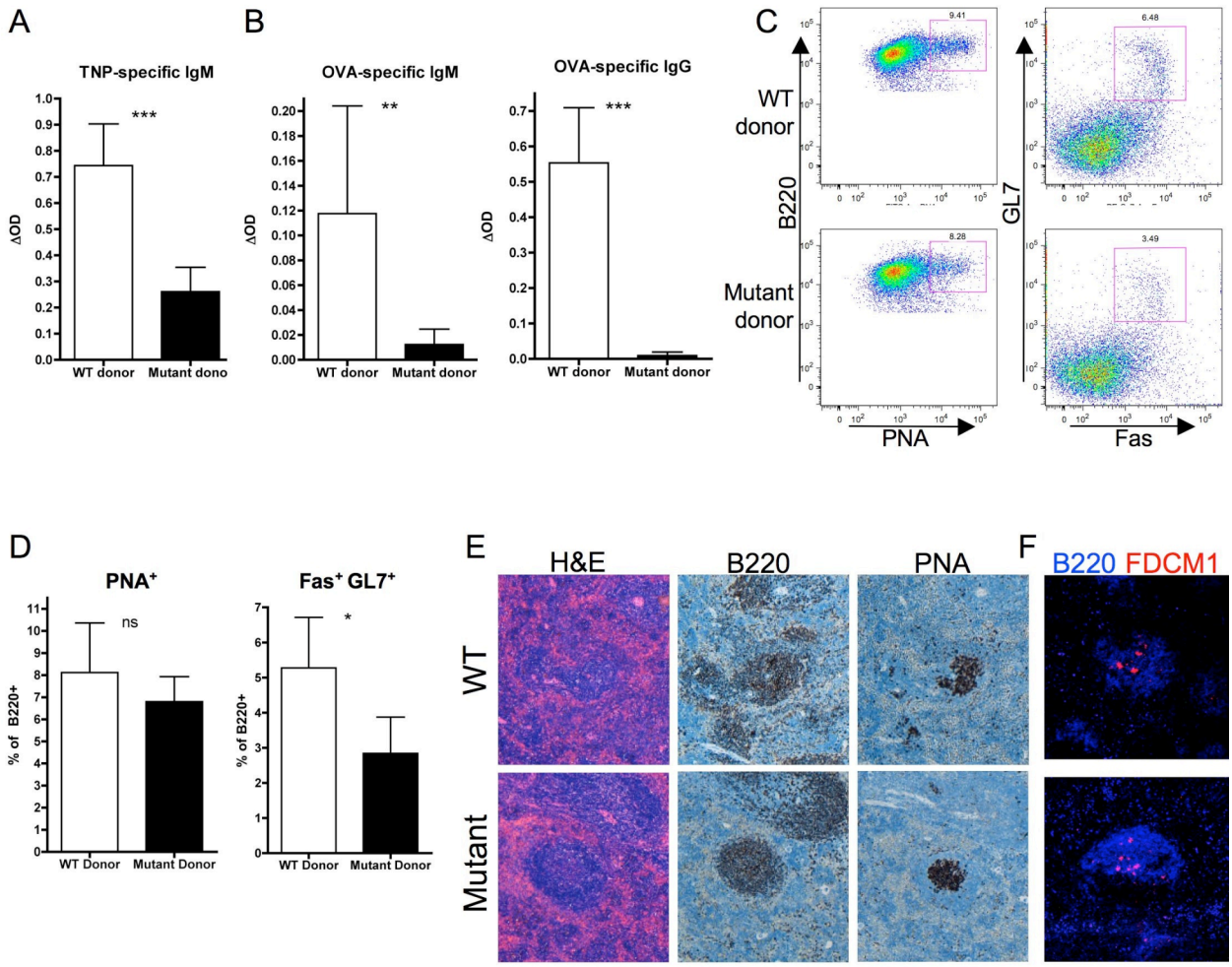

Figure 3.11. Rag2$^{-/-}$ mice reconstituted with IκBα mutant bone marrow can form PNA^{+} germinal centers, but do not produce specific antibodies

A. TNP-specific serum Igs after immunization with TNP-Ficoll, reported as the difference in absorbance between day 14 and day 0 for each chimera. **B**. OVA-specific serum Igs after immunization with OVA, reported as the difference in absorbance between day 21 and day 0 for each chimera. **C**.Representative plot and **D**. quantification of flow cytometric analysis of spleens after 10-day immunization with OVA (gated on B220+). **E**. Spleen sections from Rag2$^{-/-}$ bone marrow chimeras after 10-day immunization with OVA. Paraffin sections were stained with H&E, B220 or PNA. **F**. Immunofluorescent staining of spleen stroma for FDCs, red: FDCM1, blue: B220.

mice as evidenced by staining for peanut agglutinin (PNA). In contrast, GC development was severely deficient in IκBα mutant mice (Fig. 3.10D). The percentage of $B220^+PNA^+$ and $B220^+Fas^+GL7^+$ GC B cells in the spleen was significantly lower in OVA immunized IκBα mutant mice than WT controls (Fig. 3.10E,F). IκBα mutant B cells have a modest proliferation defect and the mutant mice are unable to form germinal centers and mount a specific antibody response to antigens.

The defect in antibody production in IκBα mutant mice is intrinsic to B cells. To determine if the defective antibody production in IκBα mutant mice was intrinsic to the B cells, we examined $Rag2^{-/-}$ chimeric mice. Antibody responses to the TI antigen TNP-Ficoll and to the TD antigen OVA were significantly lower in IκBα mutant chimeras than in control WT chimeras (Fig. 3.11A, B). Examination of spleens from IκBα mutant chimeras revealed the presence of follicles that were comparable in size and number to those in WT chimeras (Fig. 3.11E, left panel). Following i.p. immunization with OVA, the percentage of $B220^+PNA^+$ and $B220^+Fas^+GL7^+$ cells in the spleens of immunized mice was comparable in IκBα mutant chimeras and WT chimeras (Fig. 3.11C, D), but antibody response remained deficient, indicating that an intrinstic defect exists in the B cells of IκBα mutant chimeras. IκBα mutant chimeras developed PNA^+ GCs in their spleens which were similar to control WT chimeras (Fig. 3.11E, middle and right panels). $CD35^+$ follicular dendritic cells are absent in $Rag2^{-/-}$ mice[23], but were readily and comparably detectable in spleens of IκBα mutant and WT OVA-immunized chimeras (Fig. 3.11F). Therefore, in chimeric mice, where the stroma is WT,

spleen follicle, follicular dendritic cells and germinal center formation are supported.

DISCUSSION

We have generated knock-in mice heterozygous for the S32I mutation in IκBα that abolishes ligand-induced IκBα phosphorylation and causes ED-ID in patients. In addition to ED, the mice lacked LN, PP, splenic follicles and FDCs, had severely impaired delayed contact hypersensitivity and antibody responses and failed to form germinal centers. All these defects, except for the defective antibody responses, were corrected in IκBα mutant chimeras, and thus they likely resulted from a defect in stromal cells.

The IκBα S32I mutant mice had ectodermal dysplasia, similar to ED-ID patients carrying the same mutation and *tabby* mice, which have a mutation in the EDA gene[8]. The size and weight of the mutant mice were smaller than those of their WT littermates, possibly due to poor ability to compete against WT littermates for food and/or to their ectodermal defects. One ED-ID patient with the S32I mutation in IκBα had a reduced response to growth hormone (GH)[24]. The response to GH remains to be investigated in the mutant mice.

The total amount of IκBα protein appeared to be comparable in mutant and WT fibroblasts. Since IκBα is under transcriptional regulation by NFκB, diminished NFκB activation in the mutant would result in lower expression of both alleles. However, this would be counterbalanced by decreased degradation of mutant protein, leading to a relative increase of IκBα mutant protein compared to WT protein. This would explain the comparable amounts of total IκBα protein in mutant and WT fibroblasts. We were unable to evaluate the relative expression levels of the mutant and WT proteins in the mutant fibroblasts, because the two

proteins migrate together and there are no available antibodies that distinguish between them. Nevertheless, a portion of the protein does not degrade after stimulation, and the disease is recapitulated in these mice.

Following IL-1 stimulation, virtually 100% of the IκBα protein was degraded in WT fibroblasts. In contrast, IL-1 stimulation resulted in the degradation of only ~20% of IκBα protein in the mutant fibroblasts. Assuming a comparable translation efficiency of WT and mutant mRNA, this result strongly suggests that the mutant protein accumulates to a higher level than the WT protein. In addition, the mutant might interfere with the degradation of WT protein by sequestering the IKK complex, and undegraded WT protein would account for some of the IκBα protein that remains intact following IL-1 stimulation of the mutant. One or both of these mechanisms would explain the previous observation that the S32I mutant acts as a dominant negative in an NFκB reporter gene assay[9].

IκBα mutant mice completely lacked LN and PP. The formation of LN and PP depends on the interaction of stromal cells with $CD4^+CD3^-IL\text{-}7R\alpha^+$ LTi cells, which express TNFα and LTαβ. This results in the activation of the NFκB pathway in stromal cells, which is essential for LN formation. This is evidenced by the observation that $LT\beta R^{-/-}$ $LT\alpha^{-/-}$ and $RelA^{-/-}/TNFR^{-/-}$ mice have absent LN and PP, while $TNF\alpha^{-/-}$ and $TNFR^{-/-}$ mice have poorly formed PP. LTi cells do not depend on NFκB for their development, as they are present in normal numbers in $RelA^{-/-}/TNFR^{-/-}$ mice[25]. We therefore do not expect their numbers to be reduced in

the IκBα mutant mice. Direct proof of normal LTi numbers in the mutant mice will require direct examination of $CD4^+CD3^-$IL-7Rα^+ LTi cells in embryonic intestines.

TNFα and LTβR signaling in stromal cells results in the expression of adhesion molecules, including VCAM1, which are essential for LN and PP formation[19]. We gathered strong evidence that TNFα signaling and signaling via LTβR are deficient in the mutant. Using MEFs, we showed that TNFα and ligation of LTβR by agonistic mAb failed to upregulate the expression of the adhesion molecule VCAM1 in the mutant. This result strongly suggested that impaired NFκB signaling in stromal cells underlies the failure of IκBα mutant mice to form LN and PP. This was supported by the observation that BM cells from the mutant reconstituted LN and PP in $Rag2^{-/-}$ recipients. The observation that IκBα mutant lymphocytes populated LN, PP (data not shown) and spleen in $Rag2^{-/-}$ recipients also rules out a homing defect in lymphocytes from IκBα mutant mice.

IκBα mutant mice lacked MZ and $B220^+CD21^+CD23^-$ MZ B cells in their spleens. $MOMA^+$ macrophages which are normally adjacent to MZ B cells and form a ring-like structure outside the follicle, were present in apparently normal numbers, but were dispersed. Proper MZ formation, like LN and PP formation, depends on TNFα and LTβR activation of the NFκB pathway in stromal cells. This is evidenced by the observation that LTβR$^{-/-}$, LTα$^{-/-}$ and $p50^{-/-}$ mice have no MZ B cells, and $TNF^{-/-}$ and $TNFR^{-/-}$ mice have reduced MZ[26]. TNFα and LTβR signaling in stromal cells results in NFκB mediated upregulation of the expression of the adhesion molecule MAdCAM1, which is critical for MZ formation[27]. MAdCAM1 expression was absent in spleens from mutant mice

(data not shown), implicating failure to express MAdCAM1 in the lack of MZ development in these mice. MZ formation has been reported to be dependent on BCR dependent NFκB activation in B cells[28]. MZ B cells were reconstituted in IκBα mutant Rag2$^{-/-}$ chimeras indicating that a B cell intrinsic defect did not contribute to the lack of MZ in the mutant. This is consistent with findings in RelA$^{-/-}$/TNFR$^{-/-}$->Rag2$^{-/-}$ chimeras[25].

IκBα mutant mice lacked FDCs and B cell follicles, and failed to form GCs. Spleens from IκBα mutant mice lacked FDCM1^{+} cells and had poorly formed follicles. Following i.p. immunization with OVA, IκBα mutant mice failed to develop GCs, as evidenced by lack of PNA^{+} staining of spleen sections and lack of B220^{+}PNA^{+} and B220^{+}Fas^{+}GL7^{+} cells by FACS analysis. FDCs are derived from non-hematopoietic stromal cell precursors and play an important role in the formation of follicles and GCs. NFκB activation by TNFR and LTβR signaling in stromal cells and TNFα and LT$\alpha_1\beta_2$ expression on B lymphocytes are important for FDC development and the formation of B cell follicles and GCs. This is evidenced by the observation that LTβR$^{-/-}$, LTα$^{-/-}$, LTβ$^{-/-}$ TNFα$^{-/-}$ and TNFR$^{-/-}$ mice, and mice whose B cells lack TNFα and LTβ have no FDCs and do not form follicles or GCs[26, 29]. FDCs, follicles and GC formation were all restored in IκBα mutant Rag2$^{-/-}$ chimeras. This observation, together with the finding that T cells from IκBα mutant mice proliferated normally to OVA and expressed normal amounts of CD40 ligand following anti-CD3 stimulation, rules out a role for a T cell defect in the failure of GC formation in these mice. Taken together, these results strongly suggest that impaired NFκB signaling in stromal cells resulted in

the failure of FDC development, and the subsequent failure to form follicles and GCs in IκBα mutant mice.

Except for the lack of MZ B cells, T and B cell numbers and subset distribution in the spleen were comparable in numbers and percentages in the spleen of IκBα mutant mice. This is consistent with a normal T and B cell distribution in the peripheral blood of ED-ID patients with the same IκBα mutation[9, 10]. GCs are not formed, so post-GC subsets were not enumerated in these mice. There was no discernable intrinsic defect in T cells from IκBα mutant mice. Splenic T cells from these mice proliferated and secreted IL-2 normally in response to anti-CD3 and antigen administered i.p. In contrast, CHS hypersensitivity was severely impaired in IκBα mutant mice. Successful sensitization to skin painting with hapten requires the encounter between hapten-laden DCs and recirculating antigen specific T cells in skin draining LN [30]. This is evidenced by the observation that CHS is severely deficient in $LT\alpha^{-/-}$ mice, which lack LN [31]. CHS was restored in IκBα mutant chimeras, indicating that the defective CHS in IκBα mutant mice was not due to an intrinsic T cell defect, but to their lack of LN. In contrast to T cells from our mutant mice, T cells from ED-ID patients with the same IκBα S32I mutation have impaired proliferation to anti-CD3, which, however, was restored by anti-CD28 or IL-2[9, 10]. The reason for this difference is not clear but may relate to the persistent presence of infections in the patients, and the absence of obvious infections in the IκBα mice which were kept in autoclaved cages in a specific pathogen free facility and on oral sulfamethoxazole and trimethoprim prophylaxis.

B cells from IκBα mutant mice had a modest, but significant reduction in their ability to proliferate in response to all stimuli tested. These included BCR ligation with anti-IgM (BCR crosslinking), anti-CD40+IL-4 (CD40 ligation) and LPS+IL-4 (TLR ligation). B cells from IκBα mutant mice also secreted less IgM and IgG in response to anti-CD40+IL-4 and LPS+IL-4 compared to WT B cells, but only the difference in IgM secretion was significant. The decreased IgM and IgG production *in vitro* is consistent with the decreased B cell proliferation. Serum IgM was normal, IgG was low, and IgA was undetectable in the mutant mice. This profile is similar to that of ED-ID patients with the same mutation. Decreased isotype switching could be explained by the known role of NFκB in driving the expression of AID and germline transcripts in B cells[32], as well as the structural defects preventing T and B cells from meeting their antigens. Absence of PP in IκBα mutant mice is likely involved in their total lack of serum IgA. The normal serum IgM in IκBα mutant mice may reflect increased differentiation of their B cells into IgM producing plasma cells, because of the impaired isotype switching.

Lack of specific antibody responses to vaccines has been documented in ED-ID patients with IκBα mutations[9-11]. Similarly, IκBα mutant mice did not produce specific antibodies to immunization with T-dependent or T-independent antigens. Defective TD antibody responses in IκBα mutant mice were expected from their failure to form GCs. However, TD antibody responses remained deficient in IκBα mutant chimeras, despite the formation of GCs. These findings suggest that failure to form GCs and an intrinsic B cell defect in responding to T cell help are both operative in the IκBα mutant mice. Given the importance of

CD40L-CD40 interactions in TD antibody responses, a likely element of this intrinsic defect in responding to TD antigen is the impaired response of IκBα mutant B cells to CD40 ligation. An intrinsic B cell defect was also demonstrated to underlie defective TI antibody responses in these mice, since these responses also remained deficient in the IκBα mutant Rag2$^{-/-}$ chimeras. Impaired responses to TLR and BCR ligation likely underlie the defective response of IκBα mutant B cells to TI type I and II antigens.

The poor response to immunization is a two-fold problem, in that the mutant B cells do not respond well *in vitro*, nor can they form proper GC. In the IκBα mutant chimeras, even when FDCs were present and GCs were formed, they were not functional and did not produce specific antibody. A reduced B cell response to CD40 ligation may account for the lack of functional GCs in the IκBα mutant chimeras, as it would impair selection and T cell help. Given our results, it is likely that the reported failure of the patients to mount antibody responses to specific antigens is due to failure to generate antigen specific helper T cells because of potential lack of LN that drain the site of intramuscular antigen administration of TD antigens, as well as to an intrinsic B cell defect that impair their B cell responses to both TI and TD antigens.

Based on our observations, the development of secondary lymphoid organs might be impaired in ED-ID patients with the IκBα S32I mutation, because of an intrinsic defect in non-hematopoietic cells. Furthermore, one would expect that allogeneic hematopoietic stem cell transplantation (HSCT) may fall short of reconstituting the immune response of these patients. There is no report

on the status of LN in these patients. However, it has been reported that the single patient with the S32I mutation who has survived HSCT does not have visible tonsils or palpable LN during infections. In addition, the patient has needed to be kept on intravenous gammaglobulin replacement therapy and prophylactic antibiotics. These findings are consistent with poor lymphoid organogenesis and persistent failure to mount protective antibody responses following HSCT. Current experiments are directly addressing this issue in our IκBα mutant mouse model. Failure of HSCT to correct lymphoid organogenesis and immune function in the mutant mice has important implications for the treatment of patients as it will strongly suggest that HSCT may not correct their immunodeficiency.

REFERENCES

1. Bonizzi G, Karin M. The two NF-kappaB activation pathways and their role in innate and adaptive immunity. Trends Immunol 2004; 25:280-8.
2. Hayden MS, Ghosh S. NF-kappaB, the first quarter-century: remarkable progress and outstanding questions. Genes Dev; 26:203-34.
3. Hayden MS, West AP, Ghosh S. NF-kappaB and the immune response. Oncogene 2006; 25:6758-80.
4. Orange JS, Geha RS. Finding NEMO: genetic disorders of NF-[kappa]B activation. J Clin Invest 2003; 112:983-5.
5. Smahi A, Courtois G, Rabia SH, Doffinger R, Bodemer C, Munnich A, et al. The NF-kappaB signalling pathway in human diseases: from incontinentia pigmenti to ectodermal dysplasias and immune-deficiency syndromes. Hum Mol Genet 2002; 11:2371-5.
6. Puel A, Picard C, Ku CL, Smahi A, Casanova JL. Inherited disorders of NF-kappaB-mediated immunity in man. Curr Opin Immunol 2004; 16:34-41.
7. Kere J, Srivastava AK, Montonen O, Zonana J, Thomas N, Ferguson B, et al. X-linked anhidrotic (hypohidrotic) ectodermal dysplasia is caused by mutation in a novel transmembrane protein. Nat Genet 1996; 13:409-16.
8. Srivastava AK, Durmowicz MC, Hartung AJ, Hudson J, Ouzts LV, Donovan DM, et al. Ectodysplasin-A1 is sufficient to rescue both hair growth and sweat glands in Tabby mice. Hum Mol Genet 2001; 10:2973-81.

9. Courtois G, Smahi A, Reichenbach J, Doffinger R, Cancrini C, Bonnet M, et al. A hypermorphic IkappaBalpha mutation is associated with autosomal dominant anhidrotic ectodermal dysplasia and T cell immunodeficiency. J Clin Invest 2003; 112:1108-15.

10. Janssen R, van Wengen A, Hoeve MA, ten Dam M, van der Burg M, van Dongen J, et al. The same IkappaBalpha mutation in two related individuals leads to completely different clinical syndromes. J Exp Med 2004; 200:559-68.

11. McDonald DR, Mooster JL, Reddy M, Bawle E, Secord E, Geha RS. Heterozygous N-terminal deletion of IkappaBalpha results in functional nuclear factor kappaB haploinsufficiency, ectodermal dysplasia, and immune deficiency. J Allergy Clin Immunol 2007; 120:900-7.

12. Lopez-Granados E, Keenan JE, Kinney MC, Leo H, Jain N, Ma CA, et al. A novel mutation in NFKBIA/IKBA results in a degradation-resistant N-truncated protein and is associated with ectodermal dysplasia with immunodeficiency. Hum Mutat 2008; 29:861-8.

13. Ohnishi H, Miyata R, Suzuki T, Nose T, Kubota K, Kato Z, et al. A rapid screening method to detect autosomal-dominant ectodermal dysplasia with immune deficiency syndrome. J Allergy Clin Immunol; 129:578-80.

14. Dupuis-Girod S, Cancrini C, Le Deist F, Palma P, Bodemer C, Puel A, et al. Successful allogeneic hemopoietic stem cell transplantation in a child who had anhidrotic ectodermal dysplasia with immunodeficiency. Pediatrics 2006; 118:e205-11.

15. Tsitsikov EN, Gutierrez-Ramos JC, Geha RS. Impaired CD19 expression and signaling, enhanced antibody response to type II T independent antigen and reduction of B-1 cells in CD81-deficient mice. Proc Natl Acad Sci U S A 1997; 94:10844-9.

16. Cariappa A, Takematsu H, Liu H, Diaz S, Haider K, Boboila C, et al. B cell antigen receptor signal strength and peripheral B cell development are regulated by a 9-O-acetyl sialic acid esterase. J Exp Med 2009; 206:125-38.

17. Kranich J, Krautler NJ, Heinen E, Polymenidou M, Bridel C, Schildknecht A, et al. Follicular dendritic cells control engulfment of apoptotic bodies by secreting Mfge8. J Exp Med 2008; 205:1293-302.

18. Koduru S, Kumar L, Massaad MJ, Ramesh N, Le Bras S, Ozcan E, et al. Cdc42 interacting protein 4 (CIP4) is essential for integrin-dependent T-cell trafficking. Proc Natl Acad Sci U S A; 107:16252-6.

19. van de Pavert SA, Mebius RE. New insights into the development of lymphoid tissues. Nat Rev Immunol; 10:664-74.

20. Fu YX, Chaplin DD. Development and maturation of secondary lymphoid tissues. Annu Rev Immunol 1999; 17:399-433.

21. Dejardin E, Droin NM, Delhase M, Haas E, Cao Y, Makris C, et al. The lymphotoxin-beta receptor induces different patterns of gene expression via two NF-kappaB pathways. Immunity 2002; 17:525-35.

22. Rajewsky K. Clonal selection and learning in the antibody system. Nature 1996; 381:751-8.

23. Fu YX, Huang G, Wang Y, Chaplin DD. B lymphocytes induce the formation of follicular dendritic cell clusters in a lymphotoxin alpha-dependent fashion. J Exp Med 1998; 187:1009-18.

24. Wu S, Walenkamp MJ, Lankester A, Bidlingmaier M, Wit JM, De Luca F. Growth hormone and insulin-like growth factor I insensitivity of fibroblasts isolated from a patient with an I{kappa}B{alpha} mutation. J Clin Endocrinol Metab; 95:1220-8.

25. Alcamo E, Hacohen N, Schulte LC, Rennert PD, Hynes RO, Baltimore D. Requirement for the NF-kappaB family member RelA in the development of secondary lymphoid organs. J Exp Med 2002; 195:233-44.

26. Seymour R, Sundberg JP, Hogenesch H. Abnormal lymphoid organ development in immunodeficient mutant mice. Vet Pathol 2006; 43:401-23.

27. Zindl CL, Kim TH, Zeng M, Archambault AS, Grayson MH, Choi K, et al. The lymphotoxin LTalpha(1)beta(2) controls postnatal and adult spleen marginal sinus vascular structure and function. Immunity 2009; 30:408-20.

28. Cariappa A, Liou HC, Horwitz BH, Pillai S. Nuclear factor kappa B is required for the development of marginal zone B lymphocytes. J Exp Med 2000; 192:1175-82.

29. Alimzhanov MB, Kuprash DV, Kosco-Vilbois MH, Luz A, Turetskaya RL, Tarakhovsky A, et al. Abnormal development of secondary lymphoid tissues in lymphotoxin beta-deficient mice. Proc Natl Acad Sci U S A 1997; 94:9302-7.

30. Krasteva M, Kehren J, Ducluzeau MT, Sayag M, Cacciapuoti M, Akiba H, et al. Contact dermatitis I. Pathophysiology of contact sensitivity. Eur J Dermatol 1999; 9:65-77.

31. Rennert PD, Hochman PS, Flavell RA, Chaplin DD, Jayaraman S, Browning JL, et al. Essential role of lymph nodes in contact hypersensitivity revealed in lymphotoxin-alpha-deficient mice. J Exp Med 2001; 193:1227-38.

32. Jabara HH, Weng Y, Sannikova T, Geha RS. TRAF2 and TRAF3 independently mediate Ig class switching driven by CD40. Int Immunol 2009; 21:477-88.

Conclusions and Future Directions

Conclusions and Future Directions

Why study primary immunodeficiency?

The study of patients with primary immunodeficiency (PID) gives insights into the *in vivo* function of the different effectors of the immune system. This concept has been evident for the past 50 years since Dr. Robert A. Good described how PID bisected the microbial world into microbes that require T cells for clearance (i.e. opportunistic infections, fungi and systemically invasive viruses) and microbes that require humoral, antibody mediated immunity (e.g. encapsulated bacteria, and viruses that infect the mucosae)[1]. The consequences of mutations in genes that are important for immune cell development and function can vary from severe, sometimes fatal susceptibility to infection by a broad range of microorganisms, as in the case of genes that underlie severe combined immunodeficiency (SCID) with lack of T cells, to a narrow predisposition to infections by certain organisms, for example mycobacteria or Candida[2, 3]. Several genes have been discovered by studying patients with PID e.g. WASP[4]. In addition, the function of several previously known genes has become better understood by the study of patients carrying mutations in those genes e.g. ATM, IL-7Rα[3].

Ectodermal dysplasia with immunodeficiency (ED-ID) is a PID with a clinical spectrum that includes susceptibility to recurrent pyogenic infections; hypogammaglobulinemia with low IgG and variable IgM and IgA; specific antibody deficiency, particularly to polysaccharide antigens; and decreased

cytokine and type I interferon production in response to TLR ligation[5]. Mutations in the NEMO gene were discovered to cause X-linked ED-ID when patients with ED-ID were compared to those with incontinentia pigmenti (IP). IP affects only women who are heterozygous for mutations in NEMO that abolish its activity. Patients with IP do not suffer from immunodeficiency because of non-random X-inactivation. All male progeny of IP mothers who inherit the nonfunctional NEMO allele die *in utero* because NFκB activation depends on NEMO and is essential for normal cell survival. For the same reason, skin lesions are present in those few locations populated by the progeny of epidermal cells that have inactivated the normal X chromosome. Since it was known that amorphic mutations in NEMO caused IP, and that NEMO is essential for NFκB function, which is important for B and T cell responses, Zonana, et al hypothesized that "milder" mutations in NEMO may cause ED-ID[6]. However, as predicted by Zonana, et al, a number of groups reported the presence of hypomorphic NEMO mutations in males with ED-ID, while genes known to cause ED alone were found to be normal in the ED-ID patients[6, 7]. The function of NEMO has been studied by linking the mutation site to patient phenotype. Certain mutations are selectively associated with ED, deficient CD40 signaling, osteopetrosis, or specific infections[8].

Several PIDs with a defined clinical presentation have been found to be caused by mutations in genes that lie in the same signaling pathway. Examples include Hyper-IgM syndrome where mutations in the CD40 ligand, CD40, AICDA and UNG genes have been found[9]. Another example is T^-B^+ SCID where

mutations in IL-7Rα, IL-2γc and Jak3 have been reported[10, 11]. In the case of the canonical NFκB signaling pathway, mutations in NEMO and IκBα have been described, and we discuss in detail two novel mutations that have taught us important lessons about the function of these genes in ED-ID.

The genes responsible for PID often carry mutations in their coding sequence. However this is not always the case. This is important to remember, as targeted exon sequencing and whole exome sequencing have reached clinical practice. In Chapter 1, we illustrated how a mutation in the 5'UTR of NEMO can cause disease by impairing mRNA and protein expression levels of NEMO.

The majority of the genes known to cause PID to date are homozygous autosomal mutations, compound heterozygous autosomal mutations, or mutations on X chromosomes in males that impair protein function. However, in a number of cases a heretozygous autosomal mutation may also interfere with function by causing haploinsufficiency or by acting as a dominant negative. Examples of the former include TACI deficiency, where haploinsufficiency interferes with the response to T-independent type II antigens[12], and C1 esterase inhibitor deficiency, which leads to uncontrolled activation of the complement system in response to infection and injury[13]. Autosomal dominant mutations include mutations in the STAT3 [14] and Fas genes[15]. In Chapter 2, we described an IκBα mutation that results in functional insufficiency with 50% residual activation of NFκB. The resulting ED-ID phenotype is markedly milder than that of the S32I mutation in the same gene, which results in a dominant negative. The reasons for this difference are also discussed in Chapter 2.

The severity of the immunodeficiency that results from a mutation in a certain gene depends on at least three factors. One is the location of the mutation within the gene itself. This determines whether the mutant protein is present or absent, and if present, which of its biological activities is affected, how severely it is affected, and whether the mutant will act as a dominant negative. Another important determinant is the genetic background of the affected individual. The same mutation may result in variable degrees of disease severity in different siblings, since modifier genes in each child may be different. Finally, the clinical severity of the resulting PID depends on the microbial load in the environment. The latter point is best illustrated by the fact that $Rag2^{-/-}$ mice do well in a specific pathogen free (SPF) facility while RAG2 deficient infants uniformly die in their first year of life unless given hematopoietic stem cell transplant (HSCT). In Chapter 3, we have used a mouse knock-in model of ED-ID on C57Bl6 background to circumvent the influence of variations in the genetic background and environment on the effect of the heterozygous S32I mutation in IκBα on immune cell development and function.

Summary of studies of patients with ED-ID

In Chapter 1, we reported a patient with recurrent infections, and a family history suggesting X-linked inheritance. Although this patient had no features of ED, he had deficient cytokine production in response to stimulation with TLR ligands *in vitro*. Furthermore, the patient's cells exhibited decreased phosphorylation of IκBα, diminished IκBα degradation and impaired NFκB

activation following IL-1 stimulation. The patient's cells were also found to have very low levels of NEMO mRNA and protein. Analysis of genomic DNA revealed no mutation in the coding sequence of the *NEMO* gene, but the presence of a novel mutation in the NEMO 5' UTR. This mutation was the first to be reported in the 5'UTR of NEMO and was shown to result in aberrant splicing of the untranslated exons as evidenced by analysis of the cDNA. The fact that reduced NEMO expression and reduced NFκB activation resulted in impaired innate and adaptive immunity, but allowed normal ectodermal development strongly suggested a hierarchy in the requirement for NFκB activation for ectodermal development and innate immune responses. We suggested that NEMO protein levels should be examined in boys with dysgammaglobulinemia and an infection history consistent with a defect in NEMO, but whose NEMO sequence is normal. Decreased NEMO levels in such patients warrant examination of the 5' and 3' sequences to search for defects in transcription or mRNA stability, respectively.

In Chapter 2, we presented the first case of a female with ED-ID caused by a heterozygous mutation in IκBα that resulted in N-terminal truncation of the protein. The mutation in this patient replaced the codon that encoded for a tryptophan at position 11 with a stop codon (W11X). The clinical presentation of this patient was milder than that of the two previously reported ED-ID patients, both of whom had a heterozygous S32I substitution that abrogated phosphorylation of the mutant. TLR function in our patient with the IκBα W11X mutation was impaired. The truncated IκBα protein did not undergo ligand-induced phosphorylation or degradation following IL-1 stimulation. Moreover,

about 50% of the p65 NFκB subunit was retained in the cytoplasm by the mutant protein and NFκB DNA binding by nuclear extracts was decreased by ~50%. We have referred to this defect as a "functional haploinsufficiency".

How does the mis-spliced NEMO transcript affect protein levels?

There are four first exons in the NEMO gene, 1A-D. They are each alternatively spliced to the ATG-containing second exon, resulting in mRNAs that are translated into an identical protein product. Lymphocytes express NEMO transcripts containing exons 1A, 1B and 1C but not 1D, spliced to exon 2. Exon 1B-containing transcripts are much more abundant than transcripts containing exons 1A or 1C. Liver cells are reported to use exon 1D[16]. The patient's exon 1B-containing transcripts are mis-spliced, and we showed that his NEMO mRNA levels are decreased compared to normal controls, but we did not formally show that the mis-spliced exon 1B-containing transcripts are the cause for the low mRNA level. Biochemical studies would also allow us to measure the translation efficiency of the mis-spliced transcripts, as well as their stability in the cell. It would be interesting to show directly how the mutation affects the amount of mRNA and protein in different cell types. We postulate that the amount of NEMO in the patient's liver is normal, because it relies less on exon 1B transcripts. However it is impossible to study this directly because liver material is not available from the patient.

A mouse model of ED-ID with S32I mutation in IκBα

We have created a mouse model of ED-ID by introducing the S32I mutation into one allele of the IκBα gene. The mutant mice had ED, increased mortality, complete lack of lymph nodes and Peyer's patches, and disorganized spleens that lacked follicles, marginal zone B cells and follicular dendritic cells. T cell function was normal *in vitro*, but contact hypersensitivity *in vivo* was severely impaired. B cell function *in vitro* and antibody response to T-dependent and T-independent antigens were severely reduced. All immune defects, except those that affected B cell function, were absent in IκBα S32I mutant $Rag2^{-/-}$ bone marrow chimeras. This indicates that defects in stromal cells play a major role in the immunodeficiency of patients with ED-ID due to mutations in IκBα and other genes that impair the NFκB signaling pathway. This has important clinical implications, as bone marrow transplant may not be able to correct immune function in such patients.

Why does the S32I mutation appear to be more severe than the N-terminal truncations of IκBα?

It is expected that the product of a mutant non-degradable IκBα allele will be present at a higher level than the product of the WT allele, because both are equally subject to NFκB-induced expression but only the WT allele is degraded each time NFκB is activated. If this is the case, more than 50% of the NFκB molecules will be sequestered in the cytoplasm. In addition, if the mutant allele retains the capacity to engage the IKK complex, it will compete with the WT allele for the IKK complex.

Close examination of the Western blots of IκBα from the W11X[17] and Q9X[18] patients reveals three bands. The highest molecular weight band corresponds to normal-sized IκBα protein, the product of the WT allele. The middle band corresponds in size to the product of transcription reinitiation at Met 13, and the lowest band to reinitiation at Met 37. The protein beginning at Met 13 could possibly be phosphorylated and degraded, since it contains both the phosphorylation and ubiquitination sites. The protein beginning at Met 37 would contain neither, and has already been shown to act as a non-degradable inhibitor of NFκB[19]. The W11X patient has milder symptoms than the S32I patients because she may have a greater proportion of IκBα that can be degraded than the S32I patients, that is: the sum of the WT protein and the Met 13 protein. In addition, if the IKK complex anchors at the N-terminus of IκBα, her non-degradable Met 37 mutant protein may not compete for IKK. This may explain why 50% of the IκBα is degraded in this patient, as demonstrated by retention of only 50% of p65 in the cytoplasm compared to 0% in the control following IL-1 stimulation. This contrasts with phosphorylation of 10% of the IκBα in the S32I patient and of 30% in the IκBα S32I mutant mice.

It should be noted that overexpression experiments showed that the IκBα W11X plasmid inhibited NFκB activation to the same degree as the IκBα WT plasmid in a reporter gene assay in transfected 293T cells. In contrast, Courtois et al, had reported that transfection of the IκBα S32I mutant, but not of WT IκBα, inhibited NFκB activation in 293T cells transfected with plasmids in comparable

amounts to what we used. The reason why they did not observe the expected inhibition of NFκB activation by the WT protein is unclear.

Will bone marrow transplants in the S32I IκBα deficiency restore immune function?

Transplant of mutant bone marrow into $Rag2^{-/-}$ mice showed that non-lymphoid cells were necessary to form proper B cell follicles and germinal centers (GCs). The reverse experiment will also be necessary to see if mutants receiving WT bone marrow can respond to antigens. This important experiment will have direct clinical implications, since it would be similar to the hematopoietic stem cell transplants performed in patients and would indicate to what extent WT lymphocytes would be able to cure immunodeficiency in the patients. Since the non-lymphoid stroma of the mutant mice will still lack normal NFκB function, we hypothesize that the lymph nodes (LN) and Peyer's patches (PP) may not be restored, and that the splenic architecture will continue to be disorganized. If this is the case, it will be unlikely to find mature follicular dendritic cells (FDCs) or GC formation in immunized IκBα mutant mice who have received WT bone marrow. In addition, specific antibody production will not be expected. The patient carrying the S32I mutation who survived transplant had an increase in his response to tetanus toxoid from a post-transplant immunization[20]. However the patient was reported not to have tonsils and not to have palpable LN during infection. It will be important to determine how T cells and B cells from the transplanted mutant mice respond to immunization both intraperitoneally and cutaneously.

Defective NFκB signaling in mutant mice

In the case of the IκBα S32I mice, we cannot easily determine the ratio of protein expression from the mutant and WT alleles as we did in the W11X patient, since they are of the same molecular weight. Assuming efficient transcription from both alleles, it is quite interesting that only 20% of the protein is degraded after IL-1 stimulation. There are a couple of possibilities for why this is so. The mutant protein may build up in the cells. Upon stimulation, only the WT protein is degraded, but NFκB drives IκBα transcription from both WT and mutant alleles. A second possible reason is lower than expected degradation of the WT allele, because the mutant protein could compete for IKK binding and interfere with the phosphorylation of the WT protein.

Are these mutations dominant negative?

IκBα function can be represented by a spectrum of mutations. Normal mice would lie at the center of the spectrum, while IκBα$^{-/-}$ mice, with no IκBα function would lie at one end, and mice with the non-degradable IκBα would lie at the other. Since there is little NFκB negative regulation in IκBα$^{-/-}$ mice, there is increased inflammation and the mice die in the second week of life[21]. The IκBα S32I mice, which express non-degradable IκBα, have little NFκB signaling because of too much negative regulation.

Since the IκBα mutations are gain-of-function mutations, are they necessarily dominant *negative*? The overall effect in the IκBα S32I mutant is loss

of more than 50% of NFκB signaling, thus they would fit the definition of dominant negative. We have no direct evidence that the mutant protein interferes with the function of product from the WT IκBα allele. In particular, IκBα is not known to dimerize. Thus the likely cause for the dominant negative effect is an excess of mutant protein, which in addition may also compete with the WT protein for IKK. It should be noted that IκBα$^{+/-}$ mice are completely normal and have no evidence of constitutive NFκB activation[21]. This suggests that there is normally an excess of IκBα over p50:p65 or that there is a compensatory increase in the level of IκBα to reset the normal IκBα:NFκB balance in IκBα$^{+/-}$ cells.

How much NFκB activity is present in IκBα mutant cells?

In order to compare NFκB function in the IκBα S32I model to WT mice, nuclear translocation of p50 and p65 in fibroblasts after stimulation with IL-1 or TNFα will be measured by Western blot. These experiments will help elucidate how much residual NFκB activity is present in the mutant cells. Other experiments in this vein include electrophoretic mobility shift assays (EMSA) in order to measure NFκB DNA binding in lysates after stimulation in fibroblasts, as shown in Chapter 2. Courtois, et al unexpectedly found that an excess of mutant IκBα S32I, but not of WT IκBα, inhibited NFκB luciferase activity. I plan to repeat this experiment in order to verify whether the mutant has a more inhibitory effect than the WT in a transient transfection assay, which would indicate a “true” dominant negative effect.

As expected from impaired canonical NFκB signaling, IκBα mutant mice had no FDCs, B cell follicles or GCs in the spleen. Unexpectedly, they also had no LN or PP which have been reported to depend on the LTβR driven non-canonical pathway of NFκB signaling[22, 23]. It is therefore important to examine directly whether the IκBα mutant protein interferes with the non-caninocal pathway. This could result from downregulation of p100 and RelB expression, which are subject to regulation by the canonical pathway. We will measure p100 and RelB protein expression in MEFs and lymphocytes.

It has been reported that LTβR also activates the canonical NFκB pathway to upregulate adhesion molecules, but relies on the non-canonical pathway to induce the expression of chemokines that are essential to attract LTi cells and lymphocytes[22]. We propose to study the upregulation of CXCL13, CCL19 and CCL21 in the MEF system by flow cytometry and quantitative PCR. A defect in this pathway would give further insight into the mechanism for the lack of LN formation and improper splenic architecture in these mice, as CXCL13 and its receptor CXCR5 are essential for successful secondary lymphoid organogenesis[24].

Are IκBα mutant mice more susceptible to infection?

A quintessential question when considering whether a patient has an NFκB deficiency is the ability of the patient's peripheral blood mononuclear cells (PBMCs) to produce cytokines after stimulation with a panel of TLR ligands[25]. Since IκBα phosphorylation and degradation after LPS stimulation was reduced

in fibroblasts and B cells (data not shown), it is expected that bone marrow-derived macrophages and dendritic cells from IκBα mutant bone marrow would be impaired in their ability to secrete cytokines in response to TLR ligands. If this is the case, the mice would not be able to sense pathogens well and would be more susceptible to infection.

Susceptibility to infection has not been directly tested in these mice. The mice have been kept in autoclaved cages and on prophylactic antibiotics in an SPF environment. In order to more thoroughly characterize the phenotype, it would be necessary to keep some mice under conventional conditions in order to determine whether they develop any lesions, or are susceptible to opportunistic infections such as *pneumocystis jiroveci*, like ED-ID patients[8, 26]. We have shown that the response to TNP-LPS, TNP-ficoll and OVA immunization is defective in IκBα mutant mice. A next step would be to infect the mice with known amounts of a pathogen, such as *Streptococcus pneumonia* intranasally or *Staphyloccus aureus* cutaneously and evaluate bacterial clearance and inflammatory responses[27].

Are IκBα mutant mice more susceptible to LPS shock?

As mentioned previously, IκBα phosphorylation and degradation following LPS stimulation was reduced. However, when the mice were immunized with TNP-LPS, some of the IκBα mutant mice died within a few days (6/7 mice in experiment 1, 3/6 mice in experiment 2). This is similar to the phenotype of the $p50^{-/-}$ mice that die from LPS shock. The phenotype is lymphocyte-independent

and depends on elevated levels of TNF[28]. It would be interesting to see if IκBα mice also produce high amounts of TNF after LPS administration, and if their survival in response to LPS is similar to $p50^{-/-}$ or $p65^{+/-}p50^{-/-}$ mice.

A closer look at immunoglobulin isotype switching in the IκBα mutant mice

Class switch recombination is also reported to require NFκB, as evidenced by germline transcripts and switching to certain Ig constant regions in $p50^{-/-}$ mice[29]. In the IκBα mutant mice, serum IgM was normal, serum IgG was low (due mostly to a defect in IgG1 subclass switching; data not shown) and serum IgA was absent. Mutant splenic B cells stimulated with anti-CD40+IL-4 or LPS+IL4 did not have a significant defect in IgG production. However these experiments used total B cells. We need to use naïve B cells to determine if isotype switching to IgG and IgE following anti-CD40+IL-4 and LPS+IL4 is impaired. We will use LPS and TGFβ to examine switching to IgA. NFκB regulates the expression of IgG and IgE germ line transcripts and AICDA expression[30]. We will use quantitiative PCR to determine the expression of these genes in stimulated naïve B cells from mutant mice.

Increased B1b cells in IκBα mutant mice?

One possible reason for why the IκBα mutant mice do not have low serum IgM may be that in the absence of normal isotype switching, the IgM^+ B cells differentiate into plasma cells. Alternatively, the increased number of B1b-like cells which were found in the bone marrow (Fig. C.1) and spleen but not in the

peritoneum, may account for the normal serum IgM in the mutant mice. B1 cells produce natural antibodies and autoantibodies. We plan to explore the natural serum antibody levels to known antigens such as α-gal[31] pneumococcal and other bacterial antigens. We will also screen the sera from IκBα mice for autoantibodies using a commercial screen for autoantigens.

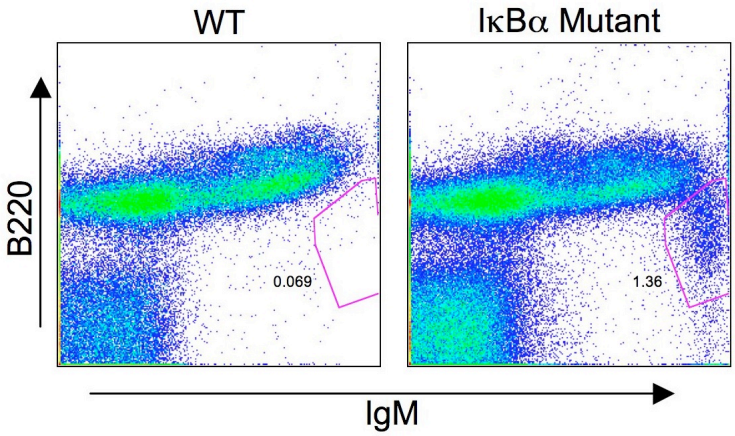

Figure C.1. B1b-like population in bone marrow from IκBα mutant mice.

The IgM^{high}B220^{low} population is IgD^{-}CD43^{+}CD23^{low}CD11b^{+}CD5^{-}CD93^{-}CD138^{-}, consistent with B1b cells. A similar population was found in the spleens of IκBα mutant mice.

Dermatitis in IκBα mutant mice

IκBα mutant mice develop skin lesions at varying ages with thickened epidermis and an intense dermal infiltrate of neutrophils, lymphocytes and eosinophils (Fig. C.2). Lesional skin becomes thick and scaly and the hair is lost. Even non-lesional skin contains more neutrophils than WT. Staining for bacteria was negative and we have failed to culture bacteria from these lesions. All mice have patches of hyperkeratosis, particularly around the eyes (data not shown); it is not known if this is immune in nature or if it is the mouse correlate of periorbital

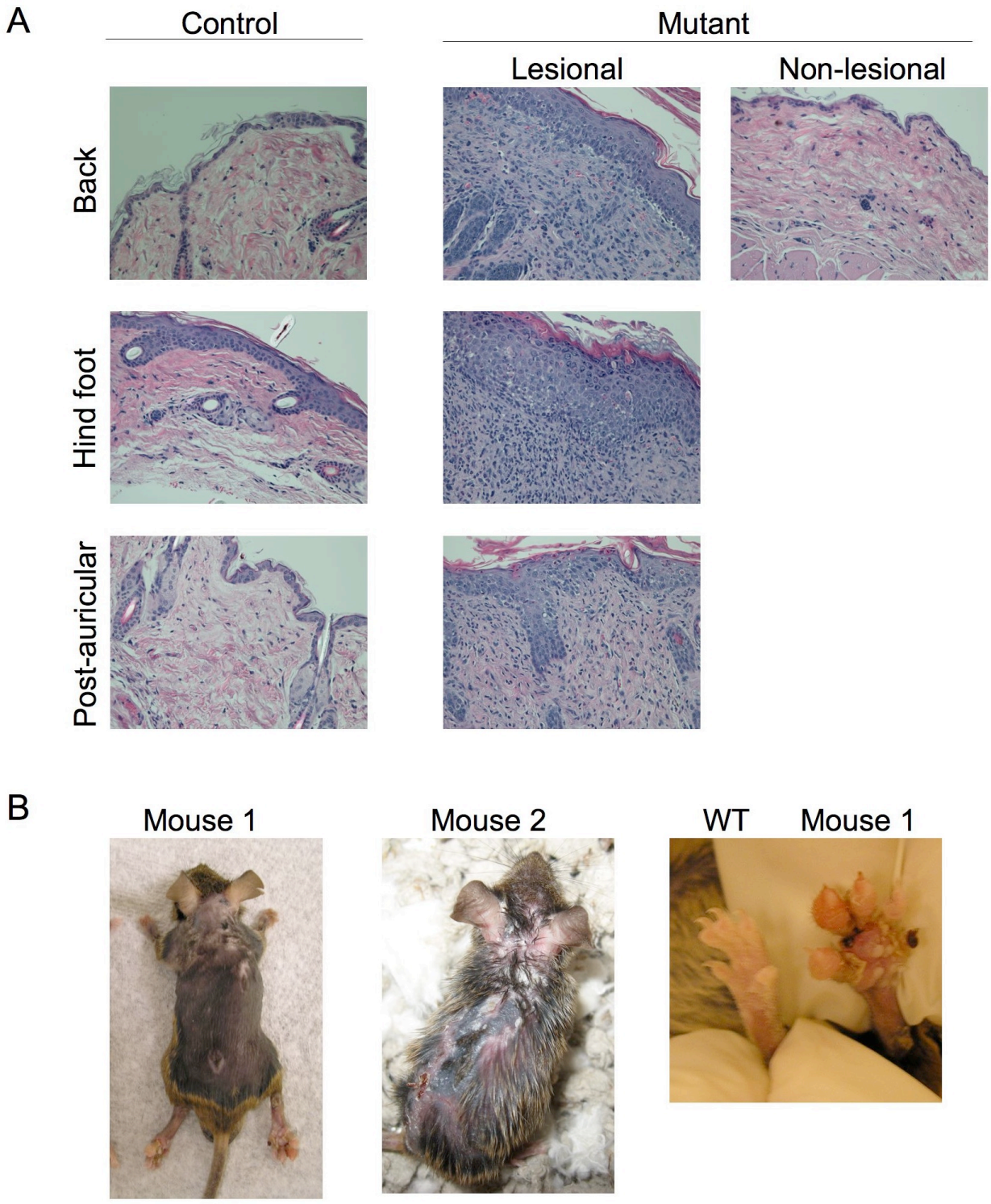

Figure C.2. Dermatitis in IκBα mutant mice.

A. H&E staining of sections from several tissues. **B**. Photos showing dermatitis and foot swelling in IκBα mutant mice.

wrinkling seen in some patients with ED. A small percentage of mice develop severe scaling and swelling of the feet. The dermatitis appears to be hematopoietically transferred, since one-quarter of the $Rag2^{-/-}$ mice that received IκBα mutant bone marrow also developed severe dermatitis.

Dermatitis is not uncommon in NFκB family transgenic mice. $IκBα^{-/-}$ mice have perinatal lethality and severe inflammatory dermatitis[21]. Mice with a degradation-resistant IκBα (Δ1-36) transgene under the control of the Keratin5/14 promoter had TNFα-dependent keratinocyte hyperproliferation associated with immune infiltrates[32]. Skin grafts from RelA/c-Rel/TNFα triple KO embryos onto $Rag^{-/-}$ mice also develop TNFα-induced hyperplasia[19].

In order to better describe the dermatitis, we plan to stain the skin sections to look for Ig deposition and complement deposition, and to count various cell types in the infiltrate using H&E staining. T cell subsets in the infiltrate will be stained and enumerated by immunohistochemistry. Because of the presence of eosinophils in the infiltrate, IgE levels will also be compared between affected and unaffected IκBα mutant mice and their WT littermates. Expression of cytokines and chemokines in the lesional and non-lesional skin of mutant mice will be analyzed by quantitiative PCR and compared to that in skin of WT littermates.

T cell development

Skin-resident regulatory T cells (T_{reg}) are essential for maintaining normal immune homeostasis in the skin[33], and the T_{reg} deficient scurfy mice develop skin

inflammation that can be transferred to Rag1$^{-/-}$ recipients[34]. We have evidence of a 3-fold decrease in the number of CD25^{+}Foxp3^{+} regulatory CD4^{+} T cells in the spleen (data not shown). We plan to analyze T_{reg} cell function. The mice will be bred with Foxp3-EGFP mice and EGFP^{+} cells will be sorted and their function assessed using standard assays[35].

While the numbers and percentages of T cell subsets in the thymus from IκBα mutant mice appeared to be intact, there was abnormal thymic architecture. Further immunohistochemical studies on the thymus will show whether there is a defect in thymic epithelial cell development, and whether there is proper AIRE expression. If AIRE expression is impaired, there is a possibility that T cells escape from negative selection and contribute to autoimmunity and dermatitis in these mice. To address this issue we will analyze the T cell repertoire of these mice by flow cytometry and analysis of V_{β} region expression.

Conclusion

Through these mouse model experiments we will gain insight into the consequences of impaired NFκB signaling due to the IκBα S32I mutation, a mutation that severely impairs NFκB signaling and results in severe disease that appears to be not well controlled by bone marrow transplantation.

ED-ID covers a spectrum of patient presentations depending on the location of the mutation within the gene and the gene affected. NFκB signaling is complex with interplay between the canonical and non-canonical pathways. The lessons we will learn from these studies may be applicable to other mutations

that severely impair NFκB signaling and have important implications for the treatment of patients who carry these mutations.

REFERENCES

1. Good RA. Cellular immunology in a historical perspective. Immunol Rev 2002; 185:136-58.
2. Casanova JL, Abel L. Genetic dissection of immunity to mycobacteria: the human model. Annu Rev Immunol 2002; 20:581-620.
3. Fischer A. Human primary immunodeficiency diseases. Immunity 2007; 27:835-45.
4. Ochs HD, Thrasher AJ. The Wiskott-Aldrich syndrome. J Allergy Clin Immunol 2006; 117:725-38; quiz 39.
5. Puel A, Picard C, Ku CL, Smahi A, Casanova JL. Inherited disorders of NF-kappaB-mediated immunity in man. Curr Opin Immunol 2004; 16:34-41.
6. Zonana J, Elder ME, Schneider LC, Orlow SJ, Moss C, Golabi M, et al. A novel X-linked disorder of immune deficiency and hypohidrotic ectodermal dysplasia is allelic to incontinentia pigmenti and due to mutations in IKK-gamma (NEMO). Am J Hum Genet 2000; 67:1555-62.
7. Jain A, Ma CA, Liu S, Brown M, Cohen J, Strober W. Specific missense mutations in NEMO result in hyper-IgM syndrome with hypohydrotic ectodermal dysplasia. Nat Immunol 2001; 2:223-8.
8. Hanson EP, Monaco-Shawver L, Solt LA, Madge LA, Banerjee PP, May MJ, et al. Hypomorphic nuclear factor-kappaB essential modulator mutation database

and reconstitution system identifies phenotypic and immunologic diversity. J Allergy Clin Immunol 2008; 122:1169-77 e16.

9. Davies EG, Thrasher AJ. Update on the hyper immunoglobulin M syndromes. Br J Haematol; 149:167-80.

10. Notarangelo LD, Giliani S, Mazza C, Mella P, Savoldi G, Rodriguez-Perez C, et al. Of genes and phenotypes: the immunological and molecular spectrum of combined immune deficiency. Defects of the gamma(c)-JAK3 signaling pathway as a model. Immunol Rev 2000; 178:39-48.

11. Puel A, Leonard WJ. Mutations in the gene for the IL-7 receptor result in T(-)B(+)NK(+) severe combined immunodeficiency disease. Curr Opin Immunol 2000; 12:468-73.

12. Rachid R, Castigli E, Geha RS, Bonilla FA. TACI mutation in common variable immunodeficiency and IgA deficiency. Curr Allergy Asthma Rep 2006; 6:357-62.

13. Frank MM. The C1 esterase inhibitor and hereditary angioedema. J Clin Immunol 1982; 2:65-8.

14. Sowerwine KJ, Holland SM, Freeman AF. Hyper-IgE syndrome update. Ann N Y Acad Sci; 1250:25-32.

15. Siegel RM, Chan FK, Chun HJ, Lenardo MJ. The multifaceted role of Fas signaling in immune cell homeostasis and autoimmunity. Nat Immunol 2000; 1:469-74.

16. Fusco F, Mercadante V, Miano MG, Ursini MV. Multiple regulatory regions and tissue-specific transcription initiation mediate the expression of NEMO/IKKgamma gene. Gene 2006; 383:99-107.

17. McDonald DR, Mooster JL, Reddy M, Bawle E, Secord E, Geha RS. Heterozygous N-terminal deletion of IkappaBalpha results in functional nuclear factor kappaB haploinsufficiency, ectodermal dysplasia, and immune deficiency. J Allergy Clin Immunol 2007; 120:900-7.

18. Ohnishi H, Miyata R, Suzuki T, Nose T, Kubota K, Kato Z, et al. A rapid screening method to detect autosomal-dominant ectodermal dysplasia with immune deficiency syndrome. J Allergy Clin Immunol; 129:578-80.

19. Gerondakis S, Grumont R, Gugasyan R, Wong L, Isomura I, Ho W, et al. Unravelling the complexities of the NF-kappaB signalling pathway using mouse knockout and transgenic models. Oncogene 2006; 25:6781-99.

20. Dupuis-Girod S, Cancrini C, Le Deist F, Palma P, Bodemer C, Puel A, et al. Successful allogeneic hemopoietic stem cell transplantation in a child who had anhidrotic ectodermal dysplasia with immunodeficiency. Pediatrics 2006; 118:e205-11.

21. Beg AA, Sha WC, Bronson RT, Baltimore D. Constitutive NF-kappa B activation, enhanced granulopoiesis, and neonatal lethality in I kappa B alpha-deficient mice. Genes Dev 1995; 9:2736-46.

22. Dejardin E, Droin NM, Delhase M, Haas E, Cao Y, Makris C, et al. The lymphotoxin-beta receptor induces different patterns of gene expression via two NF-kappaB pathways. Immunity 2002; 17:525-35.

23. Seymour R, Sundberg JP, Hogenesch H. Abnormal lymphoid organ development in immunodeficient mutant mice. Vet Pathol 2006; 43:401-23.

24. Weih F, Caamano J. Regulation of secondary lymphoid organ development by the nuclear factor-kappaB signal transduction pathway. Immunol Rev 2003; 195:91-105.

25. Karin M. Signal transduction and gene control. Curr Opin Cell Biol 1991; 3:467-73.

26. Salt BH, Niemela JE, Pandey R, Hanson EP, Deering RP, Quinones R, et al. IKBKG (nuclear factor-kappa B essential modulator) mutation can be associated with opportunistic infection without impairing Toll-like receptor function. J Allergy Clin Immunol 2008; 121:976-82.

27. Pittet LA, Quinton LJ, Yamamoto K, Robson BE, Ferrari JD, Algul H, et al. Earliest innate immune responses require macrophage RelA during pneumococcal pneumonia. Am J Respir Cell Mol Biol; 45:573-81.

28. Gadjeva M, Tomczak MF, Zhang M, Wang YY, Dull K, Rogers AB, et al. A role for NF-kappa B subunits p50 and p65 in the inhibition of lipopolysaccharide-induced shock. J Immunol 2004; 173:5786-93.

29. Snapper CM, Zelazowski P, Rosas FR, Kehry MR, Tian M, Baltimore D, et al. B cells from p50/NF-kappa B knockout mice have selective defects in proliferation, differentiation, germ-line CH transcription, and Ig class switching. J Immunol 1996; 156:183-91.

30. Jabara HH, Weng Y, Sannikova T, Geha RS. TRAF2 and TRAF3 independently mediate Ig class switching driven by CD40. Int Immunol 2009; 21:477-88.

31. Takeuchi Y, Liong SH, Bieniasz PD, Jager U, Porter CD, Friedman T, et al. Sensitization of rhabdo-, lenti-, and spumaviruses to human serum by galactosyl(alpha1-3)galactosylation. J Virol 1997; 71:6174-8.

32. Zhang JY, Green CL, Tao S, Khavari PA. NF-kappaB RelA opposes epidermal proliferation driven by TNFR1 and JNK. Genes Dev 2004; 18:17-22.

33. Dudda JC, Perdue N, Bachtanian E, Campbell DJ. Foxp3+ regulatory T cells maintain immune homeostasis in the skin. J Exp Med 2008; 205:1559-65.

34. Sharma R, Sung SS, Fu SM, Ju ST. Regulation of multi-organ inflammation in the regulatory T cell-deficient scurfy mice. J Biomed Sci 2009; 16:20.

35. Chauhan SK, Saban DR, Lee HK, Dana R. Levels of Foxp3 in regulatory T cells reflect their functional status in transplantation. J Immunol 2009; 182:148-53.